NON-ORTHOGONAL MULTIPLE ACCESS WITH TWO SETS OF ORTHOGONAL SIGNAL WAVEFORMS

by

Ersoy Çalışkan

B.S., Electrical and Electronics Engineering, Boğaziçi University, 2015

Submitted to the Institute for Graduate Studies in
Science and Engineering in partial fulfillment of
the requirements for the degree of
Master of Science

Graduate Program in Electrical and Electronics Engineering
Boğaziçi University

2019

ACKNOWLEDGEMENTS

I dedicate this thesis to my family who supports me unconditionally. My father, mother and sister are the most precious things I have.

I owe special thanks to my supervisor Prof. Mutlu Koca. In addition I would like to thanks Prof. Emin Anarım and Prof. Erdal Panayırcı who accepted to being my thesis jury.

I also thank to Prof. Hikmet Sarı who proposed the method which my whole thesis is based on. I am always proud to work with him.

I thank to my whole friends especially the member of WCL. Oğuz Kışlal, Negin Kazemi, Bayram Akdeniz, Abdullah Sarıduman, Can Karamanlı, Öykü Tuncel, Reza Asrafi, Özgün Demir, Numan Su and İsmail Coşandal helps me on my whole thesis duration and I would like to thank them. Lastly I would like to thanks my dear friend Okan Ulusoy who stands with me on my hard times.

ABSTRACT

NON-ORTHOGONAL MULTIPLE ACCESS WITH TWO SETS OF ORTHOGONAL SIGNAL WAVEFORMS

The rapid development of the mobile systems causes dramatic increase on data traffic. Due to the bandwidth scarcity, existing multiple access systems may not overcome this problem [1]. These multiple access techniques are called as orthogonal multiple access (OMA) in which different users utilize orthogonal resource blocks such as frequency, time or code domain. Therefore the number of the users which can be supported by a wireless system is strictly restricted by the number of the resource blocks. However in non-orthogonal multiple access (NOMA), orthogonal resource blocks are shared by different users. Interference cancellation method is used by receiver at the cost of complexity. Thanks to NOMA, users more than orthogonal resource block size, can communicate. In addition to that, NOMA is more spectral efficient multiple access technique than OMA. For instance even if a user has poor channel condition, she/he occupies at least one resource block in OMA. This situation reduces total throughput of the overall system. However in NOMA, since all resource blocks are shared by more than one user, weak users do not occupy any resource block on his own. Existing NOMA techniques can be divided into two main categories as code domain and power domain NOMA [2]. Power differences between non-orthogonal users are very important for power domain NOMA. Weakness of the code domain is that even if the number of the users do not exceed the number of the orthogonal blocks, non-orthogonality still occurs. These problems can be overcome by using two sets orthogonal signal waveforms which are non-orthogonal to each others [3]. In addition to that, its error performance on different channel conditions is encouraging.

ÖZET

DİKGEN İKİ DALGA BİÇİMİ KÜMESİ İLE DİKGEN OLMAYAN ÇOKLU ERİŞİM

Mobil sistemlerin hızlı gelişimi, veri trafiğinde hızlı bir artışa neden olmaktadır. Bant genişliği yetersizliği nedeniyle, mevcut çoklu erişim sistemleri bu sorunun üstesinden gelemeyebilir [1]. Bu çoklu erişim teknikleri, farklı kullanıcıların frekans, zaman veya kod düzlemi gibi dikgen kaynak bloklarını kullandığı, dikgen çoklu erişim (DÇE) olarak adlandırılır. Bu nedenle, bir kablosuz sistem tarafından desteklenebilen kullanıcıların sayısı, kaynak bloklarının sayısı ile sınırlıdır. Bununla birlikte, dikgen olmayan çoklu erişimde (DOÇE), dikgen kaynak blokları farklı kullanıcılar tarafından paylaşılmaktadır. Girişim iptal yöntemi, alıcı tarafından, dikgen olmayan sinyalleri ayrıştırmak için kullanılır. DOÇE sayesinde, bir kablosuz sistemde, dikgen kaynak blok sayısından daha fazla kullanıcı iletişim kurabilir. Buna ek olarak, DOÇE, DÇE'den bant kullanımı açısından daha verimlidir. Örneğin, bir kullanıcının kanal durumu kötü olsa bile, DÇE'de en az bir kaynak bloğu işgal eder. Bu durum, genel sistemin toplam verimini azaltır. Ancak DOÇE'de, tüm kaynak blokları birden fazla kullanıcı tarafından paylaşıldığından, zayıf kullanıcılar kendi başlarına herhangi bir kaynak bloğunu işgal etmemektedir. Mevcut DOÇE teknikleri, kod düzlemi ve güç düzlemi DOÇE [2] olarak iki ana kategoriye ayrılabilir. Dikgen olmayan kullanıcılar arasındaki güç farklılıkları, güç düzlemi DOÇE için çok önemlidir. Kod düzlemi DOÇE'de ise, kullanıcı sayısı dikgen blokların sayısını aşmasa bile, girişimin hala mevcut olmaktadır. Bu sorunlar, birbirleriyle dikgen olmayan iki küme dikgen sinyal dalga biçimi kullanılarak aşılabilir [3]. Buna ek olarak, bu yöntemin farklı kanal koşullarındaki hata performansı da umut vericidir.

TABLE OF CONTENTS

LIST OF FIGURES

LIST OF SYMBOLS

$\vec{a}$	OFDMA symbols' vector
a_n	n^{th} element of the $\vec{a}$
$\vec{b}$	MC-CDMA symbols' vector
b_n	n^{th} element of the $\vec{b}$
$H_{(m)}$	Diagonal MC-CDMA coefficient matrix
$H_{(o)}$	Diagonal OFDMA coefficient matrix
$\vec{u}$	Noise vector
u_n	n^{th} element of the $\vec{u}$
W	Walsh-Hadamard matrix
$\vec{x}$	Received signals' vector
x_n	n^{th} element of the $\vec{x}$
η	Additive white noise
λ	Soft decision coefficient

LIST OF ACRONYMS/ABBREVIATIONS

AWGN	Additive White Gaussian Noise
BER	Bit Error Rate
bps	Bits per Second
BS	Base Station
CDMA	Code Division Multiple Access
dB	Decibel
DFT	Discrete Fourier Transform
FDMA	Frequency Division Multiple Access
IFFT	Inverse Fast Fourier Transform
ISI	Inter Symbol Interference
LDS-CDMA	Low Density Signature Code Division Multiple Access
LDS-OFDM	Low Density Signature Orthogonal Frequency Division Multiplexing
MA	Multiple Access
MC-CDMA	Multi-Carrier Code Division Multiple Access
MISO	Multiple Input Single Output
ML	Maximum Likelihood
MMSE	Minimum Mean Square Error
NOMA	Non-Orthogonal Multiple Access
OF	Overload Factor
OFDM	Orthogonal Frequency Division Multiplexing
OFDMA	Orthogonal Frequency Division Multiple Access
OMA	Orthogonal Multiple Access
PDF	Probability Density Function
S/I	Signal to Interference Ratio
SCMA	Sparse Code Multiple Access
SIC	Successive Interference Cancellation
SNR	Signal to Noise Ratio
TDMA	Time Division Multiple Access

1. INTRODUCTION

1.1. Multiple Access

In communication systems, if a channel in which data transfer be realized is shared by multiple users, it is called as multiuser channel. There are two different the type as uplink and downlink transmission which are illustrated in figure 1.1(a) and 1.1(b).

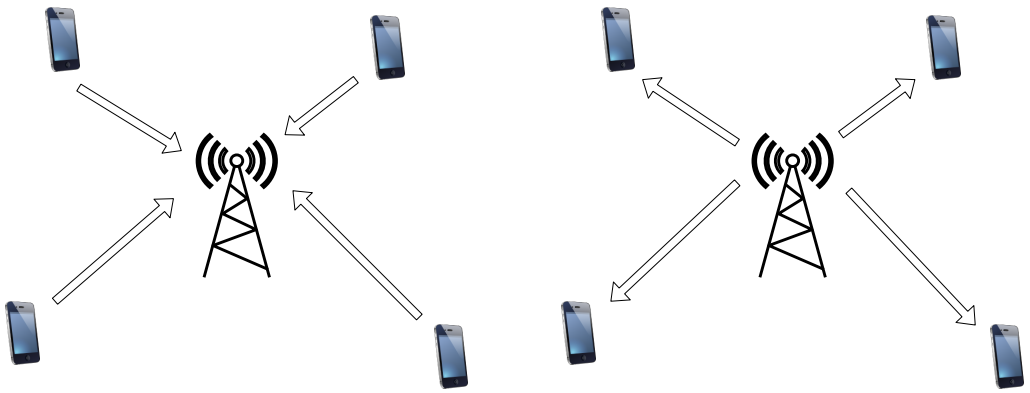

(a) Uplink channel. (b) Downlink channel.

Figure 1.1. Uplink and downlink channels.

Downlink channel also known as broadcast channel, one transmitter transmits its signal to many receivers. In contrast to it, many transmitters send their signal to one receiver in uplink. For both systems, since multiple users share same medium in order for data transfer (this medium is air for mobile communication) their signals have to be separated somehow. These separations techniques are called as Multiple Access (MA) [4]. If the separated resource blocks can be detected without any interference from each others, it is named as Orthogonal Multiple Access. Main OMA techniques are Frequency Division Multiple Access (FDMA), Time Division Multiple Access (TDMA) and Code Division Multiple Access (CDMA). In FDMA, resource blocks are divided along the frequency dimension. Each users use non-overlapping (i.e. orthogonal) different frequency blocks as in figure 1.2(a). TDMA system provides distinct time slot (or resource blocks) to communicate for each users. Figure 1.2(b) shows

to the main idea of the system. Although users shares same frequency band, they receive and transmit data at different time instances. CDMA brings a new dimension which can be named as code domain among time and frequency. Orthogonal, more precisely orthonormal codes are used to distinguish different users' signal from each others (see figure 1.2(c)).

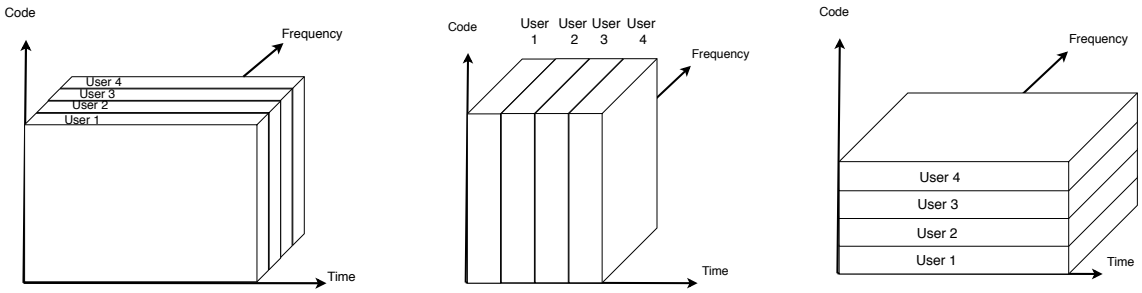

(a) FDMA Structure. (b) TDMA Structure. (c) CDMA Structure.

Figure 1.2. Main OMA Structures.

1.2. Non-Orthogonal Multiple Access (NOMA)

Non-Orthogonal Multiple Access is a multiple access technique in which dedicated channel resource blocks are not orthogonal to each other. For instance, if these non-orthogonality is realized in frequency domain this situation can be visualized as figure 1.3(b). User 1 and 2 shares same bandwidth as opposed to OMA in figure 1.3(a). They can be distinguished at receiver side thanks to their power level differences. Therefore it can be said that NOMA introduces a new domain and it is called as power domain [5].

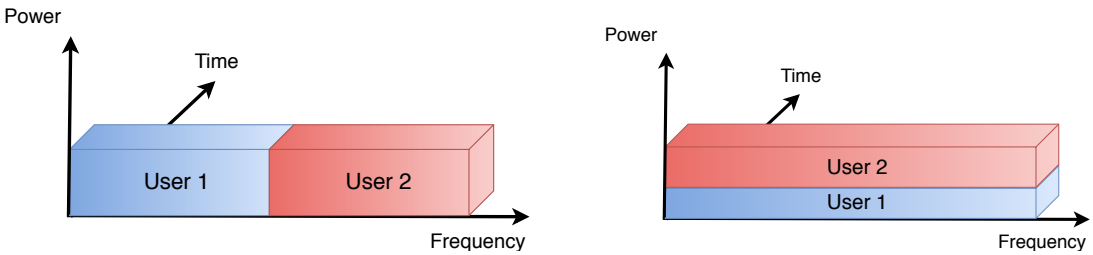

(a) OMA structure. (b) NOMA structure.

Figure 1.3. Basic illustration of the OMA vs NOMA.

Main reason of the NOMA usage is supporting higher mobile users than the number of the resource blocks [2]. The cost is receiver complexity and the increase of

the calculation cost. For instance in order to detect the signals of the user 1 and 2 in figure 1.3(b) first of all user 2's signal should be detected. In this step, user 1's signal is an interferer for user 2. Then detected user 2 signal is subtracted from received one and user 1 signal is detected from this subtraction. It is called as Successive Interference Cancellation (SIC). Difference between users' power is very important for this NOMA concept and it makes power control highly critical. This point can be written into negative aspect of NOMA.

1.3. Multi-Carrier Modulation

In wireless communication, due to multipath fading, a received symbol can be interfered with subsequent symbols. This distortion is named as inter symbol interference (ISI). From frequency domain perspective this phenomena known as frequency selective fading. If the channel is thought as a finite impulse response filter, it can restrain some specific frequencies of the signal. When data is transmitted with only one carrier, even if small portion of the its frequency is faded by channel, whole data is distorted. However if same data is sent by multiple carrier with lower bandwidth (total bandwidth remains same), channel response becomes relatively flat according to new narrow carrier spectrum as seen in figure 1.4(a) and 1.4(b). This method called as Multi-Carrier Modulation. Because symbols are modulated over multiple carriers.

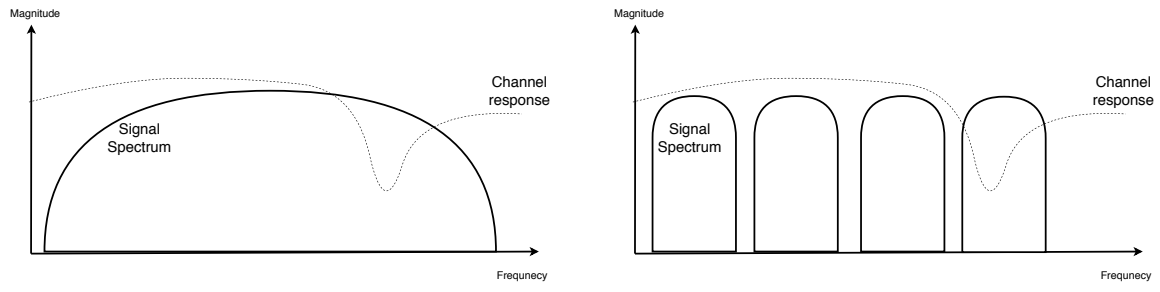

(a) Single Carrier Transmission. (b) Multi-Carrier Transmission.

Figure 1.4. Multi-Carrier Modulation.

1.4. Orthogonal Frequency Division Multiple Access (OFDMA)

Orthogonal Frequency Division Multiple Access or OFDMA is a type of multiple access technique which is based on a discrete implementation of the multi-carrier modulation. It is known as Orthogonal Frequency Division Multiplexing (OFDM). Before OFDMA, OFDM concept should be explained.

Since OFDM is an implementation of the multi-carrier modulation, it includes multiple carriers. First important property of the OFDM is that their frequency blocks are orthogonal however they overlap with each others. This point is the important differences of OFDM and FDMA. Because of the guard bands between consecutive carriers in FDMA as seen in 1.5(a) OFDM is more efficient for the perspective of the band usage than FDMA.

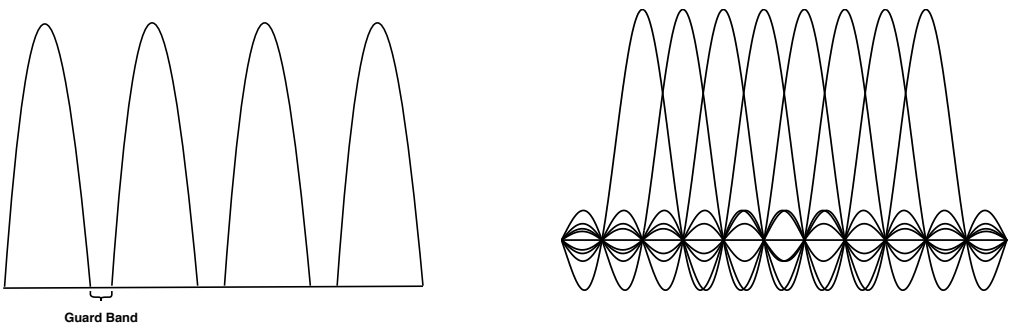

(a) FDMA carriers. (b) OFDM carriers.

Figure 1.5. Overlapped but Orthogonal OFDM carriers.

Another key feature of the OFDM is producing multiple carriers with single up-converter. It is realized by IFFT and digital to analog converter as seen in figure 1.6(a) and 1.6(b). Output of the both figures are same.

In OFDMA, sub-carriers which are produced by OFDM are assigning to different users [6]. These sub-carriers are also separated in time domain like TDMA. It provides more flexibility for channel assignment. As a result, more than one user can communicate via air medium thanks to OFDMA.

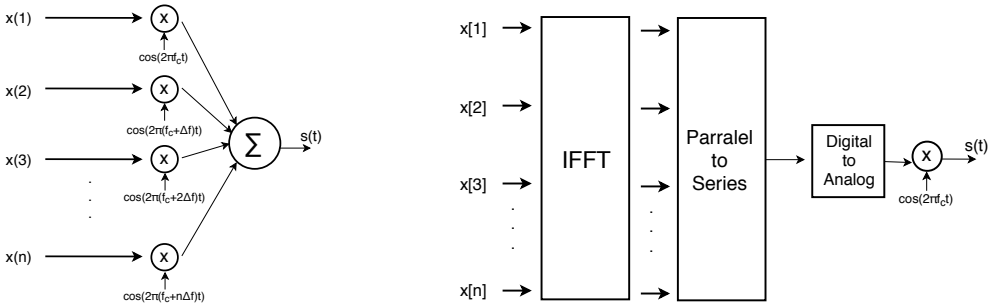

(a) With multiple up-converter.

(b) With single up-converter.

Figure 1.6. Producing multiple carriers with single and multi up-converters.

1.5. Multi-Carrier Code Division Multiple Access (MC-CDMA)

MC-CDMA is like classical CDMA however each chip of the direct sequence spread data symbol is transmitted with different OFDM sub-carriers in parallel [7]. Figure 1.7 illustrates MC-CDMA structure. Here $[c_1,\ c_2,\ ...c_8]$ are code sequence and s is symbol.

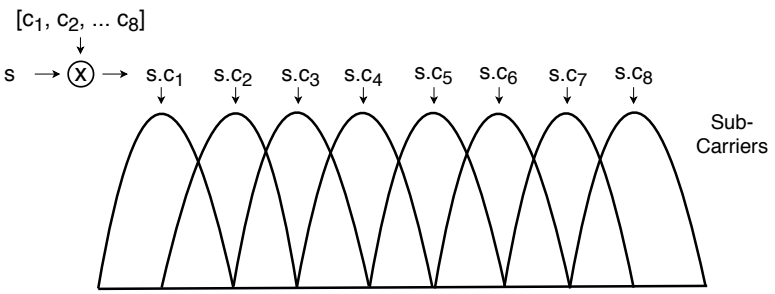

Figure 1.7. Structure of the MC-CDMA.

The other users also transmits their spread symbols onto same sub-carriers. Therefore n^{th} sub-carrier includes n^{th} chips of the all users. Codes are orthogonal to each others hence users' symbol can be detected without any interference.

1.6. Channel Capacity

Channel capacity is the maximum bit number per channel use (or per second) in which information can be sent with low error [8]. It can be thought as theoretical

maximum speed of a communication system. Capacity of the additive white Gaussian channel (AWGN) is given as

$$C = \frac{1}{2}\log\left(1 + \frac{P}{N}\right) \tag{1.1}$$

bits per channel use. C is channel capacity, P is average symbol power and N is the noise power.

In real life, wireless communication is realized over specific band intervals i.e. channel is band limited. Assume that bandwidth is W. According to Nyquist theory, there should be $2W$ samples in a second. The power spectral density (power per frequency) of the noise is $N_0/2$. In T seconds signal energy $T \cdot P$ and sample number becomes $T \cdot 2W$. Then signal energy per sample is $T \cdot P/(T \cdot 2W) = P/2W$. Since signal is real, its frequency domain representation has to be symmetric according to y-axis. Therefore if a channel bandwidth is W, it must have same frequency interval at negative part. For this reason noise power is $2W \cdot N_0/2 = W \cdot N_0$. In this situation, noise energy in time interval T is $T \cdot W \cdot N_0$ and noise energy per sample $T \cdot W \cdot N_0/(T \cdot 2W) = N_0/2$. If signal energy per sample and noise energy per sample are added to equation (1.1),

$$C = \frac{1}{2}\log\left(1 + \frac{\frac{P}{2W}}{N_0/2}\right) = \frac{1}{2}\log\left(1 + \frac{P}{N_0 W}\right) \tag{1.2}$$

bits per sample. Since there are $2W$ samples in one second channel capacity is,

$$C = 2W \cdot \frac{1}{2}\log\left(1 + \frac{P}{N_0 W}\right) = W\log\left(1 + \frac{P}{N_0 W}\right) \tag{1.3}$$

bits per second.

1.7. Iterative Successive Interference Cancellation (Iterative SIC)

SIC is based on the idea that in a multiuser detection process, if users' signals are interfering with each other, detected symbols are subtracted from received signal

in order to remove interference [9]. For instance in a NOMA system received signal is $s_1 + s_2 + n$ where s_1 and s_2 are users' symbols and n is additive noise. Assume symbol power s_1 is greater than s_2. First s_1 is detected while s_2 is treated as a Gaussian noise then $\hat{s}_1$ is subtracted from received signal. This subtraction is used to detect s_2. Up to this point described system is classical SIC and it can be seen as first step of the iterative SIC. In order to increase precision this process can be continued. Detected $\hat{s}_2$ is subtracted from received signal and $\hat{s}_1$ is updated. Then new $\hat{s}_1$ is subtracted and $\hat{s}_2$ is detect again. It is the second iteration of the iterative SIC and it is described in [3]. Detection iterations can continue as many steps as needed.

1.8. Multi-User Detection

Multi-user and single-user detections are detection techniques in which received symbols are map onto possible symbols sequences [9]. Difference between them is that in single-user detection, only channel state information of the detected user is used however in multi-user detection channel state informations of the all users are used to detect any user. Therefore the performance of the multi-user detection technique is higher than single-user.

1.9. Rayleigh Channel Model

In real life because of the Doppler effect and multi-path spread, a wireless channel can act as time-variant filter [10]. In discrete time domain, this channel characterization can be shown as,

$$Y[m] = \sum_{l} H[l]X[m-l] + U[m] \tag{1.4}$$

where Y is received, X is transmitted signal, H is channel impulse responses' tap and U is corresponding noise. According to probabilistic model of the channel taps H, different discrete channel models are occurred. In the absence of the line of sight or dominant component, one of the simplest and common model is Rayleigh in which

magnitude of the channel taps are Rayleigh distributed random variables.

Statistical characteristic of Rayleigh channel in frequency domain should be investigated in order to clarify some points for OFDMA system's behavior in Rayleigh channel. Assume equation (1.4) represents an OFDM system. After removing cyclic prefix and inverse Fourier transform equation (1.4) turns into,

$$y[m] = h[m]x[m] + u[m]. \tag{1.5}$$

Regardless of the taps' number of the channel impulse response in time domain, if frequency and time inter-leaver with sufficient interleaving depth is applied, fading on adjacent data symbols after inverse Fourier transform and de-interleaving can be assumed uncorrelated Rayleigh distributed random variables as stated in [7]. This channel model is named as uncorrelated Rayleigh channel. Channel coefficient h is a complex number and it is,

$$h = \alpha \cdot e^{j\theta} \tag{1.6}$$

where α is fading magnitude and it is generated by a Rayleigh distribution and θ is phase which is uniformly distributed between $[0,\ 2\pi)$. If fading coefficients are same for OFDMA sub-carriers during a symbol period, then channel is called as non-frequency selective Rayleigh or Rayleigh flat fading channel. However if channel coefficient is varied sub-carrier to sub-carrier it is called as frequency selective Rayleigh channel.

2. NON-ORTHOGONAL MULTIPLE ACCESS

2.1. Channel Capacity of NOMA

2.1.1. Downlink

Assume that there are only two mobile users. Transmitted signal is $\sqrt{P_1}s_1+\sqrt{P_2}s_2$ where s_1 and s_2 are symbols of the user 1 and 2 with power P_1 and P_2 respectively. Received signal for i^{th} user is,

$$y_i = h_i x + n_i, \tag{2.1}$$

where h_i is the channel coefficient and n_i is the noise of i^{th} user. x is transmitted signal $\sqrt{P_1}s_1 + \sqrt{P_2}s_2$. Assume first 2. user is decoded. 2. user symbol is subtracted from received signal and then 1. user is tried to be detected. If channel bandwidth is 1, power spectral density of noise is same for both users N_0 and there is no error at the detection of 2. user, channel capacities are

$$\begin{aligned} R_1 &= \log_2\Big(1 + \frac{|h_1|^2 \cdot P_1}{N_0}\Big), \\ R_2 &= \log_2\Big(1 + \frac{|h_2|^2 \cdot P_2}{|h_2|^2 \cdot P_1 + N_0}\Big), \end{aligned} \tag{2.2}$$

bits per second per Hertz according to equation (1.3). If the total signal power is P, P_1 and P_2 can be expressed as $P \cdot \alpha$ and $P \cdot (1-\alpha)$ where $\alpha \in [0,\ 1]$ respectively. Equation (2.2) turns into

$$\begin{aligned} R_1 &= \log_2\Big(1 + \frac{|h_1|^2 \cdot P\alpha}{N_0}\Big), \\ R_2 &= \log_2\Big(1 + \frac{|h_2|^2 \cdot P(1-\alpha)}{|h_2|^2 \cdot P\alpha + N_0}\Big). \end{aligned} \tag{2.3}$$

Channel capacity of the NOMA is greater than the corresponding OMA system [11]. To make fair comparison, total signal power in the OMA system should be P, total bandwidth is 1 and power spectral density of noise is N_0 for both users. If bandwidth of the user 2 is $\beta \in [0,\ 1]$, channel capacities of the OMA are

$$\begin{aligned} R_1 &= (1-\beta)\cdot \log_2\left(1+\frac{|h_1|^2\cdot P\alpha}{(1-\beta)\cdot N_0}\right), \\ R_2 &= \beta\cdot \log_2\left(1+\frac{|h_2|^2\cdot P(1-\alpha)}{\beta\cdot N_0}\right). \end{aligned} \tag{2.4}$$

Assume $P = 1$, $N_0 = 0.1$ and $h_1 = h_2 = 1$. When α in equation (2.3) is tuned from 0 to 1, channel capacity of the user 1 and 2 in NOMA are shown in 2.1(a). At the same figure, OMA capacities are also illustrated. As seen in equation (2.4) there are two parameters that effects the capacity. These are β and α, i.e. the bandwidth and power allocation between users 1 and 2. For a fixed α, β is altered from 0 to 1 and one of the blue lines at the below figure is obtained. This process is repeated for different

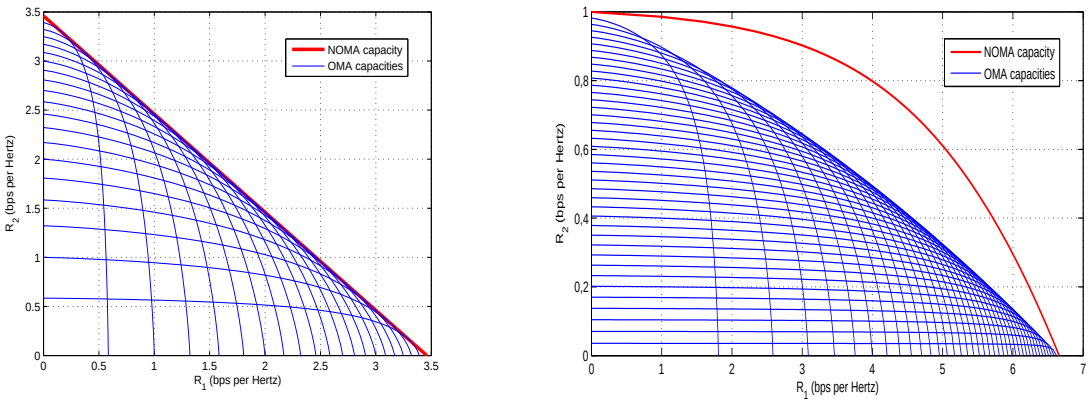

(a) $|h_1|^2 = |h_2|^2 = 1$. (b) $|h_1|^2 = 10$, $|h_2|^2 = 0.1$.

Figure 2.1. Downlink channel capacities of the NOMA and OMA.

α values. As a result only for a specific pair of β and α, OMA capacity caught NOMA only on a single point. However NOMA capacity, regardless of the power allocation between users always on the optimal line.

Now consider a flat fading channel. Assume $|h_1|^2 = 10$ and $|h_2|^2 = 0.1$. Rest of the values are same with AWGN channel scenario. According to this situation, NOMA

capacity with SIC are superior than OMA as seen in figure 2.1(b).

As a result of the figure 2.1(a) and 2.1(b) it can be said that, when the channel conditions betweens users are same, OMA can catch NOMA capacity performance only on a specific power and band allocation. However when the channel gain differences between users are increase, NOMA capacity becomes greater than OMA.

2.1.2. Uplink

In the uplink system received signal y is

$$y = h_1 x_1 + h_2 x_2 + n \tag{2.5}$$

where x_1 is $\sqrt{p_1}s_1$ and x_2 is $\sqrt{p_2}s_2$. Note that $|s_i|^2 = 1$ for $i = 1,\ 2$. Bandwidth is 1, noise spectral density is $N_0/2$ and total signal power is P i.e. $P_1 + P_2 = P$. The first thing it can be observed that any user capacity cannot exceed the capacity with single user regardless of the decoding order [8]. For instance in the absence of user 2, received signal is $h_2 x_2 + n$ and in this situation achievable maximum rate is $\log_2\left(1 + P_2/N_0\right)$. In the same manner maximum rate for user 1 is $\log_2\left(1 + P_1/N_0\right)$. This situation is formulated as

$$\begin{aligned} R_1 &\leq \log_2\Big(1 + \frac{|h_1|^2 \cdot P_1}{N_0}\Big), \\ R_2 &\leq \log_2\Big(1 + \frac{|h_2|^2 \cdot P_2}{N_0}\Big). \end{aligned} \tag{2.6}$$

If user 1 is decoded firstly capacities become

$$\begin{aligned} R_1 &= \log_2\Big(1 + \frac{|h_1|^2 \cdot P_1}{|h_2|^2 \cdot P_2 + N_0}\Big), \\ R_2 &= \log_2\Big(1 + \frac{|h_2|^2 \cdot P_2}{N_0}\Big). \end{aligned} \tag{2.7}$$

If user 2 is decoded at first capacities are

$$\begin{aligned} R_1 &= \log_2\Big(1+\frac{|h_1|^2\cdot P_1}{N_0}\Big), \\ R_2 &= \log_2\Big(1+\frac{|h_2|^2\cdot P_2}{|h_1|^2\cdot P_1+N_0}\Big). \end{aligned} \tag{2.8}$$

Total capacity in the equation (2.7) is

$$\begin{aligned} R_1+R_2 &= \log_2\Big(1+\frac{|h_1|^2\cdot P_1}{|h_2|^2\cdot P_2+N_0}\Big)+\log_2\Big(1+\frac{|h_2|^2\cdot P_2}{N_0}\Big) \\ &= \log_2\Big(\Big[1+\frac{|h_1|^2\cdot P_1}{|h_2|^2\cdot P_2+N_0}\Big]\cdot\Big[1+\frac{|h_2|^2\cdot P_2}{N_0}\Big]\Big) \\ &= \log_2\Big(1+\frac{|h_1|^2\cdot P_1}{|h_2|^2\cdot P_2+N_0}+\frac{|h_2|^2\cdot P_2}{N_0}+\frac{|h_1|^2\cdot P_1}{|h_2|^2\cdot P_2+N_0}\cdot\frac{|h_2|^2\cdot P_2}{N_0}\Big) \\ &= \log_2\Big(1+\frac{|h_1|^2\cdot P_1\cdot(|h_2|^2\cdot P_2+N_0)+|h_2|^2\cdot P_2\cdot(|h_2|^2\cdot P_2+N_0)}{(|h_2|^2\cdot P_2+N_0)\cdot N_0}\Big) \\ &= \log_2\Big(1+\frac{|h_1|^2\cdot P_1+|h_2|^2\cdot P_2}{N_0}\Big). \end{aligned} \tag{2.9}$$

In the second scenario in which capacities are given in equation (2.8), total capacity is

$$\begin{aligned} R_1+R_2 &= \log_2\Big(1+\frac{|h_1|^2\cdot P_1}{N_0}\Big)+\log_2\Big(1+\frac{|h_2|^2\cdot P_2}{|h_1|^2\cdot P_1+N_0}\Big) \\ &= \log_2\Big(\Big[1+\frac{|h_1|^2\cdot P_1}{N_0}\Big]\cdot\Big[1+\frac{|h_2|^2\cdot P_2}{|h_1|^2\cdot P_1+N_0}\Big]\Big) \\ &= \log_2\Big(1+\frac{|h_1|^2\cdot P_1}{N_0}+\frac{|h_2|^2\cdot P_2}{|h_1|^2\cdot P_1+N_0}+\frac{|h_1|^2\cdot P_1}{N_0}\cdot\frac{|h_2|^2\cdot P_2}{|h_1|^2\cdot P_1+N_0}\Big) \\ &= \log_2\Big(1+\frac{|h_1|^2\cdot P_1\cdot(|h_1|^2\cdot P_1+N_0)+|h_2|^2\cdot P_2\cdot(|h_1|^2\cdot P_1+N_0)}{N_0\cdot(|h_1|^2\cdot P_1+N_0)}\Big) \\ &= \log_2\Big(1+\frac{|h_1|^2\cdot P_1+|h_2|^2\cdot P_2}{N_0}\Big). \end{aligned} \tag{2.10}$$

As seen in equations (2.9) and (2.10), regardless of the decoding order, total capacity is same and optimum. Because $|h_1|^2\cdot P_1+|h_2|^2\cdot P_2$ is total received power and according to equation (1.3) total capacity cannot exceed $W_{tot}\cdot\log_2\left(1+\frac{P_{tot}}{W_{tot}\cdot N_0}\right)$ where W_{tot} is total bandwidth and P_{tot} is total power. However there are some restrictions

on this optimum region for static power allocation that states in equation (2.6). If this result is combined with (2.6) we gets

$$\begin{aligned} R_1 &\leq \log_2\left(1+\frac{|h_1|^2\cdot P_1}{N_0}\right) \\ R_2 &\leq \log_2\left(1+\frac{|h_2|^2\cdot P_2}{N_0}\right) \\ R_1+R_2 &\leq \log_2\left(1+\frac{|h_1|^2\cdot P_1+|h_2|^2\cdot P_2}{N_0}\right). \end{aligned} \tag{2.11}$$

On contrary OMA capacity in uplink system is straightforward:

$$\begin{aligned} R_1 &= (1-\beta)\cdot\log_2\left(1+\frac{|h_1|^2\cdot P_1}{(1-\beta)\cdot N_0}\right), \\ R_2 &= \beta\cdot\log_2\left(1+\frac{|h_2|^2\cdot P_2}{\beta\cdot N_0}\right). \end{aligned} \tag{2.12}$$

where β is bandwidth of the user 2 and it is between 0 and 1. When $P_1 = P_2 = 0.5$, $N_0 = 0.1$, channel is AWGN (i.e. $|h_1|^2 = |h_2|^2 = 1$) and β is changed from 0 to 1, figure 2.2(a) is obtained.

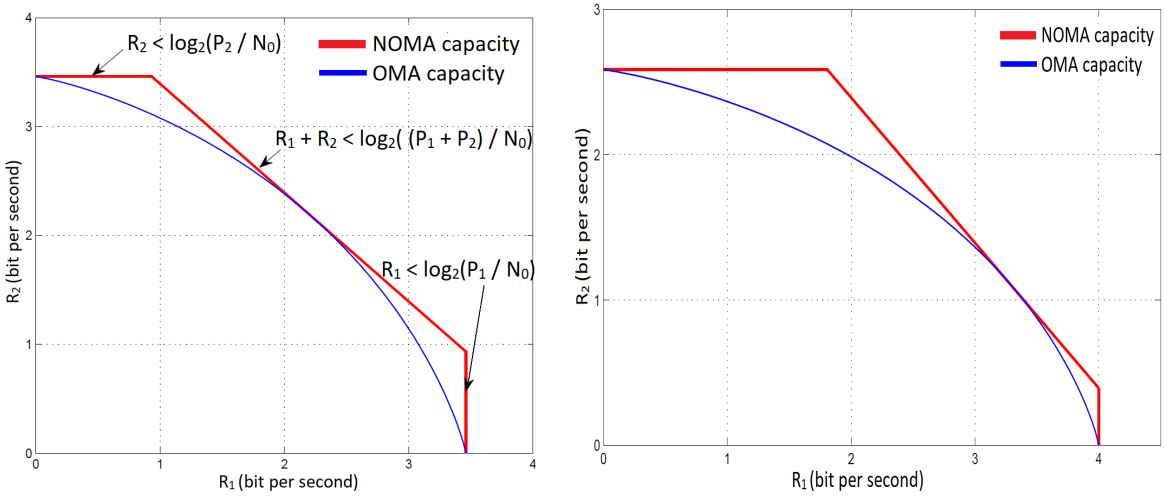

(a) $|h_1|^2 = |h_2|^2 = 1$, $N_0 = 0.1$ and $P_1 = P_2 = 0.5$.

(b) $|h_1|^2 = 2$, $|h_2|^2 = 0.5$, $N_0 = 0.1$ and $P_1 = P_2 = 0.5$.

Figure 2.2. Uplink channel capacities of the NOMA and OMA.

According to figure 2.2(a), capacity of the OMA only catch the NOMA capacity on a single point. In fading case this situation does not change. For instance if $|h_1|^2$ is

2 and $|h_2|^2$ is 0.5, then NOMA and OMA capacities follows to same features as shown in figure 2.2(b)

2.2. Existing NOMA Techniques

Several NOMA techniques were proposed until today. Power domain NOMA [5, 12], sparse code multiple access [13], pattern division multiple access [14] and multi-user shared access [15] are the examples of the proposed NOMA techniques. These NOMA concepts can be categorized in different ways. In [16], NOMAs are divided into two main groups which are single and multi-carrier NOMA. However in this thesis, existing NOMA techniques will be divided into two main groups as done in [2]. These groups are called as code domain NOMA (such as [13, 17–19]) and power domain NOMA (such as [20–23]). In addition to these, there are two more NOMA concepts as frequency domain and time domain NOMA that will be introduced in this chapter [24].

2.2.1. Power Domain NOMA

In power domain NOMA, users' informations are transmitted through same time slot, frequency bandwidth or spreading code but different power levels. Multiple access i.e. decomposing users' signal is realized thanks to this power differences. For this reasons power allocation between users are very critical. From information theoretical perspective, in order for optimality of the channel capacity, users with better channel state conditions are allocated less power at downlink [25]. According to power allocation policy there are different power domain NOMA systems such as cognitive radio NOMA. In this NOMA schemes some or all of the users' quality of service (QoS) requirements must be satisfied [16].

2.2.2. Code Domain NOMA

In code domain NOMA, multiple users are transmitted through same time and frequency slot with different codes. Number of the users are greater than length of the code or spreading sequence. Low-density signature CDMA (LDS-CDMA), low-

density signature OFDM (LDS-OFDM) and sparse code multiple access (SCMA) are the examples of code domain NOMA [25]. Low-density signature is a type of code sequence which includes lots of zero (low density comes from existing of zeros). The aim of becoming low-density or including many zeros is to decrease multiuser detection complexity. For example 9 chip sequences with length 6 are given as [26],

$$\mathbf{S}_{6,9} = \begin{pmatrix} 0 & 0 & a_0 & 0 & 0 & 0 & a_1 & 0 & a_2 \\ 0 & a_0 & 0 & a_1 & 0 & 0 & a_2 & 0 & 0 \\ 0 & 0 & a_0 & a_1 & 0 & a_2 & 0 & 0 & 0 \\ a_0 & 0 & 0 & 0 & a_1 & 0 & 0 & 0 & a_2 \\ a_0 & 0 & 0 & 0 & 0 & a_1 & 0 & a_2 & 0 \\ 0 & a_0 & 0 & 0 & a_1 & 0 & 0 & a_2 & 0 \end{pmatrix} \tag{2.13}$$

where $a_k = e^{j\frac{2\pi}{3}k}$. Each columns of the matrix $\mathbf{S}_{6,9}$ represents a different spread sequence. In LDS-CDMA this chip sequences are located on different time slots and in LDS-OFMD each distinct sequence of a code is mapped into OFDM sub-carriers like MC-CDMA. It can be said that LDS-OFDM is multi-carrier version of the LDS-CDMA.

2.2.3. Time Domain NOMA

In time domain NOMA, users' signals are transmitted, same frequency and spread sequence, different but overloaded time slots. Example of this type NOMA is given in [3] and [24]. It is simply superimposing CDMA and TDMA as seen in figure 2.3. In this figure there are N time slots with duration T_c and each of them is a different TDMA resource block. On the other hand, one chip of a CDMA code sequence is overlaying one time slots. Hence for instance third TDMA resource block and third chip of the all CDMA sequences are conflicted. If orthonormal (orthogonal with unit magnitude) code block Walsh-Hadamard (WH) is used for CDMA users, they becomes orthogonal with each others. Now CDMA and TDMA are orthogonal to themselves however non-orthogonal against each other. Since CDMA symbols are normalized its instantaneous power is $1/N$ times TDMA power. Both CDMA and TDMA symbols' energy are same and it is equals to $N \cdot P \cdot T_c$. As it can be seen there is no need to

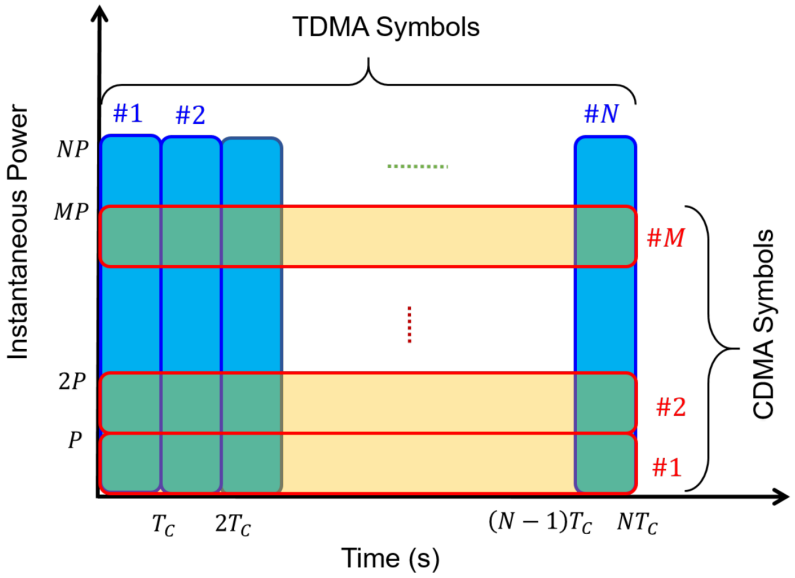

Figure 2.3. Illustration of the time domain NOMA with TDMA and CDMA combination.

power balance between users.

2.2.4. Frequency Domain NOMA

Users in this type NOMA shares same time and code domain but overloaded frequency slots. This type of NOMA described in [3], [24] and [27]. It is like time domain NOMA, however instead of TDMA and CDMA, OFDMA and MC-CDMA are combined respectively.

Every OFDMA sub-carrier is taken by one OFDMA user and one of the corresponding m MC-CDMA users' chip. According to figure 2.4 one sub-carrier has $1/(NT)$ Hz bandwidth. Power spectrum densities are $N \cdot D$ and D for OFDMA and MC-CDMA respectively. Hence total power is same for both modulation type and it is equals to N/T. As a result power allocation is not required.

This NOMA concept has some advantages over time domain NOMA. It is compatible with 4G since it is based on OFMDA technology. Therefore in this thesis frequency domain NOMA will be investigated in detail.

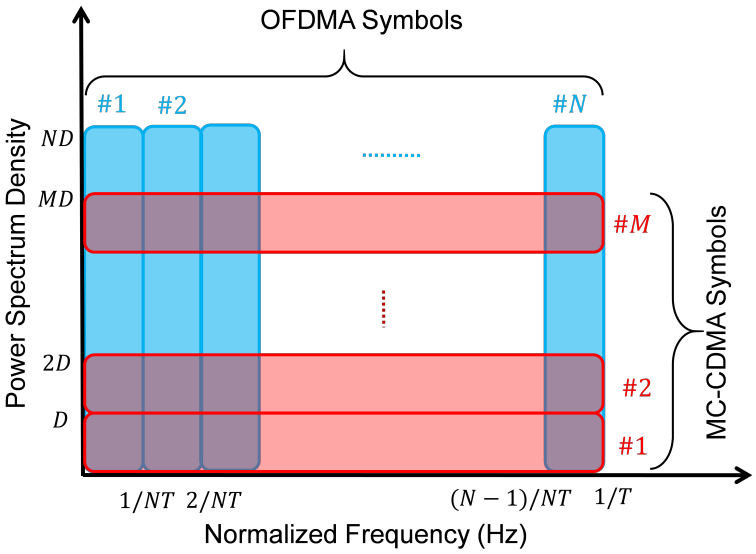

Figure 2.4. Illustration of the frequency domain NOMA with OFDMA and MC-CDMA combination.

To sum up, non-orthogonal multiple access is more efficient that orthogonal multiple access in terms of channel capacity for both uplink and downlink. In addition to that NOMA concepts can be divided into four main groups in which non-orthogonality is realized in different domains.

3. FREQUENCY DOMAIN NOMA: CLOSER LOOK

As stated before, frequency domain NOMA can be easily adopted to 4G technology which is based on OFDMA. There will be introduced two types of the frequency domain NOMA as NOMA 2000 and channel overloading NOMA. Detection mechanisms will be also given and their bit error rate performances will be demonstrated.

3.1. NOMA 2000

First frequency domain NOMA concept is introduced at [24] in year 2000 therefore it can be called as NOMA 2000. Its principal is visualized in figure 2.4. For transmitted signal in AWGN channel, if n^{th} sub-carrier where $n = 1,\ 2,\ \cdots,\ N$ is shown as x_n, it is equals to

$$x_n = a_n + \frac{1}{\sqrt{N}} \sum_{m=1}^{M} w_{m,n} b_m + u_n \tag{3.1}$$

in which a_n is n^{th} OFDMA symbol, b_m is m^{th} MC-CDMA symbol, $w_{m,n}$ is n^{th} chip of the m^{th} WH code sequence and u_n is corresponding noise. $1/\sqrt{N}$ provides normalization since $w_{m,n}$ is either 1 or -1.

Detection process start with a_n. Let assume detected a_n is denoted with $\hat{a}_n$ and it is detected without error. Then $\hat{a}_n$ is subtracted from x_n and if resulted signal is demonstrated by y_n, it is equals to

$$\begin{aligned} y_n &= a_n - \hat{a}_n + \frac{1}{\sqrt{N}} \sum_{m=1}^{M} w_{m,n} b_m + u_n, \\ &= \frac{1}{\sqrt{N}} \sum_{m=1}^{M} w_{m,n} b_m + u_n. \end{aligned} \tag{3.2}$$

This operation is realized for every possible n values which range from 1 to N. After that MC-CDMA symbols are detected. Assume in order to detect k^{th} MC-CDMA user

where $k = 1,\ 2,\ \cdots,\ M$; subtracted signal is despreaded by corresponding WH code sequence. If despreaded symbol is shown by z_k,

$$\begin{aligned} z_k &= \frac{1}{\sqrt{N}} \sum_{n=1}^{N} w_{k,n} y_n \\ &= \frac{1}{\sqrt{N}} \sum_{n=1}^{N} w_{k,n} \left(\frac{1}{\sqrt{N}} \sum_{m=1}^{M} w_{m,n} b_m + u_n \right) \\ &= b_k + \frac{1}{\sqrt{N}} \sum_{n=1}^{N} w_{k,n} u_n. \end{aligned} \tag{3.3}$$

According to equation (3.3) new noise is $\frac{1}{\sqrt{N}} \sum_{n=1}^{N} w_{k,n} u_n$. Its power found as

$$\begin{aligned} E\Big[\big(\frac{1}{\sqrt{N}} \sum_{n=1}^{N} w_{k,n} u_n \big)^2 \Big] &= E\Big[\big(\frac{1}{\sqrt{N}} \sum_{n=1}^{N} w_{k,n} u_n \big) \cdot \big(\frac{1}{\sqrt{N}} \sum_{t=1}^{N} w_{k,t} u_t \big) \Big] \\ &= \frac{1}{N} \sum_{n=1}^{N} \sum_{t=1}^{N} w_{k,n} w_{k,t} \cdot E[u_n u_t] \\ &\overset{(a)}{=} \frac{1}{N} \sum_{n=1}^{N} w_{k,n}^2 \cdot E[u_n u_n] \\ &\overset{(b)}{=} \frac{1}{N} \sum_{n=1}^{N} E[u_n^2] \\ &= E[u_n^2] \end{aligned} \tag{3.4}$$

where step (a) comes from that noises are uncorrelated for different sub-carriers i.e. $E[u_n u_t] = 0$ if $n \neq t$. The reason of the step (b) is that $w_{k,n}$ is either 1 or -1. As it can be seen in equation (3.4), noise power hence signal to noise ration (SNR) does not change. The matrix representation of the equation (3.1) and (3.2) are

$$\begin{aligned} \vec{x} &= \vec{a} + (1/\sqrt{N}) \cdot W \cdot \vec{b} + \vec{u} \\ \vec{y} &= \vec{x} - \hat{\vec{a}} \end{aligned} \tag{3.5}$$

respectively. Vector $\vec{x}$ is $[x_1,\ x_2,\ \cdots,\ x_N]^T$, vector $\vec{a} = [a_1,\ a_2,\ \cdots,\ a_N]^T$, in the same manner vector $\hat{\vec{a}} = [\hat{a}_1,\ \hat{a}_2,\ \cdots,\ \hat{a}_N]^T$, vector $\vec{b}$ is $[b_1,\ b_2,\ \cdots,\ b_M]^T$ and $\vec{u}$ is $[u_1,\ u_2,\ \cdots,\ u_N]^T$ where operation $.^T$ is transpose (not conjugate transpose) of a vector or matrix. Matrix W is Hadamard matrix with dimension $N \times M$ and its element $w_{q,p}$ locates on q^{th} row and p^{th} column. This matrix is demonstrated as,

$$W = \begin{bmatrix} w_{1,1} & w_{1,2} & ..... & w_{1,M} \\ w_{2,1} & w_{2,2} & ..... & w_{2,M} \\ \vdots & \vdots & \ddots & \vdots \\ w_{N,1} & w_{N,2} & ..... & w_{N,M} \end{bmatrix}_{N \times M} \tag{3.6}$$

Notice that $[(1/\sqrt{N}) \cdot W]^T \cdot [(1/\sqrt{N}) \cdot W]$ gives $M \times M$ identity matrix. Then equation (3.3) can be shown as

$$\begin{aligned} \vec{z} &= \big[\frac{1}{\sqrt{N}} W\big]^T \vec{y} \\ &= \big[\frac{1}{\sqrt{N}} W\big]^T \cdot \big[\frac{1}{\sqrt{N}} W \cdot \vec{b} + \vec{u}\big] \\ &= I \cdot \vec{b} + \frac{1}{\sqrt{N}} W^T \cdot \vec{u} \\ &= \vec{b} + \vec{u}'. \end{aligned} \tag{3.7}$$

As stated in equation (3.4), variance or noise power of the $\vec{u}'$ is same with $\vec{u}$.

3.1.1. Detection

At the detection part, iterative SIC is used in order to increase precision of the detection. First step is detecting OFDMA symbol. Assume $T[.]$ is simple threshold detector function. Then,

$$\hat{\vec{a}}_1 = T[\vec{x}] \tag{3.8}$$

where $\vec{x}$ is received signal which is given in equation (3.5) and $\hat{\vec{a}}_1$ is detected OFDMA symbols at first step. MC-CDMA symbol detection at first step can be formulated as

$$\hat{\vec{b}}_1 = T\big[(1/\sqrt{N}) \cdot W^T \cdot (\vec{x} - \hat{\vec{a}}_1)\big]. \tag{3.9}$$

Above equation includes three process. First detected OFDMA symbols are subtracted from received signal $\vec{x} - \hat{\vec{a}}_1$. After that result is despreaded by $(1/\sqrt{N}) \cdot W^T$. Lastly despreaded signal is proceeded by a threshold detector.

Second step is different for OFDMA detection. First of all detected MC-CDMA symbols are re-spreaded and subtracted from received signal. Equation (3.10) shows this process,

$$\hat{\vec{a}}_2 = T\big[\vec{x} - (1/\sqrt{N}) \cdot W \cdot \hat{\vec{b}}_1\big]. \tag{3.10}$$

Multiplication $\hat{\vec{b}}_1$ with $(1/\sqrt{N}) \cdot W$ provides spreading. It is straightforward for MC-CDMA,

$$\hat{\vec{b}}_2 = T\big[(1/\sqrt{N}) \cdot W^T \cdot (\vec{x} - \hat{\vec{a}}_2)\big]. \tag{3.11}$$

As a result, for t^{th} step, iterative SIC process can be formulated as

$$\hat{\vec{a}}_t = T\big[\vec{x} - (1/\sqrt{N}) \cdot W \cdot \hat{\vec{b}}_{t-1}\big], \tag{3.12}$$

and

$$\hat{\vec{b}}_t = T\big[(1/\sqrt{N}) \cdot W^T \cdot (\vec{x} - \hat{\vec{a}}_t)\big]. \tag{3.13}$$

Figure 3.1 illustrates iterative SIC. Detection steps can be increased as many as needed. In this figure, it is assumed that signal is perfectly received at the end of the discrete Fourier transform block.

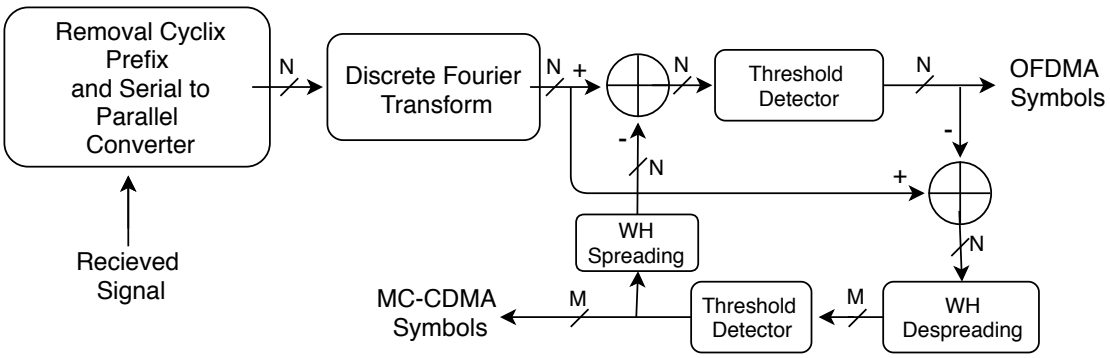

Figure 3.1. Block diagram of the iterative SIC receiver.

Another approach of the detection is using soft-decision detector which is described in [27] and [28] at subtraction process. It is a non-linear function and denoted with Ψ. In-phase and quadrature phase of the received signal is detected separately, for instance

$$\hat{a}_{soft} = \Psi[\Re(a)] + j \cdot \Psi[\Im(a)] \tag{3.14}$$

where $\Re(a)$ and $\Im(a)$ are real and imaginary part of the symbol a respectively. Assume 16-QAM modulated signal whose symbols are $\mp\{3,1\} \mp j\{3,1\}$ and its soft decision function given as

$$\Psi[k] = \begin{cases} +3, & k > 2+\lambda, \\ (k-2)/\lambda + 2, & 2+\lambda > k > 2-\lambda, \\ +1, & 2-\lambda > k > \lambda, \\ k/\lambda, & \lambda > k > -\lambda, \\ -1, & -\lambda > k > -2+\lambda, \\ (k+2)/\lambda - 2, & -2+\lambda > k > -2-\lambda, \\ -3, & -2-\lambda > k \end{cases} \tag{3.15}$$

where λ is soft detector coefficient and it is between 0 and 1. Notice that for $\lambda = 0$, $\Psi[.]$ turns into simple threshold detector. Figure 3.2 demonstrates soft decision output

that is given in equation (3.15) for $\lambda = 0.5$. As it can be seen when λ is increased, $\Psi[.]$ becomes softer and if $\lambda = 1$ functions turns into $\Psi[k] = k$ for $+3 > k > -3$.

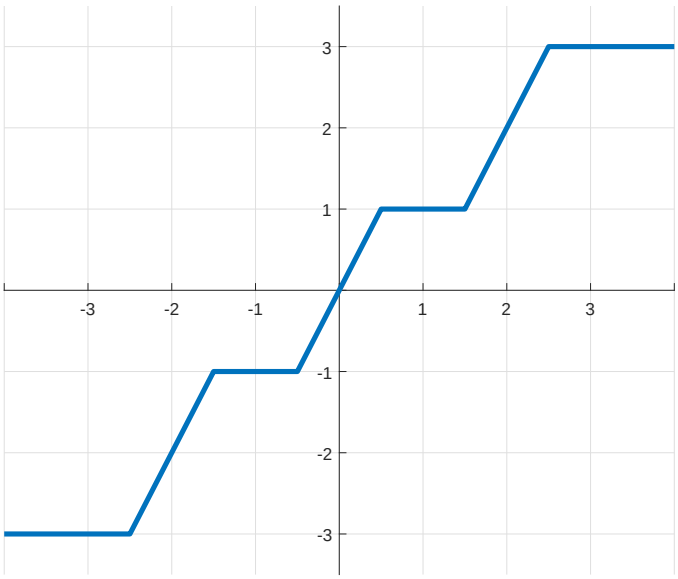

Figure 3.2. Output of the soft detector for the real part of a 16QAM modulated symbol. λ is 0.5.

Detection process of the symbols with soft decision detector similar with simple threshold detector. First step is

$$\begin{aligned} \hat{\vec{a}}_{1(s)} &= \Psi[\vec{x}] \\ \hat{\vec{b}}_{1(s)} &= \Psi[(1/\sqrt{N}) \cdot W^T \cdot (\vec{x} - \hat{\vec{a}}_{1(s)})] \end{aligned} \tag{3.16}$$

where $\vec{x}$ is received signal and it is given at (3.1). Second step,

$$\begin{aligned} \hat{\vec{a}}_{2(s)} &= \Psi[\vec{x} - (1/\sqrt{N}) \cdot W \cdot \hat{\vec{b}}_{1(s)}] \\ \hat{\vec{b}}_{2(s)} &= \Psi[(1/\sqrt{N}) \cdot W^T \cdot (\vec{x} - \hat{\vec{a}}_{2(s)})]. \end{aligned} \tag{3.17}$$

In the same manner t^{th} step given as,

$$\begin{aligned}\hat{\vec{a}}_{t(s)} &= \Psi[\vec{x} - (1/\sqrt{N}) \cdot W \cdot \hat{\vec{b}}_{t-1(s)}] \\ \hat{\vec{b}}_{t(s)} &= \Psi[(1/\sqrt{N}) \cdot W^T \cdot (\vec{x} - \hat{\vec{a}}_{t(s)})].\end{aligned} \tag{3.18}$$

Assume t^{th} step is last one. There is also one more process to convert soft symbols into hard one. It is realized by threshold detector $T[.]$ which is stated before and it can be shown as,

$$\begin{aligned}\hat{\vec{a}} &= T[\hat{\vec{a}}_{t(s)}] \\ \hat{\vec{b}} &= T[\hat{\vec{b}}_{t(s)}].\end{aligned} \tag{3.19}$$

Block diagram of the receiver structure with soft detector is given in figure 3.3. The difference between previous one is that instead of threshold detector soft decision detectors exist. There are also threshold detector at the end of the process additionally.

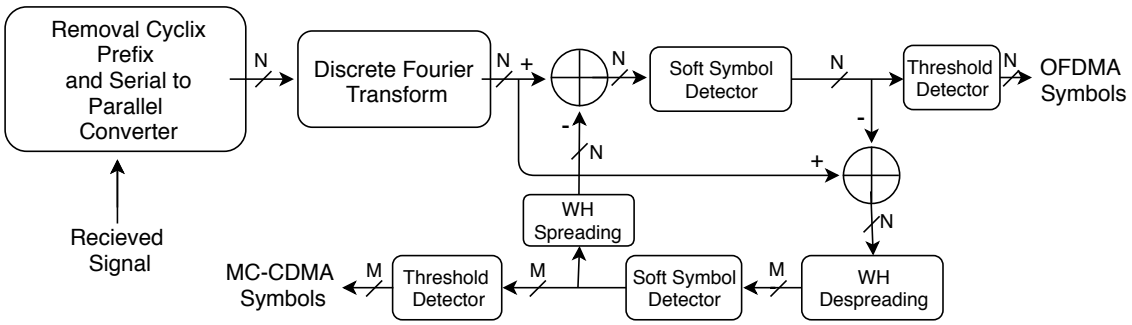

Figure 3.3. Block diagram of the iterative SIC receiver with soft decision detector.

3.1.2. Performance Results

Performances of the NOMA-2000 in AWGN channel are investigated for different modulation schemes and different detection types. Basic threshold detector is named as hard detector because it gives exact symbol values in each iterations. Total iteration number is limited to 5 for all figures. Soft decision detector coefficient λ which is stated in equation (3.15) is detected as to maximize BER performance. There is also a very important variable which is called as overload factor (OF) and it is ratio of

the MC-CDMA users to OFDMA sub-carriers' number. Because of the using different modulation schemes, instead of keeping average symbol energy, we always keep minimum distance between symbols at constellation map same. For instance if OFDMA symbols are 16QAM and MC-CDMA symbols are QPSK modulated and minimum distance between symbols is 2 then 16QAM symbols are $\pm\{3,\ 1\} \pm j\{3,\ 1\}$ and QPSK symbols $\pm\{1\} \pm j\{1\}$.

Our aim is maximizing OF while bit error rate (BER) of the NOMA system should be similar with corresponding OMA. In the absence of the noise it is expected that BER should go to zero. This situation is possible if maximum interference magnitude which is the magnitude of $\frac{1}{\sqrt{N}} \sum_{m=1}^{M} w_{m,n} b_m$ in equation (3.1) cannot exceed half of minimum OFDMA symbols' distance. Figure 3.4(a) visualize the idea. In here OFMDA symbols are 16QAM, MC-CDMA symbols are QPSK modulated. Minimum distance between symbols is 2. Only 4 of 16QAM symbols are shown and red dots represent them. Assume one of the OFDMA symbol is $1 + j$. All of the possible MC-CDMA interferers are illustrated by red lines. Magnitude of the red lines is $\sqrt{2}/\sqrt{N}$. Dashed black lines are threshold detector's borders. If interferer arrows carry $1 + j$ symbol to another region, $1 + j$ detects wrongly.

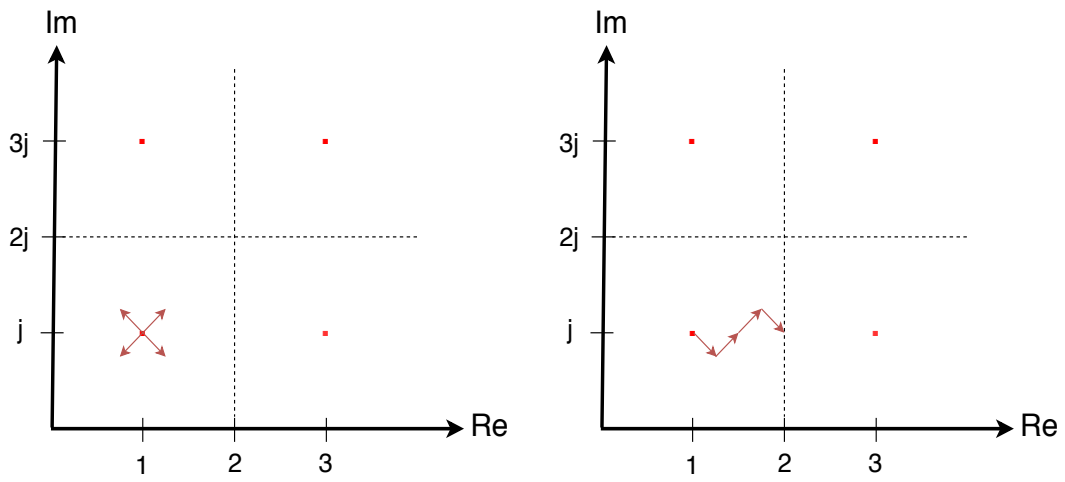

(a) Constellation diagram of the NOMA symbols.

(b) Visualization of the error occurrence in absence of noise.

Figure 3.4. Constellation maps.

For instance let say n^{th} OFDMA symbol is $1+j$ like stated before, N is 16 and M is 4. In addition to that $w_{1,m}b_1 = 1-j,\ w_{2,m}b_2 = 1+j,\ w_{3,m}b_3 = 1+j,\ w_{4,m}b_4 = 1-j$. Even if the absence of noise, according to equation (3.1) location of the point x_n in constellation map is given in figure 3.4(b). According to threshold filter definition, OFDMA symbol can be detected as $3+j$.

Notice that magnitude of the QPSK vector on x-axis is $1/\sqrt{N}$. Therefore maximum magnitude of the vector summation projection onto x-axis is $M/\sqrt{N}$. In order to detect OFDMA symbol correctly in zero noise scenario, $M/\sqrt{N}$ must be less than 1 as seen in figure 3.4(b).

This constraint is very important and it is also explained in [3] and [27] as if $M/\sqrt{N}$ is equals or greater than 1, eye diagram of the OFDMA signal is closed.

Wrong detection of the OFDMA symbols can also causes detection error for MC-CDMA symbols. Assume $\mathbb{E}$ is the collection of wrong detected OFDMA symbols index at first iteration and noise is zero. In this situation equation (3.2) can be rewritten as,

$$y_n = \sum_{e\in\mathbb{E}}(a_e - \hat{a}_e) + \frac{1}{\sqrt{N}}\sum_{m=1}^{M} w_{m,n}b_m. \tag{3.20}$$

Detection of the k^{th} MC-CDMA symbol is given in equation (3.3). This equation with interference term $\sum_{e\in\mathbb{E}}(a_e - \hat{a}_e)$ is

$$\begin{aligned} z_k &= \frac{1}{\sqrt{N}}\sum_{n=1}^{N} w_{k,n}y_n \\ &= \frac{1}{\sqrt{N}}\sum_{n=1}^{N} w_{k,n}\left(\sum_{e\in\mathbb{E}}(a_e - \hat{a}_e) + \frac{1}{\sqrt{N}}\sum_{m=1}^{M} w_{m,n}b_m\right) \\ &= \frac{1}{\sqrt{N}}\sum_{e\in\mathbb{E}} w_{k,e}(a_e - \hat{a}_e) + b_k. \end{aligned} \tag{3.21}$$

If magnitude of the interference term $\frac{1}{\sqrt{N}}\sum_{e\in\mathbb{E}} w_{k,e}(a_e - \hat{a}_e)$ is great enough, symbol b_k can be also detected wrongly. As a consequence if $M/\sqrt{N} \geq 1$ even if in the absence

of noise, BER does not goes zero. In order for zero BER in zero noise,

$$M < \sqrt{N}. \tag{3.22}$$

Equation (3.22) is very important. If M is equal or greater than $\sqrt{N}$ hard-decision detector always encounter with an error floor. Soft symbol detector can overcome with this situation. For instance in the scenario which is visualized by figure 3.4(b), OFDMA symbol is detected either $1+j$ or $3+j$ by hard detector. However soft detector output will be $2+j$. This soft symbol creates smaller error than hard detector. Still it cannot eliminate error floor completely but soft detector takes error floor down.

Now assume there are 256 OFDMA sub-carriers and each of them are assigned to different users i.e. there are also 256 OFDMA users. 44 MC-CDMA users are overloaded to OFDMA symbols. Hence OF is approximately 17.2%. Notice that 44 is grater than $\sqrt{256} = 16$. Therefore it can be said that error floor will be occurred. Since channel is AWGN there is no difference between uplink and downlink systems.

Figure 3.5(a) shows 16QAM modulated OFDMA performance with QPSK modulated MC-CDMA users. 16QAM bit error probability in AWGN can be viewed as theoretical lower limit because OFDMA users without MC-CDMA symbols BER must exactly match with this line. Soft decision detector which is shown by blue lines is significantly better than hard decision detector (red lines). BER for both hard and soft detectors improves while number of the iterations increase. In addition last iteration of the soft decision detector almost catches theoretical limit after 10 dB however hard detector cannot achieve this BER. MC-CDMA performance in the same system is given in 3.5(b). Now theoretical lower limit is QPSK bit error probability in AWGN channel for same reasons. As in the OFDMA BER, soft detector is superior to the hard one. However BER of the soft detector at last iteration follows lower limit 1 dB behind.

When both OFDMA and MC-CDMA symbols are QPSK modulated, BERs are given in figures 3.6(a) and 3.6(b) for OFDMA and MC-CDMA respectively. OF is 25%

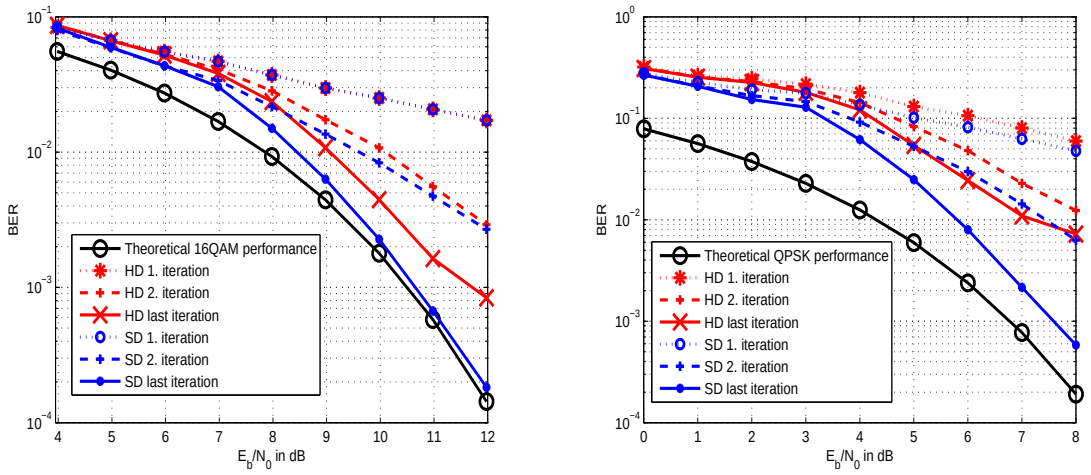

(a) OFDMA BER. (b) MC-CDMA BER.

Figure 3.5. 16QAM modulated OFDMA and QPSK modulated MC-CDMA performances of NOMA-2000 system in AWGN channel. OF = 17.2% ($N = 256$, $M = 44$).

i.e. there are 256 OFDMA and 64 MC-CDMA users. Since OFDMA is now QPSK modulated, system can tolerate more interferer users. Like in figures 3.5, soft detector performs better BER than hard one. Last iteration of the soft detector is closed to theoretical lower limit visually.

3.2. Channel Overloading NOMA

It is the special type of the NOMA-2000 and system is described in [29]. MC-CDMA symbols are spreaded over whole OFDMA sub-carriers in NOMA-2000. However for overloaded NOMA, one MC-CDMA user is spreaded over only $\lfloor N/M \rfloor$ OFDMA sub-carriers. For instance first MC-CDMA symbol is spreaded over carriers whose indexes are 1 to $\lfloor N/M \rfloor$, second MC-CDMA symbol is spreaded over $\lfloor N/M \rfloor + 1$ sub-carrier to $2\lfloor N/M \rfloor$ and so on. Figure 3.7 illustrates the signal frequencies for $N/M = 4$ or overloaded factor = 25%.

Motivation for channel overloading NOMA can be explain by an example: Assume $N = 64$ and $M = 16$ for a NOMA-2000 system. Channel overload factor is 25%. However since $16 > \sqrt{64}$ which violates equation (3.22) an error floor will occur. If

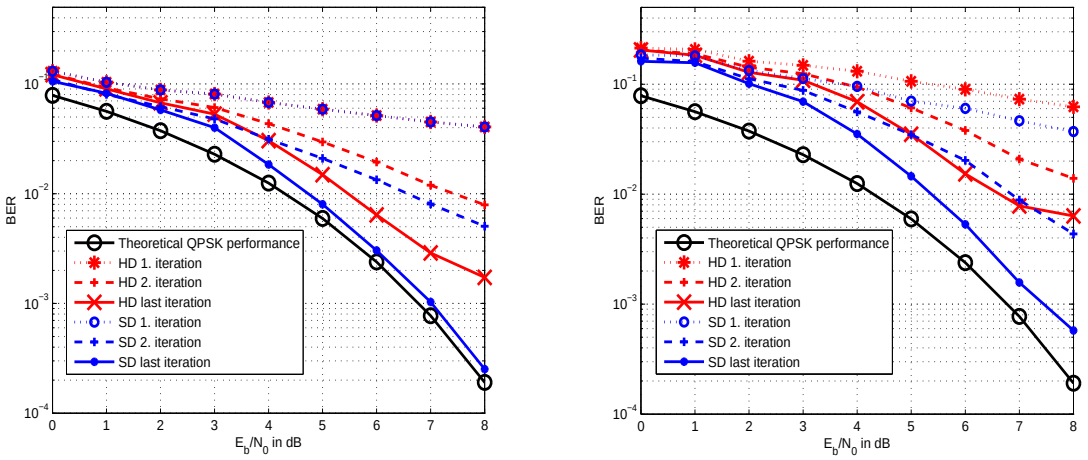

(a) OFDMA BER. (b) MC-CDMA BER.

Figure 3.6. QPSK modulated OFDMA and QPSK modulated MC-CDMA performances of NOMA-2000 system in AWGN channel. OF = 25% ($N = 256$, $M = 64$).

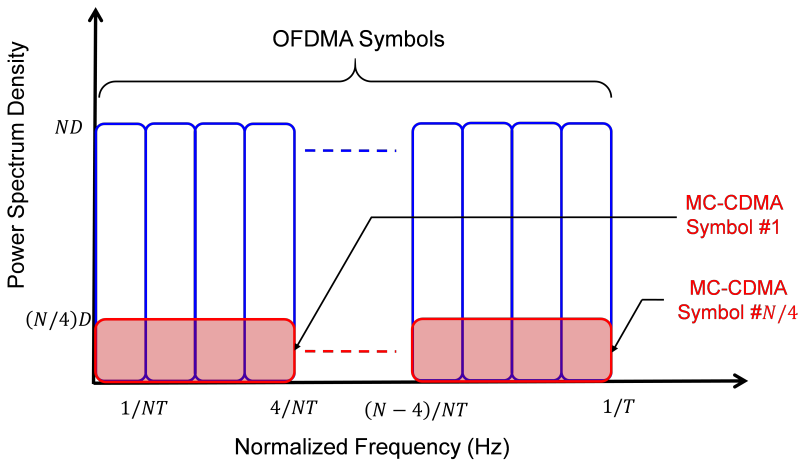

Figure 3.7. A channel overloading system for $N/M = 4$.

this system is converted to overloading NOMA, every MC-CDMA user is spreaded over $\lfloor 64/16 \rfloor = 4$ sub-carriers. 4 OFMDA with 1 MC-CDMA combinations are sent by side by side, therefore there is no interaction between groups. Even if OF is same for both system, since number of interferer user for one group is 1 and it is smaller than $\sqrt{4}$ in channel overloading NOMA, error floor will not occur.

In addition MC-CDMA users are spreaded with normalized reputation code. Assume $k = \lfloor N/M \rfloor$ then normalized reputation code is $(1/\sqrt{k}) \cdot [1,\ 1,\ \cdots,\ 1]$ which includes k elements. Notice that k and so that OF take any value.

3.2.1. Detection

As state in [9], optimum detection for a multiple access system is maximum-likelihood (ML) detection. However calculation cost for ML detection can be extreme and it is depends on number of users and their modulation type. Assume OFMDA 16QAM and MC-CDMA symbols are QPSK modulated. If $\lfloor N/M \rfloor = 4$ then we have signal groups with 4 sub-carriers. This received signals are formulated as,

$$x_n = a_n + b_{\lceil n/4 \rceil}/2 + u_n \tag{3.23}$$

where $n = 1,\ 2,\ \ldots,\ N$, a_n OFDMA symbol, $b_{\lceil n/4 \rceil}$ MC-CDMA symbol, u_n noise and x_n is received signal from n^{th} sub-carrier. Notice that $\lceil n/4 \rceil$ can take values from $1,\ 2,\ \ldots,\ N/4$. MC-CDMA symbol is divided by 2 because of normalization ($\sqrt{4} = 2$). If $n = 1$, we should interested with there signals,

$$\begin{aligned} x_1 &= a_1 + b_1/2 + u_1, \\ x_2 &= a_2 + b_1/2 + u_2, \\ x_3 &= a_3 + b_1/2 + u_3, \\ x_4 &= a_4 + b_1/2 + u_4. \end{aligned} \tag{3.24}$$

In order to realize ML detection, all possible 16QAM symbols are placed into $a_1,\ a_2,\ a_3,\ a_4$ and all possible QPSK symbols are tried for symbol b_1 to minimize,

$$\sum_{n=1}^{4} |x_n - a_n - b_1/2|^2. \tag{3.25}$$

This requires trying $16^4 \times 4$ different situations and choosing the symbols combination with minimum error.

Another approach is applying threshold detectors in order to detect OFDMA symbols for all possible MC-CDMA symbols and choosing a signal group with minimum error. This method is exactly same with ML detection because for a particular b_1, x_n's are independent for $n = 1,\ 2,\ 3,\ 4$. It can be showed mathematically as,

$$E\Big[\prod_{n=1}^{N} x_n \mid b_1\Big] = \prod_{n=1}^{N} E\Big[x_n \mid b_1\Big]. \tag{3.26}$$

Equations (3.26) tells us that for given symbols b_1, minimizing error of the OFDMA symbols sequence i.e. $a_1,\ a_2,\ \cdots,\ a_N$; are same with minimizing OFMDA symbols' error individually. If we define detection process for symbols $a_1,\ a_2,\ a_3,\ a_4,\ b_1$ step by step:

• *Step-1*: Symbol b_1 is accepted as $1 + j$. Then $(1 + j)/2$ is subtracted from x_1, x_2, x_3, x_4 which are given in equation (3.24). After that subtracted symbols are given into a threshold detector in order to detect OFDMA symbols $a_1,\ a_2,\ a_3$ and a_4. Let say detected OFDMA symbols are $\hat{a}_{11},\ \hat{a}_{12},\ \hat{a}_{13},\ \hat{a}_{14}$. System's error is calculated by using equation (3.25) and let say it is represented by e_1.

• *Step-2*: Symbol b_1 is accepted as $1 - j$. Then $(1 - j)/2$ is subtracted from x_1, x_2, x_3, x_4. After that subtracted symbols are given into a threshold detector in order to detect a_1, a_2, a_3 and a_4. Detected OFDMA symbols are $\hat{a}_{21}$, $\hat{a}_{22}$, $\hat{a}_{23}$, $\hat{a}_{24}$. System's error is calculated it is represented by e_2.

• *Step-3*: Symbol b_1 is accepted as $-1 + j$. Then $(-1 + j)/2$ is subtracted from $x_1,\ x_2,\ x_3,\ x_4$. After that subtracted symbols are given into a threshold detector in

order to detect $a_1,\ a_2,\ a_3$ and a_4. Detected OFDMA symbols are $\hat{a}_{31},\ \hat{a}_{32},\ \hat{a}_{33},\ \hat{a}_{34}$. System's error is calculated it is represented by e_3.

• *Step-4*: Symbol b_1 is accepted as $-1-j$. Then $(-1-j)/2$ is subtracted from $x_1,\ x_2,\ x_3,\ x_4$. After that subtracted symbols are given into a threshold detector in order to detect $a_1,\ a_2,\ a_3$ and a_4. Detected OFDMA symbols are $\hat{a}_{41},\ \hat{a}_{42},\ \hat{a}_{43},\ \hat{a}_{44}$. System's error is calculated it is represented by e_4.

• *Step-5*: Detected symbols now become estimated symbols in previous steps whose error is minimum.

As seen above instead of huge calculation, a simple threshold detector is required for this technique. Since there is no iteration at detection process, calculation cost is smaller than NOMA-2000 and there is no error floor. Moreover because of that ML is optimum detection technique iterative SIC with soft or hard decision detector cannot exceed its performance.

3.2.2. Performance Results

Performance results are given for OF = 16.7% and 25%; MC-CDMA QPKS, OFMDA symbols are 16QAM modulated in figures 3.8(a) and 3.8(b) respectively. Overload factor of the figures 3.8(a), 3.5(a) and 3.5(b) are very close. Notice that 16QAM and QPSK symbols performances are almost same for NOMA-2000 and channel overloading NOMA as seen in these figures. However calculation cost of the figure 3.8(a) are smaller than NOMA-2000 system because there is no iteration at receiver side. On the other hand as stated before error floor does not occur at channel overloading NOMA which can be observed from figures 3.8(a) and 3.8(b).

BER performance of the channel overloading NOMA is so close to theoretical lower limits for both figures. However when OF is increases SNR degradation is also increases. Nevertheless even if in OF with 25%, SNR degradation approximately 0.3 dB for 16QAM and 0.8 dB for QPSK symbols. In figure 3.9 BER of the MC-CDMA and OFDMA symbols are given. However in here both type of the symbols are QPSK modulated. Overload factors are 25% and 33% in figures 3.9(a) and 3.9(b) respectively.

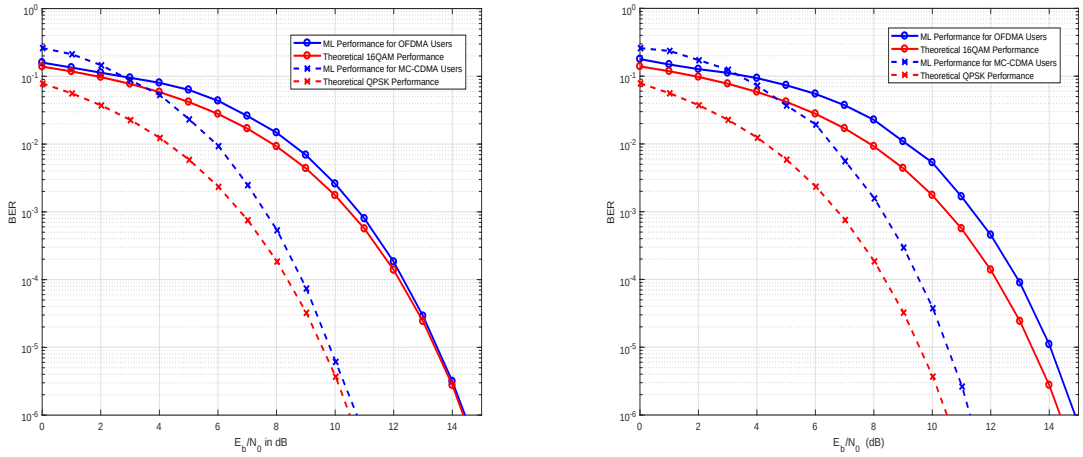

(a) Overload factor = 16.7% (b) Overload factor = 25%

Figure 3.8. BER performance of the channel overloading NOMA for 16QAM modulated OFDMA and QPSK modulated MC-CDMA in AWGN channel.

SNR degradations for 25% OF is 0.2 and 0.3 dB. For 33% OF, degradations increases as expected and they are now 0.8 dB averagely. Notice that even if OFs are same for figure 3.9(a) and 3.6, channel overloaded NOMA performs better BER than NOMA-2000. Moreover there is no error floor and it can be said that channel overloaded NOMA also support 33% percent of OF if MC-CDMA and OFDMA are both QPSK modulated.

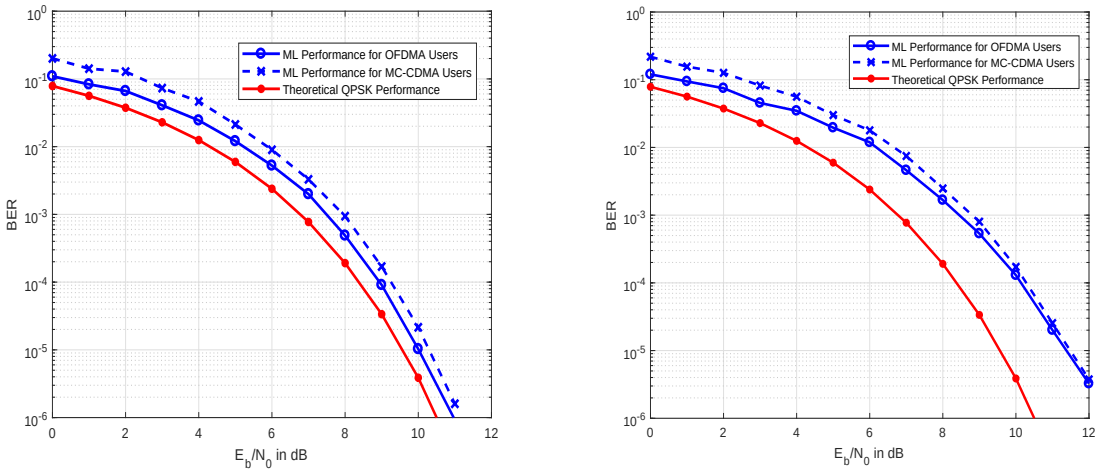

(a) Overload factor = 25% (b) Overload factor = 33.3%

Figure 3.9. BER performance of the channel overloading NOMA for QPSK modulated OFDMA and MC-CDMA in AWGN channel.

Two types of the NOMA concepts and their detection mechanism were presented. NOMA-2000 is flexible in terms of overload factor however it has sub-optimum and complex detection process. Whereas the detection process of the channel overloading NOMA is optimum and simple. However its overload factor is not flexible as NOMA-2000. In next chapter, the bit error performances of these NOMA concepts will be demonstrated for different channel conditions. In addition, in order to deal with these channel conditions, modification on the receiver side will be also given.

4. FREQUENCY DOMAIN NOMA IN RAYLEIGH FLAT FADING CHANNEL

First of all, the performances of the frequency domain NOMA on uncorrelated Rayleigh flat fading channel will be introduced in this chapter. Channel coefficients are same for different sub-carriers, if all sub-carriers are belong to same user.

4.1. NOMA-2000 Performance on Rayleigh Flat Fading Channel

4.1.1. Uplink

At a non-frequency selective Rayleigh channel in a uplink system, for a particular user, each OFDMA sub-carriers are multiplied by same Rayleigh distributed coefficient. However channel shows different fading coefficients for different users. Assume each OFDMA sub-carriers are assigned to distinct users. Received signal at n^{th} sub-carrier is x_n, a_n corresponds OFDMA symbol and u_n is noise. b_m is MC-CDMA symbol of the m^{th} user and $w_{m,n}$ is n^{th} chip of the m^{th} MC-CDMA user. $h_1,\ h_2, \cdots, h_N,\ h_{N+1}, \cdots, h_{N+M}$ are Rayleigh distributed channel coefficients. First N coefficients belong to OFDMA and from $N+1$ to $N+M$ coefficients belong to MC-CDMA users. After removing cyclic prefix and discrete Fourier transform (DFT), received signal for uplink is expressed as,

$$x_n = h_n \cdot a_n + \frac{1}{\sqrt{N}} \sum_{m=1}^{M} h_{N+m}(w_{n,m} b_m) + u_n. \tag{4.1}$$

Matrix representation of the equation (4.1) is,

$$\vec{x} = H_{(o)} \cdot \vec{a} + \frac{1}{\sqrt{N}} W \cdot H_{(m)} \cdot \vec{b} + \vec{u} \tag{4.2}$$

where vectors $\vec{x}$, $\vec{a}$, $\vec{b}$, $\vec{u}$ and matrix W have same definition with equation (3.5). $H_{(o)}$ is $N \times N$ diagonal matrix whose diagonal elements are $h_1,\ h_2,\ \cdots,\ h_N$. In the

same manner matrix $H_{(m)}$ is $M \times M$ diagonal matrix and its diagonal elements are $h_{N+1},\ h_{N+2},\ \cdots,\ h_{N+M}$.

Assume all channel coefficients and noise power are perfectly known by receiver. As stated before the best detection technique is maximum-likelihood detection (see [7] and [9]). If OFDMA symbols P-QAM and MC-CDMA symbols are T-QAM modulated, $P^N \times T^M$ different symbols combinations are placed into equation (4.2) and one of them with minimum error is chosen. Therefore it is almost impossible to implement. The second best choice is tried to remove effects of the channel coefficients then applying iterative SIC. Linear detection technique is used because of its simplicity and calculation cost efficient. Since channel state information of the all users and noise power are known minimum mean square error (MMSE) block linear equalizer is applied [7].

Assume $E_{(o)}$ and $E_{(m)}$ are equalization matrices for OFMDA and MC-CDMA symbols respectively. They are given as,

$$\begin{aligned} E_{(o)} =& \big(H_{(o)}^H \cdot H_{(o)} + I_{N\times N} \cdot SNR_{OFDMA}^{-1}\big)^{-1} \cdot H_{(o)}^H \\ E_{(m)} =& \big((\frac{1}{\sqrt{N}} W \cdot H_{(m)})^H \cdot (\frac{1}{\sqrt{N}} W \cdot H_{(m)}) + I_{M\times M} \cdot SNR_{CDMA}^{-1}\big)^{-1} \\ & \cdot (\frac{1}{\sqrt{N}} W \cdot H_{(m)})^H \\ =& \big(H_{(m)}^H \cdot H_{(m)} + I_{M\times M} \cdot SNR_{CDMA}^{-1}\big)^{-1} \cdot H_{(m)}^H \cdot \frac{1}{\sqrt{N}} W^H \end{aligned} \tag{4.3}$$

where I is identity matrix. Notice that equalizer matrix $E_{(m)}$ also include despreading. Hard and soft detector functions are $T[.]$ and $\Psi[.]$ that is defined in equation (3.15)

respectively. Hard detection with t step is,

$$\begin{aligned}
\hat{\vec{a}}_1 &= T[E_{(o)} \cdot \vec{x}], \\
\hat{\vec{b}}_1 &= T[E_{(m)} \cdot (\vec{x} - H_{(o)} \cdot \hat{\vec{a}}_1)], \\
\hat{\vec{a}}_2 &= T[E_{(o)} \cdot (\vec{x} - H_{(m)} \cdot \hat{\vec{b}}_1)], \\
\hat{\vec{b}}_2 &= T[E_{(m)} \cdot (\vec{x} - H_{(o)} \cdot \hat{\vec{a}}_2)], \\
&\vdots \\
\hat{\vec{a}}_t &= T[E_{(o)} \cdot (\vec{x} - H_{(m)} \cdot \hat{\vec{b}}_{t-1})], \\
\hat{\vec{b}}_t &= T[E_{(m)} \cdot (\vec{x} - H_{(o)} \cdot \hat{\vec{a}}_t)].
\end{aligned} \tag{4.4}$$

Important point is that before subtraction of the estimated symbols they are multiplied with channel coefficients. In the same manner, t step detection process with soft decision detector is,

$$\begin{aligned}
\hat{\vec{a}}_{1(s)} &= \Psi[E_{(o)} \cdot \vec{x}], \\
\hat{\vec{b}}_{1(s)} &= \Psi[E_{(m)} \cdot (\vec{x} - H_{(o)} \cdot \hat{\vec{a}}_{1(s)})], \\
\hat{\vec{a}}_{2(s)} &= \Psi[E_{(o)} \cdot (\vec{x} - H_{(m)} \cdot \hat{\vec{b}}_{1(s)})], \\
\hat{\vec{b}}_{2(s)} &= \Psi[E_{(m)} \cdot (\vec{x} - H_{(o)} \cdot \hat{\vec{a}}_{2(s)})], \\
&\vdots \\
\hat{\vec{a}}_{t(s)} &= \Psi[E_{(o)} \cdot (\vec{x} - H_{(m)} \cdot \hat{\vec{b}}_{t-1(s)})], \\
\hat{\vec{b}}_{t(s)} &= \Psi[E_{(m)} \cdot (\vec{x} - H_{(o)} \cdot \hat{\vec{a}}_{t(s)})], \\
\hat{\vec{a}}_t &= T[\hat{\vec{a}}_{t(s)}], \\
\hat{\vec{b}}_t &= T[\hat{\vec{b}}_{t(s)}].
\end{aligned} \tag{4.5}$$

The last step of the equation (4.5) is converting soft symbols into hard.

4.1.2. Downlink

Since channel is non-frequency selective, channel coefficient between a user and base station is constant for all sub-carriers in one symbol period time. Therefore

received signal at n^{th} sub-carrier is,

$$x_n = h \cdot \left[a_n + \frac{1}{\sqrt{N}} \sum_{m=1}^{M} w_{n,m} b_m \right] + u_n \tag{4.6}$$

where h is complex coefficient and constant for all sub-carriers. Matrix representation of the equation (4.6) is

$$\begin{aligned} \vec{x} &= H \cdot \left[\vec{a} + \frac{1}{\sqrt{N}} W \cdot \vec{b} \right] + \vec{u} \\ &= H \cdot \vec{a} + \frac{1}{\sqrt{N}} H \cdot W \cdot \vec{b} + \vec{u} \end{aligned} \tag{4.7}$$

where H is $N \times N$ diagonal matrix whose diagonal elements are all h. Equalization matrices are,

$$\begin{aligned} E_{(o)} &= \left(H^H \cdot H + I_{N \times N} \cdot SNR^{-1}_{OFDMA} \right)^{-1} \cdot H^H \\ E_{(m)} &= \left((\frac{1}{\sqrt{N}} H \cdot W)^H \cdot (\frac{1}{\sqrt{N}} H \cdot W) + I_{M \times M} \cdot SNR^{-1}_{CDMA} \right)^{-1} \cdot (\frac{1}{\sqrt{N}} H \cdot W)^H \\ &= \left(\frac{1}{N} W^H \cdot H^H \cdot H \cdot W + I_{M \times M} \cdot SNR^{-1}_{CDMA} \right)^{-1} \cdot \frac{1}{\sqrt{N}} W^H \cdot H^H \end{aligned} \tag{4.8}$$

Hard and soft detection processes are same with equations (4.4) and (4.5) respectively.

4.1.3. Performance Results

For all figure in this section, total iteration number is 5. Figure 4.1 demonstrates OFDMA and MC-CDMA BER performance for uplink system. In here OFDMA symbols are 16QAM, MC-CDMA symbols are QPSK modulated. There are 256 sub-carriers and 64 MC-CDMA users i.e. OF is 25%. As seen in figures 4.1, NOMA-2000 can provides 25% overload factor for 16QAM modulated OFDMA and QPSK modulated MC-CDMA. At last iteration, hard decision detector faces with an error floor for both type of users. However soft detector catches theoretical lower limit after 10 dB.

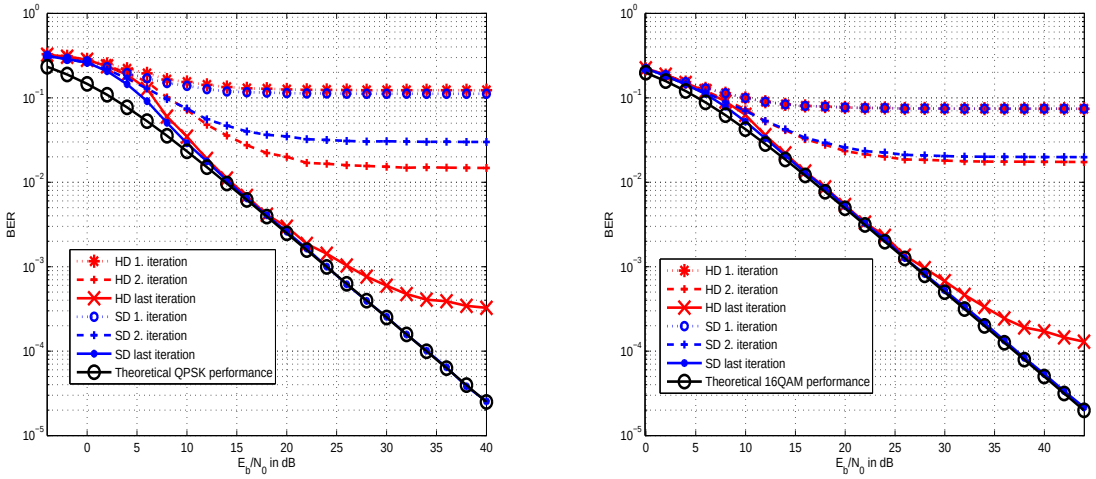

(a) MC-CDMA performance. (b) OFDMA performance.

Figure 4.1. Uplink BER performance of NOMA-2000 for 16QAM modulated OFDMA and QPSK modulated MC-CDMA. OF = 25% (i.e. 256 OFDMA vs 64 MC-CDMA)

When OF is increased to 37.5% i.e. there is 96 MC-CDMA users with 256 OFDMA sub-carriers for uplink, soft detector faces with an error floor around approximately $10^{-4}/2$ for both system. Figure 4.2 shows this situation.

If OFDMA and MC-CDMA are QPSK modulated NOMA-2000 can cope with high OF as expected. Figure 4.3 demonstrates BER performance of the OFDMA and MC-CDMA for 50% overload factor. At last iteration hard detector is faced with an error floor however there is no SNR degradation between soft detector and theoretical lower limit. However if MC-CDMA users' number is increased to 192 hence OF becomes 75% soft decision meets with an error floor for OFDMA and MC-CDMA users as seen in figure 4.4. These error floors are approximately $0.9 \cdot 10^{-3}$ for OFDMA and $0.4 \cdot 10^{-4}$ for MC-CDMA.

Downlink performance of the system is not promising as uplink. Since MC-CDMA and OFDMA symbols' coefficients are same, system treats like an AWGN with variable noise power due to channel coefficient. Figure 4.5 shows downlink performance of the 16QAM modulated OFDMA and QPSK modulated MC-CDMA with OF 12.5%. As it can be seen in figure, soft decision cannot reach theoretical lower bound.

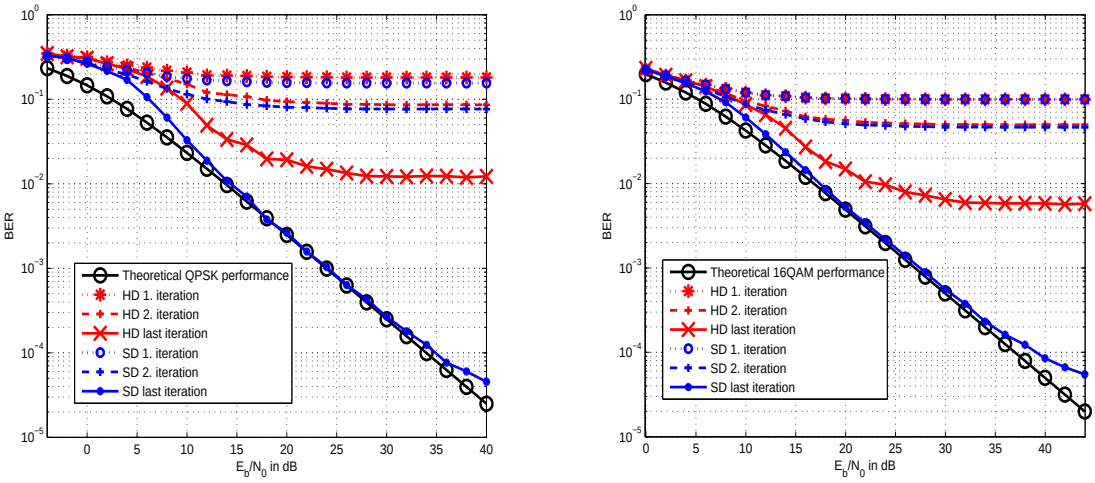

(a) MC-CDMA performance. (b) OFDMA performance.

Figure 4.2. Uplink BER performance of NOMA-2000 for 16QAM modulated OFDMA and QPSK modulated MC-CDMA. OF = 37.5% (i.e. 256 OFDMA vs 96 MC-CDMA)

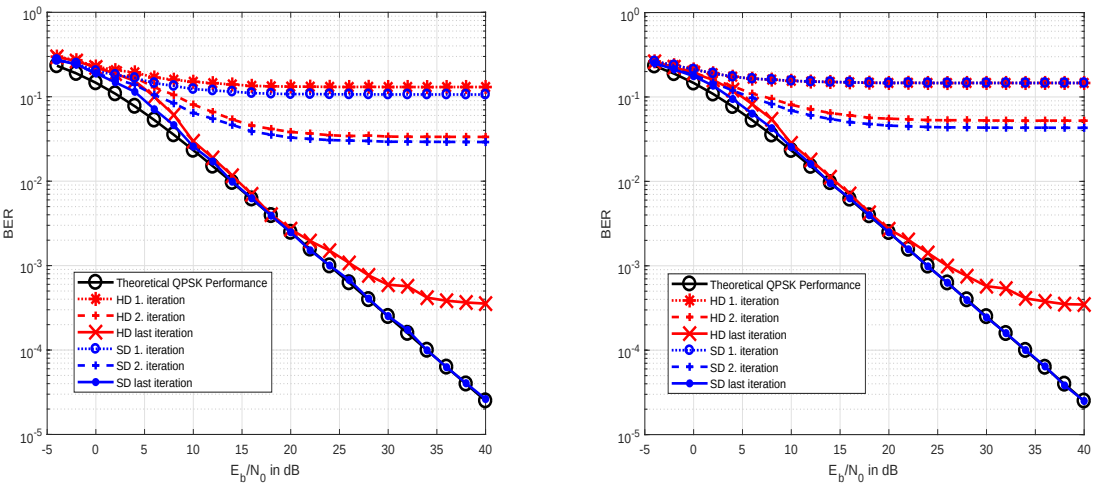

(a) MC-CDMA performance. (b) OFDMA performance.

Figure 4.3. Uplink BER performance of NOMA-2000 for QPSK modulated OFDMA and MC-CDMA. OF = 50% (i.e. 256 OFDMA vs 128 MC-CDMA)

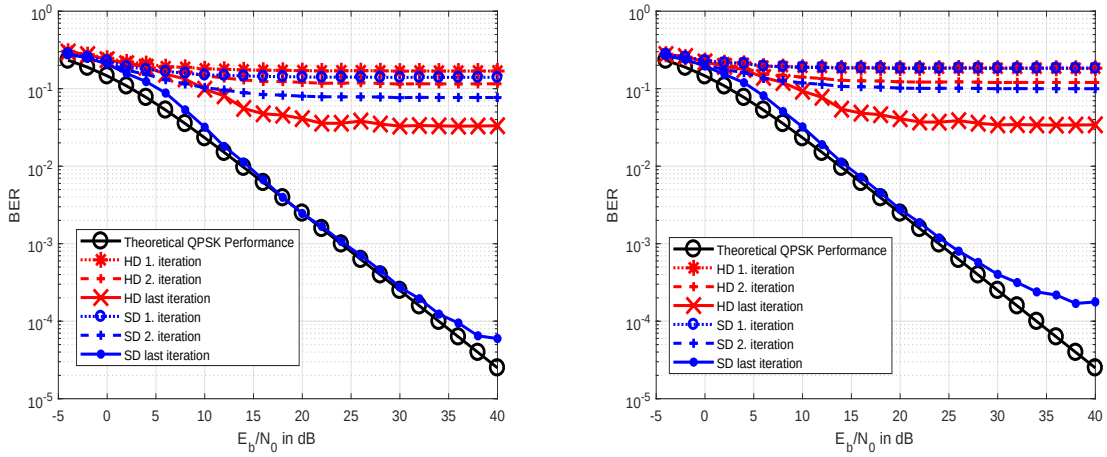

(a) MC-CDMA performance. (b) OFDMA performance.

Figure 4.4. Uplink BER performance of NOMA-2000 for QPSK modulated OFDMA and MC-CDMA. OF = 75% (i.e. 256 OFDMA vs 192 MC-CDMA)

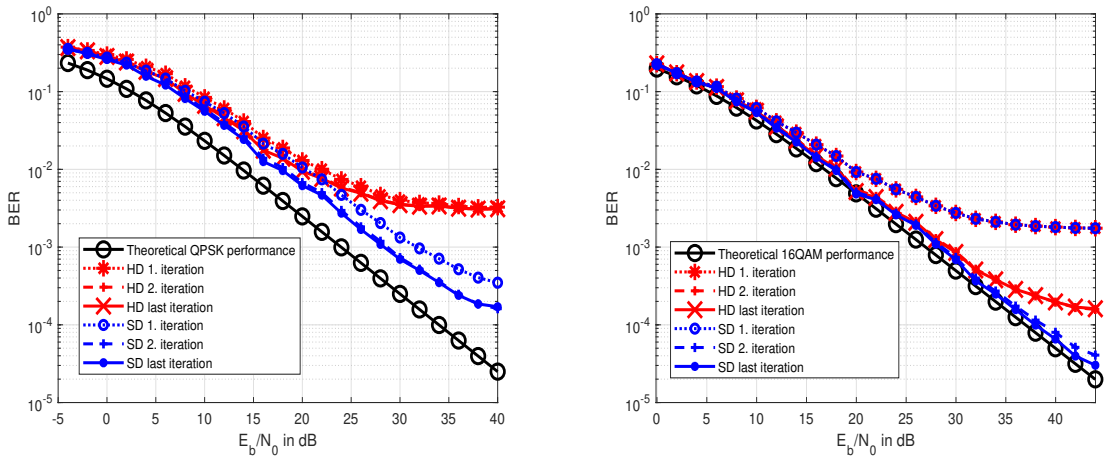

(a) MC-CDMA performance. (b) OFDMA performance.

Figure 4.5. Downlink BER performance of NOMA-2000 for 16QAM modulated OFDMA and QPSK modulated MC-CDMA. OF = 12.5% (i.e. 256 OFDMA vs 32 MC-CDMA)

When both type of the symbols are QPSK modulated performances are increase. However it is still far from uplink performance. Figure 4.6 illustrates this system with OF 25%.

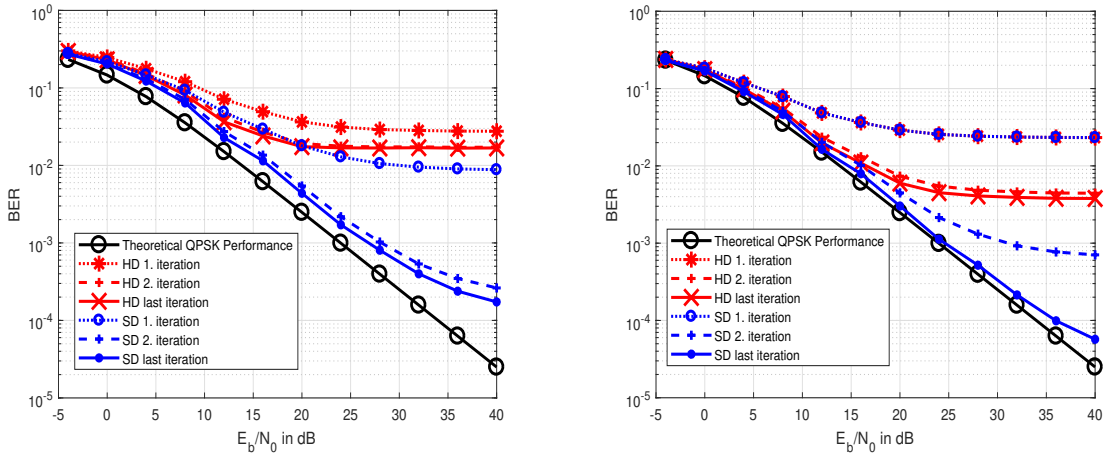

(a) MC-CDMA performance. (b) OFDMA performance.

Figure 4.6. Downlink BER performance of NOMA-2000 for QPSK modulated OFDMA and MC-CDMA. OF = 25% (i.e. 256 OFDMA vs 64 MC-CDMA)

4.2. NOMA-2000 with Dynamic User Grouping

In uplink NOMA-2000 system at non-frequency selective Rayleigh channel, received signal is expressed with equation (4.1). In order to reduce signal to interference ratio (S/I) for OFDMA symbols, these symbols are assigned to N users with strongest channel coefficient [30]. This assignment result can be formulated as,

$$Min\{|h_i|\} \geq Max\{|h_j|\} \tag{4.9}$$

for $i = 1,\ 2,\ \cdots,\ N$ and $j = M+1,\ M+2,\ \cdots,\ M+N$. However this approach is not valid for downlink system, because coefficients are same for the both type of the symbols.

This dynamic user grouping provides not only less S/I but also a fair BER for all users. Since a user's waveform is changed according to his channel coefficient magni-

tude, statistically he utilizes OFDMA with probability of $N/(N+M)$ and MC-CDMA with probability $M/(N+M)$. Therefore single user's BER is,

$$BER_{user} = \big(N \cdot BER_{OFDMA} + M \cdot BER_{MC-CDMA}\big)/(N+M) \tag{4.10}$$

Detection process is exactly same with previous system. Only difference is user assignment. Moreover dynamic user grouping provides same beneficial things with NOMA-2000 .

4.2.1. Performance Results

BER performance of the users are shown in same graph even if they have different modulation type. Because a user can be assigned to OFDMA and MC-CDMA system dynamically therefore she/he is to be OFDMA user with probability of $N/(N+M)$ and MC-CDMA user with probability of $M/(N+M)$. Hence average SNR $E_{average}/N_0$ is given as,

$$E_{average}/N_0 = \frac{N}{N+M}\cdot B_{OFDMA}\cdot(E_{OFDMA}/N_0) + \frac{M}{N+M}\cdot B_{MC-CDMA}\cdot(E_{MC-CDMA}/N_0) \tag{4.11}$$

where E_{OFDMA}/N_0 and $E_{MC-CDMA}/N_0$ are average bit to noise power of OFDMA and MC-CDMA symbols. B_{OFDMA} represents the number of bits in one OFDMA symbol, in the same manner $B_{MC-CDMA}$ is the number of bits in one MC-CDMA symbol. This average bit to noise energy $E_{average}/N_0$ are used at figures in dB to represent x-axis. In addition total iteration is limited to 5 for all figures in this section.

Theoretical lower limit is that BER of the corresponding OMA system. According to equation (4.2) received signal is demonstrated as,

$$\vec{x} = \vec{S}_{OFDMA} + \vec{S}_{MC-CDMA} + \vec{n} \tag{4.12}$$

where $\vec{S}_{OFDMA} = H_{(o)} \cdot \vec{a}$ and $\vec{S}_{MC-CDMA} = (1/\sqrt{N}) \cdot W \cdot H_{(m)} \cdot \vec{b}$.
Corresponding OMA systems are,

$$\begin{aligned} \vec{x}_{(o)} &= \vec{S}_{OFDMA} + \vec{n} \\ \vec{x}_{(m)} &= \vec{S}_{MC-CDMA} + \vec{n}. \end{aligned} \tag{4.13}$$

Notice that vector $\vec{x}_{(o)}$ contains N and $\vec{x}_{(m)}$ contains M elements. Therefore $\vec{x}_{(o)}$ has $N \cdot B_{OFDMA}$ bits while $\vec{x}_{(m)}$ has $M \cdot B_{MC-CDMA}$ bits. For this reason BER of the both system has to be normalized according to their bit numbers. Then BER of the corresponding OMA system is given as,

$$\begin{aligned} BER(OMA) = &\frac{N \cdot B_{OFDMA}}{N \cdot B_{OFDMA} + M \cdot B_{MC-CDMA}} \cdot BER(\vec{x}_{(o)}) + \\ &\frac{M \cdot B_{MC-CDMA}}{N \cdot B_{OFDMA} + M \cdot B_{MC-CDMA}} \cdot BER(\vec{x}_{(m)}). \end{aligned} \tag{4.14}$$

Equation (4.14) gives us performance lower limit of the NOMA system.

Figure 4.7 illustrates 16QAM modulated OFDMA over QPSK modulated MC-CDMA performance. According to equation (4.14) lower limits are between 16QAM and QPSK performance in Rayleigh channel. As seen in figure 4.7(a) system can overcome with 75% overload factor. However when OF becomes 100% system includes a error floor again as in figure 4.7(b).

If both OFDMA and MC-CDMA are QPSK modulated system can deal with higher OF as seen in figure 4.8. Theoretical lower limit is bit error probability of QPSK in Rayleigh fading channel because OFDMA and MC-CDMA symbols are both QPSK modulated and in this situation equation (4.14) becomes bit error probability of QPSK in Rayleigh channel. Hard decision detector also shows good performance for 75% OF. Even if 100% OF can be achieved without any SNR degradation and it is shown by figure 4.8(b).

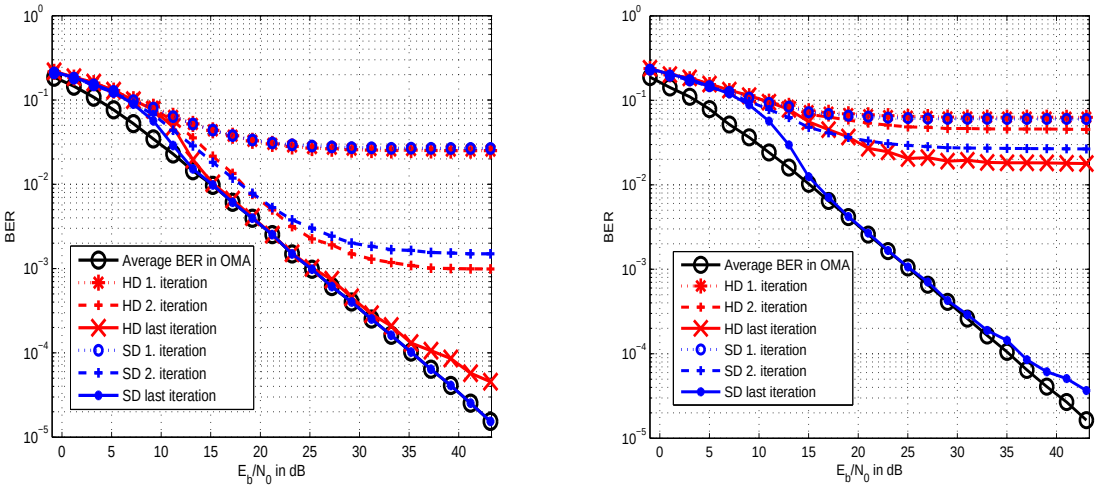

(a) OF = 75% (i.e. 256 OFDMA vs 192 MC-CDMA).

(b) OF = 100% (i.e. 256 OFDMA vs 256 MC-CDMA).

Figure 4.7. Uplink BER performance of NOMA-2000 with dynamic user grouping for 16QAM modulated OFDMA and QPSK modulated MC-CDMA.

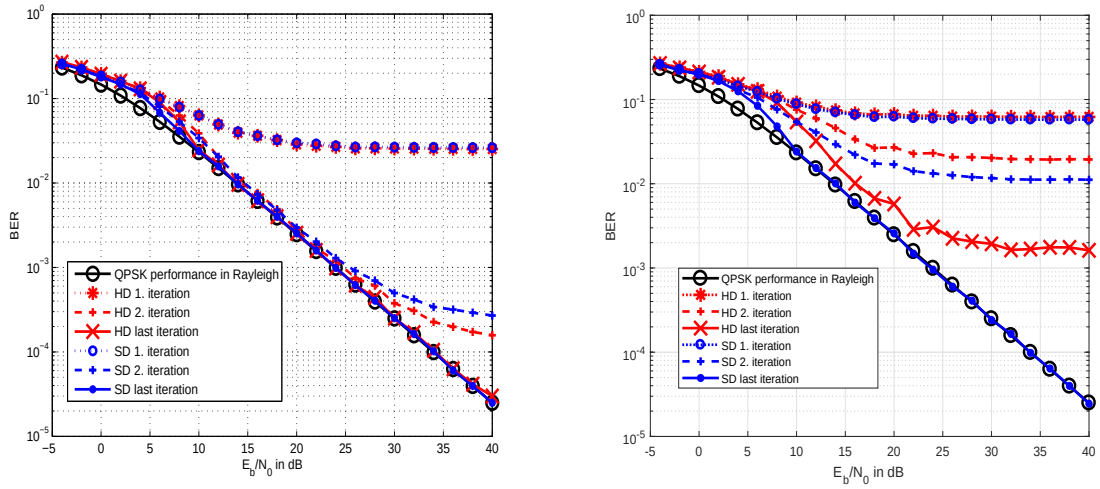

(a) OF = 75% (i.e. 256 OFDMA vs 192 MC-CDMA).

(b) OF = 100% (i.e. 256 OFDMA vs 256 MC-CDMA).

Figure 4.8. Uplink BER performance of NOMA-2000 with dynamic user grouping for QPSK modulated OFDMA and MC-CDMA.

4.3. MISO Based NOMA-2000 for Downlink

Multiple Input Single Output (MISO) wireless communication system consists of multiple transmitters and single receiver. In the downlink NOMA system, base station (BS) has 2 antennas and mobile user has single. One of the BS's antenna always radiates MC-CDMA symbols while other one radiates OFDMA symbols. Therefore received signal is,

$$\begin{aligned}\vec{x} &= h_o \cdot \vec{a} + \frac{h_m}{\sqrt{N}} \cdot W \cdot \vec{b} + \vec{u} \\ &= H_o \cdot \vec{a} + \frac{1}{\sqrt{N}} H_m \cdot W \cdot \vec{b} + \vec{u}.\end{aligned} \tag{4.15}$$

Since channel is non-frequency selective, matrix H_o is diagonal matrix and its diagonal elements are same h_o. H_m is also like H_o and assume there is no correlation between these matrices. Moreover number of the OFDMA and MC-CDMA symbols are same. It means that there is less OFDMA users that OFDMA sub-carriers. Therefore some of the $\vec{a}$ elements are 0. Assume number of the sub-carriers is N and there are $N+M$ total users. Then number of the OFDMA and MC-CDMA users are $\frac{N+M}{2}$ and $\vec{a}$ becomes $[a_1,\ a_2,\ \cdots,\ a_{(N+M)/2},\ 0,\ \cdots,\ 0]^T$.

Detection process is a little bit different from NOMA-2000. It starts with signal groups (i.e. OFDMA or MC-CDMA) whose the magnitude of the coefficient is greater. First of all received signal should be equalized in order to remove channel coefficients' effect. Equalization matrices will be like in equation (4.8). If $E_{(o)}$ is OFDMA equalization matrix and $E_{(m)}$ is for MC-CDMA, than

$$\begin{aligned}E_{(o)} =& \big(H_o^H \cdot H_o + I \cdot SNR_{OFDMA}^{-1}\big)^{-1} \cdot H_o^H \\ E_{(m)} =& \big((\frac{1}{\sqrt{N}} H_m \cdot W)^H \cdot (\frac{1}{\sqrt{N}} H_m \cdot W) + I_{M\times M} \cdot SNR_{CDMA}^{-1}\big)^{-1} \cdot \\ & (\frac{1}{\sqrt{N}} H_m \cdot W)^H \\ =& \big(\frac{1}{N} W^H \cdot H_m^H \cdot H_m \cdot W + I_{M\times M} \cdot SNR_{CDMA}^{-1}\big)^{-1} \cdot \frac{1}{\sqrt{N}} W^H \cdot H_m^H\end{aligned} \tag{4.16}$$

By using equalization matrices in equation (4.16), detection process starts like: If $\mid h_o \mid^2 > \mid h_m \mid^2$

$$\begin{aligned} \hat{\vec{a}}_1 &= F[E_{(o)} \cdot \vec{x}] \\ \hat{\vec{b}}_1 &= F[E_{(m)} \cdot (\vec{x} - H_{(o)} \cdot \hat{\vec{a}}_1')]. \end{aligned} \tag{4.17}$$

In contrast to it, if $\mid h_m \mid^2 > \mid h_o \mid^2$

$$\begin{aligned} \hat{\vec{b}}_1 &= F[E_{(m)} \cdot \vec{x}] \\ \hat{\vec{a}}_1 &= F[E_{(o)} \cdot (\vec{x} - H_{(m)} \cdot \hat{\vec{b}}_1)]. \end{aligned} \tag{4.18}$$

In equations (4.17) and (4.18), function $F[.]$ is whether hard or soft detector. Notice that when OFDMA symbols detect, after the multiplication of the signal with OFMDA equalizer, result is $N \times 1$ dimensional vector. We know that only first $\frac{N+M}{2}$ elements represent OFDMA symbol. Therefore only these elements are taken into account. However when detected OFDMA symbols are subtracted, missing elements are filled by zeros.

4.3.1. Performance Results

Performance of the this system is given in figure 4.9. OF is 43.75%, in other words there are 256 OFMDA sub-bands and 112 extra users. It means that number of the OFMDA and MC-CDMA users are 184. As seen in figures, there is a slightly error floor for both signal groups. However when this overload factor decreases for example to 37.5% error floor disappears. When figures 4.9 are compared with downlink NOMA-2000 with single transmitter system, i.e. figure 4.6, improvement on performance can be seen.

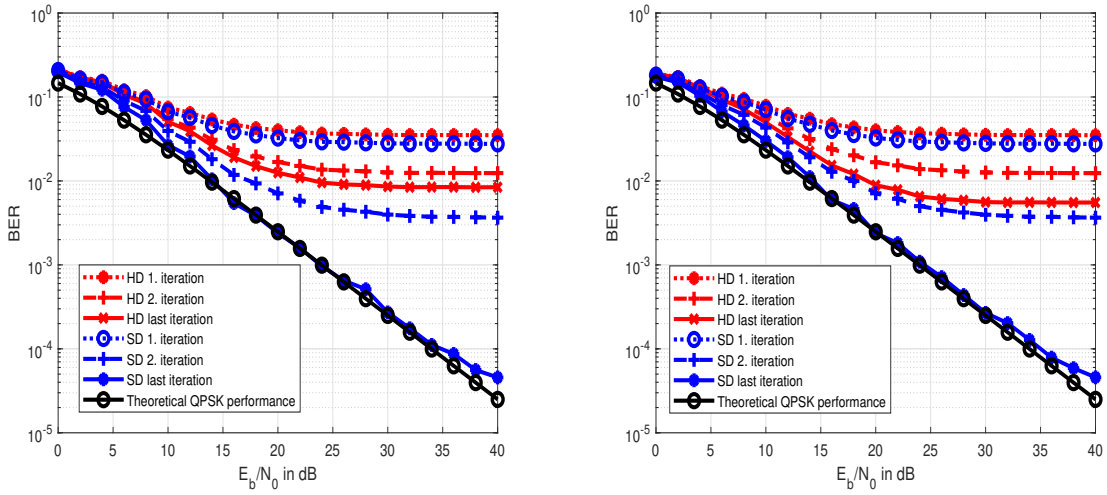

(a) OFDMA. (b) MC-CDMA.

Figure 4.9. Downlink BER performance of MISO based NOMA-2000. OF is 43.75%.

4.4. Channel Overloading NOMA Performance on Rayleigh Flat Fading Channel

4.4.1. Uplink

Assume one MC-CDMA symbol is spreaded onto k sub-carriers. Then according to equation (3.23) received signal is,

$$x_n = h_n \cdot a_n + h_{N+\lceil n/k \rceil} \cdot b_{\lceil n/k \rceil}/\sqrt{k} + u_n \tag{4.19}$$

where h's are channel coefficients. Matrix representation of the equation (4.19) for one signal group is,

$$\vec{x}_{\lceil n/k \rceil} = H_{(o)\lceil n/k \rceil} \cdot \vec{a}_{\lceil n/k \rceil} + H_{(m)\lceil n/k \rceil} \cdot \vec{b}_{\lceil n/k \rceil}/\sqrt{k} + \vec{u}_{\lceil n/k \rceil} \tag{4.20}$$

where $H_{(o)\lceil n/k \rceil}$ and $H_{(m)\lceil n/k \rceil}$ are diagonal matrices and their diagonal elements are $h_{\lceil n/k \rceil}$, $h_{\lceil n/k \rceil+1}$, $\cdots$, $h_{\lceil n/k \rceil+k-1}$ and $h_{N+\lceil n/k \rceil}$ respectively. For instance $k = 4$ and

$\lceil n/k \rceil = 1$, then,

$$\begin{bmatrix} x_1 \\ x_2 \\ x_3 \\ x_4 \end{bmatrix} = \begin{bmatrix} h_1 & 0 & 0 & 0 \\ 0 & h_2 & 0 & 0 \\ 0 & 0 & h_3 & 0 \\ 0 & 0 & 0 & h_4 \end{bmatrix} \cdot \begin{bmatrix} a_1 \\ a_2 \\ a_3 \\ a_4 \end{bmatrix} + \begin{bmatrix} h_{N+1} & 0 & 0 & 0 \\ 0 & h_{N+1} & 0 & 0 \\ 0 & 0 & h_{N+1} & 0 \\ 0 & 0 & 0 & h_{N+1} \end{bmatrix} \cdot \begin{bmatrix} b_1/2 \\ b_1/2 \\ b_1/2 \\ b_1/2 \end{bmatrix} + \begin{bmatrix} u_1 \\ u_2 \\ u_3 \\ u_4 \end{bmatrix}. \tag{4.21}$$

Detection philosophy is same with AWGN case. However phase shift on OFDMA symbols should be removed before starting process. In the sight of equation (1.6), equation (4.21) can be also shown as,

$$\begin{bmatrix} x_1 \\ x_2 \\ x_3 \\ x_4 \end{bmatrix} = \begin{bmatrix} \alpha_1 e^{j\theta_1} & 0 & 0 & 0 \\ 0 & \alpha_2 e^{j\theta_2} & 0 & 0 \\ 0 & 0 & \alpha_3 e^{j\theta_3} & 0 \\ 0 & 0 & 0 & \alpha_4 e^{j\theta_4} \end{bmatrix} \cdot \begin{bmatrix} a_1 \\ a_2 \\ a_3 \\ a_4 \end{bmatrix} + \begin{bmatrix} h_{N+1} & 0 & 0 & 0 \\ 0 & h_{N+1} & 0 & 0 \\ 0 & 0 & h_{N+1} & 0 \\ 0 & 0 & 0 & h_{N+1} \end{bmatrix} \cdot \begin{bmatrix} b_1/2 \\ b_1/2 \\ b_1/2 \\ b_1/2 \end{bmatrix} + \begin{bmatrix} u_1 \\ u_2 \\ u_3 \\ u_4 \end{bmatrix}. \tag{4.22}$$

In order to remove phase shift effect, $\vec{x}$ is multiplied by a diagonal matrix and its elements are $e^{-j\theta_1},\ e^{-j\theta_2},\ e^{-j\theta_3},\ e^{-j\theta_4}$. Assume result is $\vec{x}'$ then,

$$\begin{bmatrix} x'_1 \\ x'_2 \\ x'_3 \\ x'_4 \end{bmatrix} = \begin{bmatrix} \alpha_1 & 0 & 0 & 0 \\ 0 & \alpha_2 & 0 & 0 \\ 0 & 0 & \alpha_3 & 0 \\ 0 & 0 & 0 & \alpha_4 \end{bmatrix} \cdot \begin{bmatrix} a_1 \\ a_2 \\ a_3 \\ a_4 \end{bmatrix} + \begin{bmatrix} \frac{h_{N+1}e^{-j\theta_1}}{2} & 0 & 0 & 0 \\ 0 & \frac{h_{N+1}e^{-j\theta_2}}{2} & 0 & 0 \\ 0 & 0 & \frac{h_{N+1}e^{-j\theta_3}}{2} & 0 \\ 0 & 0 & 0 & \frac{h_{N+1}e^{-j\theta_4}}{2} \end{bmatrix} \cdot \begin{bmatrix} b_1 \\ b_1 \\ b_1 \\ b_1 \end{bmatrix} + \begin{bmatrix} u'_1 \\ u'_2 \\ u'_3 \\ u'_4 \end{bmatrix} \tag{4.23}$$

where $u'_i = u_i e^{-j\theta_i}$. Notice that,

$$\begin{aligned} E[u_i e^{-j\theta_i}] &= E[u_i] \cdot E[e^{-j\theta_i}] = E[u_i] \\ E[(u_i e^{-j\theta_i})^2] &= E[(u_i e^{-j\theta_i})(u_i e^{j\theta_i})] = E[u_i^2]. \end{aligned} \tag{4.24}$$

Equation (4.24) says that the statistical character of the noise does not change. Now detection process can be summarized as,

• *Step-1*: Symbol b_1 is accepted as $1 + j$. Then it is multiplied with its coefficient matrix that is defined in equation (4.23) and result is subtracted from $x'_1,\ x'_2,\ x'_3,\ x'_4$ or $\vec{x}'$. After that subtracted symbols are given into a threshold detector in order to detect OFDMA symbols $a_1,\ a_2,\ a_3$ and a_4. Notice that threshold detector boundaries are multiplied by α_1 for symbol a_1, α_2 for symbol a_2, α_3 for symbol a_3 and α_4 for symbol a_4. Let say detected OFDMA symbols are $\hat{a}_{11},\ \hat{a}_{12},\ \hat{a}_{13},\ \hat{a}_{14}$. System's error is calculated and let say it is represented by e_1.

• *Step-2*: Symbol b_1 is accepted as $1 - j$. Then it is multiplied with its coefficient matrix and result is subtracted from $\vec{x}'$. After that subtracted symbols are given into a threshold detector. Detected OFDMA symbols are $\hat{a}_{21},\ \hat{a}_{22},\ \hat{a}_{23},\ \hat{a}_{24}$. System's error is calculated it is represented by e_2.

• *Step-3*: Symbol b_1 is accepted as $-1 + j$. Then it is multiplied with its coefficient matrix and result is subtracted from $\vec{x}'$. After that subtracted symbols are given into a threshold detector. Detected OFDMA symbols are $\hat{a}_{31},\ \hat{a}_{32},\ \hat{a}_{33},\ \hat{a}_{34}$. System's error is calculated it is represented by e_3.

• *Step-4*: Symbol b_1 is accepted as $-1 - j$. Then it is multiplied with its coefficient matrix and result is subtracted from $\vec{x}'$. After that subtracted symbols are given into a threshold detector. Detected OFDMA symbols are $\hat{a}_{41},\ \hat{a}_{42},\ \hat{a}_{43},\ \hat{a}_{44}$. System's error is calculated it is represented by e_4.

• *Step-5*: Detected symbols now become estimated symbols in previous steps whose error is minimum.

4.4.2. Downlink

Received signal in downlink channel is,

$$x_n = h \cdot \left[a_n + b_{\lceil n/k \rceil}/\sqrt{k}\right] + u_n \tag{4.25}$$

where h is fading coefficient and one MC-CDMA symbol is spreaded onto k sub-carriers. Matrix representation of the equation (4.25) for $k = 4$ is,

$$\begin{bmatrix} x_1 \\ x_2 \\ x_3 \\ x_4 \end{bmatrix} = \begin{bmatrix} h & 0 & 0 & 0 \\ 0 & h & 0 & 0 \\ 0 & 0 & h & 0 \\ 0 & 0 & 0 & h \end{bmatrix} \cdot \begin{bmatrix} a_1 \\ a_2 \\ a_3 \\ a_4 \end{bmatrix} + \begin{bmatrix} h & 0 & 0 & 0 \\ 0 & h & 0 & 0 \\ 0 & 0 & h & 0 \\ 0 & 0 & 0 & h \end{bmatrix} \cdot \begin{bmatrix} b_1/2 \\ b_1/2 \\ b_1/2 \\ b_1/2 \end{bmatrix} + \begin{bmatrix} u_1 \\ u_2 \\ u_3 \\ u_4 \end{bmatrix}. \tag{4.26}$$

Detection process is same with uplink.

4.4.3. Performance Results

Figure 4.10 shows the performance of the channel overloading NOMA for $k = 2$ and $k = 1$ in uplink non-frequency selective Rayleigh channel. OFDMA 16QAM and MC-CDMA symbols are QPSK modulated. Their performance are compared with bit error probability of the 16QAM and QPSK in Rayleigh fading channel. In the absence of the MC-CDMA symbols, equation (4.19)

$$x_n = h_n \cdot a_n + u_n \tag{4.27}$$

and that is a simple Rayleigh flat fading channel model. In same the manner, corresponding OMA for MC-CDMA users is,

$$x_n = h_{N+\lceil n/k \rceil} \cdot b_{\lceil n/k \rceil}/\sqrt{k} + u_n. \tag{4.28}$$

If $k = 2$ and for $n = 1,\ 2$ then,

$$\begin{aligned} x_1 &= h_{N+1} \cdot b_1/\sqrt{2} + u_1, \\ x_2 &= h_{N+1} \cdot b_1/\sqrt{2} + u_2. \end{aligned} \tag{4.29}$$

Summation of the 2 signals is exactly same with,

$$x' = h_{N+1} \cdot \sqrt{2} \cdot b_1 + u_1 + u_2. \tag{4.30}$$

Notice that since noise are uncorrelated and have same variance $E[(u_1+u_2)^2] = 2 \cdot E[u_i]$ for $i = 1,\ 2$. In addition $E[(\sqrt{2} \cdot b_1)^2] = 2 \cdot E[b_1^2]$. It means that SNR is $\frac{E[h_{N+1}^2]E_{QPSK}}{E_{noise}}$. As it can be seen that corresponding OMA for MC-CDMA is exactly same with a QPSK performance in flat fading Rayleigh channel. As seen in figure 4.10(a) channel

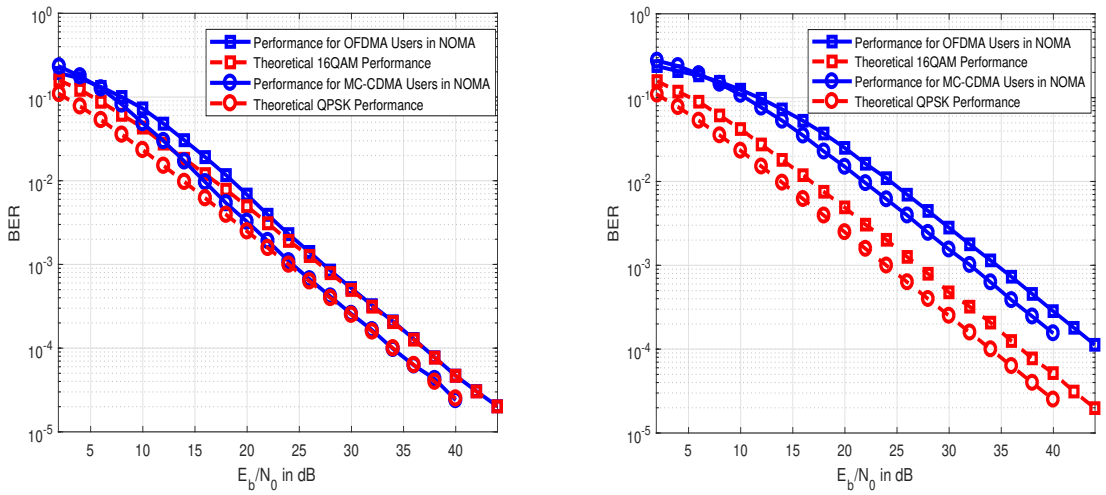

(a) OF = 50%. (b) OF = 100%.

Figure 4.10. Uplink BER performance of channel overloading NOMA for 16QAM modulated OFDMA and QPSK modulated MC-CDMA.

overloading NOMA performs very sufficient BER performance for 50% OF. However system faces with an SNR degradation about 7 dB if OF become 100%. It is easy to see that when OF is 100% system turns into simple power domain NOMA.

When both OFDMA and MC-CDMA are QPSK modulated BER performance increases according to 16QAM modulated OFDMA vs QPSK modulated MC-CDMA. However there is still SNR degradation around 5 dB for 100% OF.

In downlink system, since there is no power imbalance between OFDMA and MC-CDMA users SNR degradation is inevitable. Figure 4.12 shows SNR performance of the 16QAM and QPSK modulated OFDMA with QPSK modulated MC-CDMA

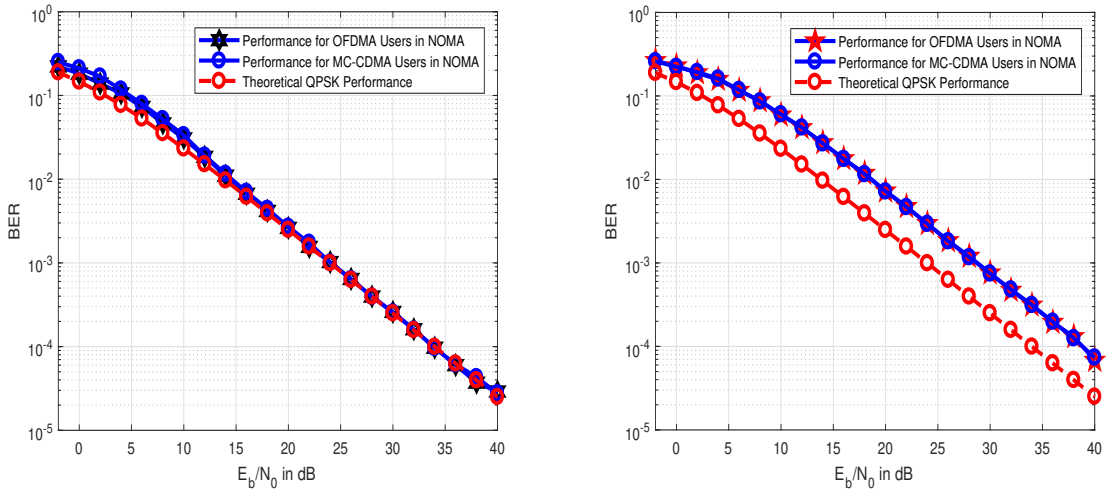

(a) OF = 50%. (b) OF = 100%.

Figure 4.11. Uplink BER performance of channel overloading NOMA for QPSK modulated OFDMA and MC-CDMA.

symbol. OF is 50%. When both symbols are QPSK modulated, SNR degradation is around 4 dB as seen in fiugre 4.12(a).

4.5. Channel Overloading NOMA with Dynamic User Grouping

In uplink system, since channel coefficients are different for each user, users with strongest channel coefficient are assigned to OFDM waveform. Hence S/I can be reduced and system can deal with higher OF. In addition since a user is assigned to OFDMA and MC-CDMA system dynamically, she/he has a fair BER performance. All these positive sights and system description were explained in section 4.2. Only difference is that $M = 1$ and N can take any value depending on desired OF. In addition to that detection process is also same with classical channel overloading NOMA.

4.5.1. Performance Results

Since users' multiple access method is determined according to their channel state information, BER performances are shown in single graph. In other words they do not be illustrated for OFDMA and MC-CDMA separately.

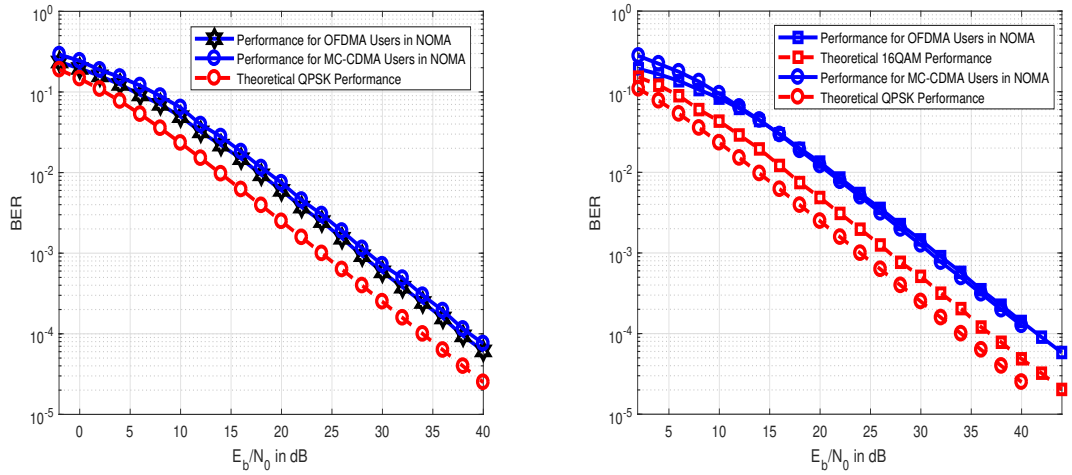

(a) OFDMA and MC-CDMA are QPSK modulated.

(b) OFDMA 16QAM, MC-CDMA is QPSK modulated.

Figure 4.12. Downlink BER performance of channel overloading NOMA for OFDMA and MC-CDMA. OF is 50%.

Figure 4.13 demonstrates 16QAM modulated OFDMA with QPSK modulated MC-CDMA performances for 50% and 100% OF. Average bit to noise ration is given in equation (4.11). Theoretical lower limit is corresponding OMA performances. As seen in figure 4.13(a), BER performance with 50% OF is very sufficient. Moreover dynamic user grouping increases BER performance when OF is 50%. However since there are only two users when OF is 100% and detection is ML, there is no differences between performances with and without user groping. When both MA systems are QPSK modulated, performances are shown in figure 4.14. Same things are also valid for this system.

In this chapter, bit error performances of the NOMA-2000 and channel overloading NOMA were given in non-frequency selective uncorrelated Rayleigh fading channel. In addition to that, modifications at the receiver side were also shown in order to cope with fading effect. Dynamic user grouping strategy and MISO based NOMA-2000 systems were suggested to increase NOMA-2000 performances in uplink and downlink channels respectively. At the next chapter, these NOMA concepts performances will be investigated in more severe channel condition.

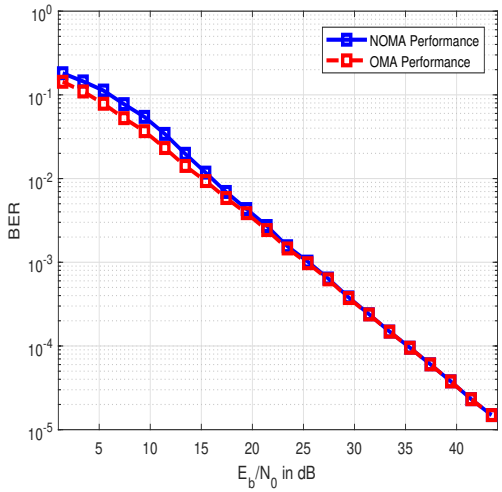

(a) OF = 50%.

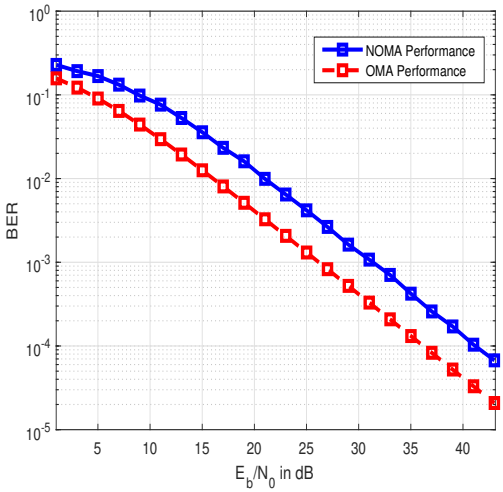

(b) OF = 100%.

Figure 4.13. Uplink BER performance of channel overloading NOMA with dynamic user grouping for 16QAM modulated OFDMA and QPSK modulated MC-CDMA.

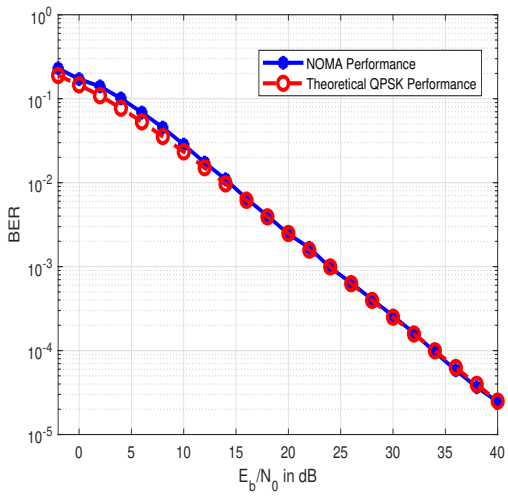

(a) OF = 50%.

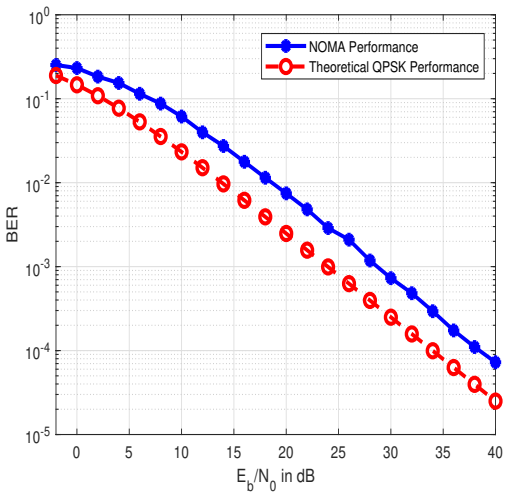

(b) OF = 100%.

Figure 4.14. Uplink BER performance of channel overloading NOMA with dynamic user grouping for QPSK modulated OFDMA and MC-CDMA.

5. FREQUENCY DOMAIN NOMA IN FREQUENCY SELECTIVE RAYLEIGH FADING CHANNEL

In this chapter, the performances of the frequency domain NOMA on uncorrelated frequency selective Rayleigh channel will be introduced. This channel conditions is more severe than previous one. Frequency selective Rayleigh channel means that channel coefficients are different for distinct sub-carriers, even if all sub-carriers are belong to same user.

5.1. NOMA-2000 Performance on Frequency Selective Rayleigh Fading Channel

5.1.1. Uplink

In frequency selective Rayleigh channel each sub-carrier is faded by different Rayleigh coefficient. Since channel model is uncorrelated Rayleigh channel, even if all sub-carriers belong to same user, we assume that there is no correlation between coefficients. In here each OFDMA sub-carriers are assigned to different users. After removing cyclic prefix and discrete Fourier transform (DFT) received signal at n^{th} sub-carrier for uplink is expressed as,

$$x_n = h_n \cdot a_n + \frac{1}{\sqrt{N}} \sum_{m=1}^{M} p_{n,m}(w_{n,m} b_m) + u_n \tag{5.1}$$

where a_n is corresponding OFDMA symbol and u_n is noise. b_m is MC-CDMA symbol of the m^{th} user and $w_{m,n}$ is n^{th} chip of the m^{th} MC-CDMA user. h_n is Rayleigh distributed channel coefficient of the n^{th} OFDMA user and $p_{n,m}$ is the channel coefficient of the n^{th} sub-carrier which belongs to m^{th} MC-CDMA user. Equation (5.1) with matrix notation is,

$$\vec{x}^{(u)} = H \cdot \vec{a} + P \cdot \vec{b} + \vec{u} \tag{5.2}$$

where $\vec{a} = [a_1, a_2, ..., a_N]^T$, $\vec{b} = [b_1, b_2, ..., b_M]^T$ and $\vec{u} = [u_1, u_2, ..., u_N]^T$. Matrices P and H are given as,

$$P = \frac{1}{\sqrt{N}} \cdot \begin{bmatrix} p_{1,1}w_{1,1} & p_{1,2}w_{1,2} & ..... & p_{1,M}w_{1,M} \\ p_{2,1}w_{2,1} & p_{2,2}w_{2,2} & ..... & p_{2,M}w_{2,M} \\ \vdots & \vdots & \ddots & \vdots \\ p_{N,1}w_{N,1} & p_{N,2}w_{N,2} & ..... & p_{N,M}w_{N,M} \end{bmatrix}_{N \times M} \tag{5.3}$$

$$H = \begin{bmatrix} h_1 & 0 & ..... & 0 \\ 0 & h_2 & ..... & 0 \\ \vdots & \vdots & \ddots & \vdots \\ 0 & 0 & ..... & h_N \end{bmatrix}_{N \times N} . \tag{5.4}$$

Assume all channel coefficients and noise power are perfectly known by receiver. The best detection technique is that maximum-likelihood detection (see [7] and [9]). If OFDMA symbols P-QAM and MC-CDMA symbols are T-QAM modulated, $P^N \times T^M$ different symbols combinations are placed into equation (4.2) and one of them with minimum error are chosen. Therefore it is almost impossible to implement. Second choice is trying to remove the effects of the channel coefficients then applying iterative SIC. Linear detection technique is used because of its simplicity and calculation cost efficient. Since channel state information of the all users and noise power are known minimum mean square error (MMSE) block linear equalizer is used [7].

Assume $E_{(o)}$ and $E_{(m)}$ are equalization matrices for OFMDA and MC-CDMA symbols respectively. They are given as,

$$\begin{aligned} E_{(o)} &= \left(H^H \cdot H + I_{N \times N} \cdot SNR^{-1}_{OFDMA}\right)^{-1} \cdot H^H \\ E_{(m)} &= \left(P^H \cdot P + I_{M \times M} \cdot SNR^{-1}_{MC-CDMA}\right)^{-1} \cdot P^H \end{aligned} \tag{5.5}$$

where I is identity matrix. Notice that equalizer matrix $E_{(m)}$ also include despreading. Hard and soft detection with t step is exactly same with equation (4.4) and (4.5). Instead of $H_{(o)}$ and $H_{(m)}$, matrices H and P are used respectively.

5.1.2. Downlink

For a particular user, there are N different channel coefficients and each of them affect a corresponding sub-carrier in downlink system. Received signal is given as,

$$x_n = h_n \cdot \left(a_n + \frac{1}{\sqrt{N}} \sum_{m=1}^{M} w_{n,m} b_m \right) + u_n \tag{5.6}$$

where h_n is the coefficient of the n^{th} sub-carrier. As seen in equation (5.6), some of the sub-carriers with low coefficient can be said eliminated. Therefore this channel is called as frequency selective channel. Matrix representation of this equation is,

$$\vec{x} = H \cdot \left(\vec{a} + \frac{1}{\sqrt{N}} W \cdot \vec{b} \right) + \vec{u} \tag{5.7}$$

where $\vec{a}$, $\vec{b}$ and $\vec{u}$ are given as in equation (5.2). Matrices W and H are given in equations (3.6) and (5.4) respectively.

5.1.3. Performance Results

The performance of the NOMA concepts are compared with corresponding OMA. It means that for uplink, according to equation (5.2) corresponding OMA systems are,

$$\begin{aligned} \vec{x}_{(o)} &= H \cdot \vec{a} + \vec{u} \\ \vec{x}_{(c)} &= P \cdot \vec{b} + \vec{u} \end{aligned} \tag{5.8}$$

for OFMDA and MC-CDMA respectively. Figure 5.1 shows 256 16QAM modulated OFDMA users and 80 QPSK modulated MC-CDMA users' performances. Notice that corresponding OMA performance for OFDMA is theoretical 16QAM Rayleigh.

When both symbol groups are QPSK modulated overload factor that system can deal

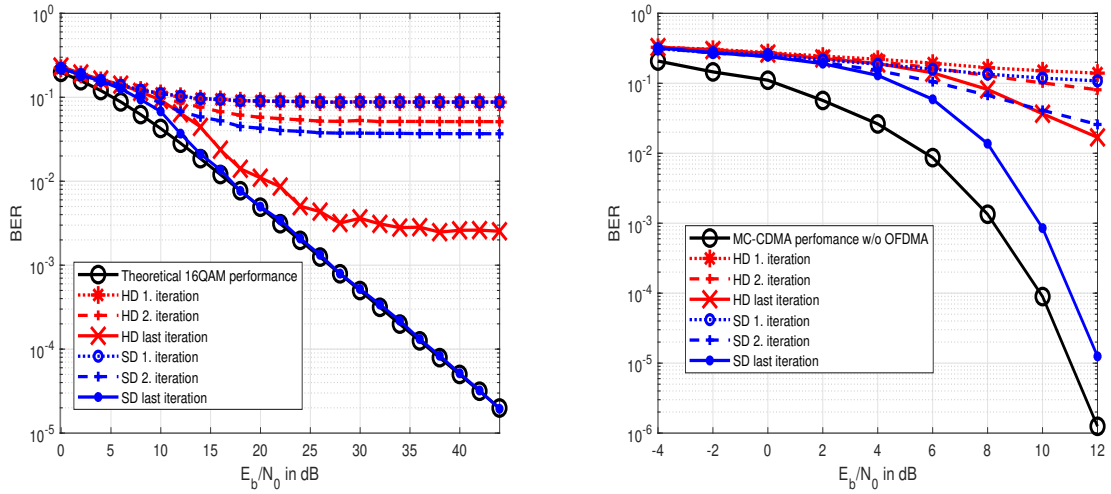

(a) OFDMA. (b) MC-CDMA.

Figure 5.1. Uplink BER performance of NOMA-2000 in frequency selective Rayleigh channel for 16QAM modulated OFDMA and QPSK modulated MC-CDMA. OF is 31.25%

with considerably less SNR degradation increases as expected. Figure 5.2 demonstrate this scenario with 116 MC-CDMA and 256 OFDMA users. Zero SNR degradation is achieved for OFDMA whereas it is not valid for MC-CDMA.

5.2. Channel Overloading NOMA Performance on Frequency Selective Rayleigh Fading Channel

5.2.1. Uplink

All sub-carriers even if they belong to same user, are faded by uncorrelated channel coefficient. If a MC-CDMA symbol is spreaded onto k sub-carrier, the received signal is,

$$x_n = h_n \cdot a_n + h_{N+n} \cdot b_{\lceil n/k \rceil}/\sqrt{k} + u_n \tag{5.9}$$

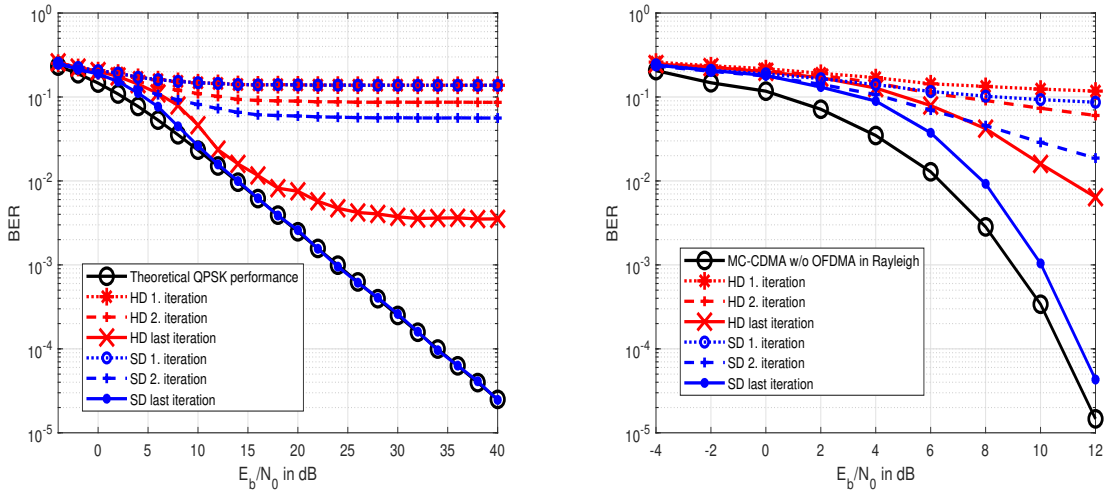

(a) OFDMA. (b) MC-CDMA.

Figure 5.2. Uplink BER performance of NOMA-2000 in frequency selective Rayleigh channel for QPSK modulated OFDMA and MC-CDMA. OF is 45.3%

where h's are channel coefficients. The matrix representation of the equation (5.9) for one signal group is,

$$\vec{x}_{\lceil n/k \rceil} = H_{(o)\lceil n/k \rceil} \cdot \vec{a}_{\lceil n/k \rceil} + H_{(m)\lceil n/k \rceil} \cdot \vec{b}_{\lceil n/k \rceil}/\sqrt{k} + \vec{u}_{\lceil n/k \rceil} \tag{5.10}$$

where $H_{(o)\lceil n/k \rceil}$ and $H_{(m)\lceil n/k \rceil}$ are diagonal matrices and their diagonal elements are $h_{\lceil n/k \rceil}$, $h_{\lceil n/k \rceil+1}$, $\cdots$, $h_{\lceil n/k \rceil+k-1}$ and h_{N+1}, h_{N+2}, $\cdots$, h_{N+k} respectively. For instance $k = 4$ and $\lceil n/k \rceil = 1$, then,

$$\begin{bmatrix} x_1 \\ x_2 \\ x_3 \\ x_4 \end{bmatrix} = \begin{bmatrix} h_1 & 0 & 0 & 0 \\ 0 & h_2 & 0 & 0 \\ 0 & 0 & h_3 & 0 \\ 0 & 0 & 0 & h_4 \end{bmatrix} \cdot \begin{bmatrix} a_1 \\ a_2 \\ a_3 \\ a_4 \end{bmatrix} + \begin{bmatrix} h_{N+1} & 0 & 0 & 0 \\ 0 & h_{N+2} & 0 & 0 \\ 0 & 0 & h_{N+3} & 0 \\ 0 & 0 & 0 & h_{N+4} \end{bmatrix} \cdot \begin{bmatrix} b_1/2 \\ b_1/2 \\ b_1/2 \\ b_1/2 \end{bmatrix} + \begin{bmatrix} u_1 \\ u_2 \\ u_3 \\ u_4 \end{bmatrix}. \tag{5.11}$$

Detection process is same with detection process that is described section 4.4.1. Only difference is that coefficients matrix of the MC-CDMA symbol in equation (4.23). Now its diagonal elements become $(h_{N+1}e^{-j\theta_1})/2$, $(h_{N+2}e^{-j\theta_2})/2$, $(h_{N+3}e^{-j\theta_3})/2$ and $(h_{N+4}e^{-j\theta_4})/2$.

5.2.2. Downlink

Received signal in downlink channel is,

$$x_n = h_n \cdot \left[a_n + b_{\lceil n/k \rceil}/\sqrt{k}\right] + u_n \tag{5.12}$$

where h is fading coefficient and one MC-CDMA symbol is spreaded onto k sub-carriers. Matrix representation of the equation (5.12) for $k = 4$ is,

$$\begin{bmatrix} x_1 \\ x_2 \\ x_3 \\ x_4 \end{bmatrix} = \begin{bmatrix} h_1 & 0 & 0 & 0 \\ 0 & h_2 & 0 & 0 \\ 0 & 0 & h_3 & 0 \\ 0 & 0 & 0 & h_4 \end{bmatrix} \cdot \begin{bmatrix} a_1 \\ a_2 \\ a_3 \\ a_4 \end{bmatrix} + \begin{bmatrix} h_1 & 0 & 0 & 0 \\ 0 & h_2 & 0 & 0 \\ 0 & 0 & h_3 & 0 \\ 0 & 0 & 0 & h_4 \end{bmatrix} \cdot \begin{bmatrix} b_1/2 \\ b_1/2 \\ b_1/2 \\ b_1/2 \end{bmatrix} + \begin{bmatrix} u_1 \\ u_2 \\ u_3 \\ u_4 \end{bmatrix}. \tag{5.13}$$

Detection process is same with uplink.

5.2.3. Performance Results

The bit error rate performances of the channel overloading NOMA are demonstrated for 25% overload factor. Blue lines represent corresponding OMA performances. MC-CDMA symbol is detected by using maximum ratio combining in OMA. according to figures 5.3, OFDM modulated symbols immediately achieve their OMA bit error rate performances at uplink. However MC-CDMA symbol is 4 dB far from its corresponding OMA performance.

The performance results are almost same for downlink. MC-CDMA symbol is now only 2 dB worse than corresponding OMA system.

In this chapter, bit error performances of the NOMA-2000 and channel overloading NOMA were given in frequency selective uncorrelated Rayleigh fading channel. In addition to that, modifications at the receiver side were also shown in order to cope with fading effect. At the next chapter, the bit error analysis of the power domain

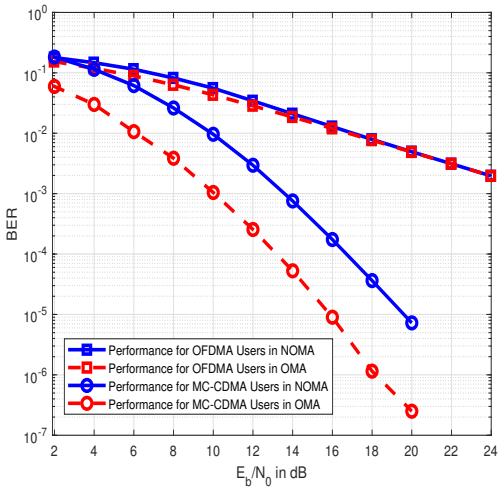

(a) OFDMA is 16QAM, MC-CDMA is QPSK modulated.

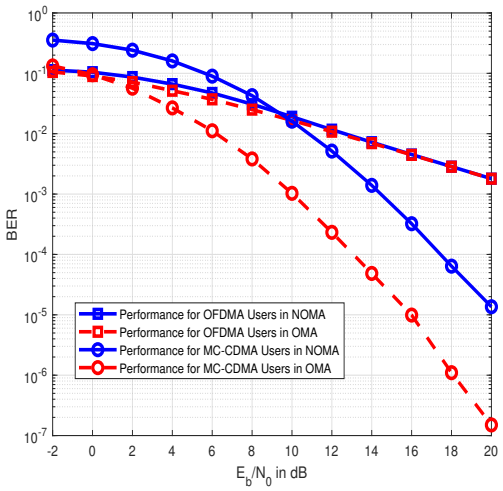

(b) OFDMA and MC-CDMA are QPSK modulated.

Figure 5.3. Uplink BER performance of the channel overloading NOMA in frequency selective Rayleigh channel. OF is 25%

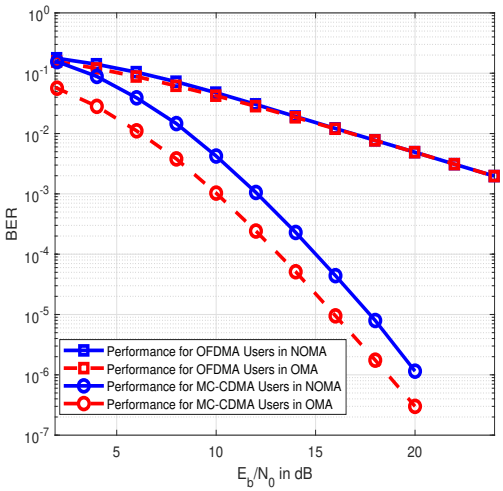

(a) OFDMA is 16QAM, MC-CDMA is QPSK modulated.

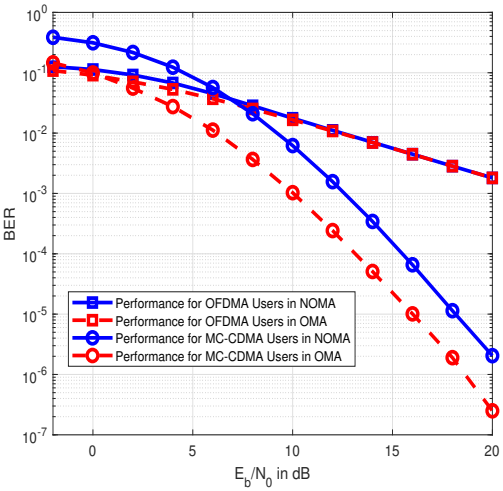

(b) OFDMA and MC-CDMA are QPSK modulated.

Figure 5.4. Downlink BER performance of the channel overloading NOMA in frequency selective Rayleigh channel. OF is 25%

NOMA and NOMA-2000 at the first iteration will be given for AWGN channels. In addition to that optimum power imbalance between users will shown for power domain NOMA in order to minimize total bit error rate.

6. ERROR ANALYSIS

6.1. Error Probability of the Simple Power Domain NOMA

In this non-orthogonal multiple access concept, there are two users and their symbols are A and B respectively. Symbol energy is $\sqrt{E_s}$, modulation is BPSK and channel is considered as AWGN for the sake of simplicity. If noise is represented with η variance is σ^2 and received signal is r,

$$r = A + h \cdot B + \eta \tag{6.1}$$

where h is coefficient of symbol B and it is between 0 and 1.

In demodulation process, first step is that symbol with higher energy is estimated. Then, this estimation is subtracted from received signal, and second symbol is tried to detect by using this subtraction,

$$r - \hat{A} = A - \hat{A} + h \cdot B + \eta. \tag{6.2}$$

Probability of the error A is,

$$\begin{aligned}
\mathbb{P}(A \neq \hat{A}) &= E_{A,B}\big[Pr(error|A,B)\big] \\
&= Pr(A = \sqrt{E_s}, B = \sqrt{E_s}) \cdot Pr(r < 0 | A = \sqrt{E_s}, B = \sqrt{E_s}) \\
&+ Pr(A = -\sqrt{E_s}, B = \sqrt{E_s}) \cdot Pr(r > 0 | A = -\sqrt{E_s}, B = \sqrt{E_s}) \\
&+ Pr(A = \sqrt{E_s}, B = -\sqrt{E_s}) \cdot Pr(r < 0 | A = \sqrt{E_s}, B = -\sqrt{E_s}) \\
&+ Pr(A = -\sqrt{E_s}, B = -\sqrt{E_s}) \cdot Pr(r > 0 | A = -\sqrt{E_s}, B = -\sqrt{E_s}).
\end{aligned} \tag{6.3}$$

Since symbols A and B are independent $Pr(A = a, B = b) = Pr(A = a) \cdot Pr(B = b)$ and all transmitted data has equal probability which is 1/2, equation (6.3) turns into,

$$\begin{aligned}\mathbb{P}(A \neq \hat{A}) =& \frac{1}{4} \cdot Pr(r < 0 | A = \sqrt{E_s}, B = \sqrt{E_s}) \\ &+ \frac{1}{4} \cdot Pr(r > 0 | A = -\sqrt{E_s}, B = \sqrt{E_s}) \\ &+ \frac{1}{4} \cdot Pr(r < 0 | A = \sqrt{E_s}, B = -\sqrt{E_s}) \\ &+ \frac{1}{4} \cdot Pr(r > 0 | A = -\sqrt{E_s}, B = -\sqrt{E_s}).\end{aligned} \tag{6.4}$$

If X is a normal distribution with variance σ^2 and mean value μ, then the probability $P(X > x) = Q(\frac{x-\mu}{\sigma})$ and $P(X < x) = Q(\frac{-x+\mu}{\sigma})$ as stated in [9]. Now, equation (6.4) with Q-function is,

$$\begin{aligned}\mathbb{P}(A \neq \hat{A}) =& \frac{1}{4} \cdot Q\Big(\frac{(1+h)\sqrt{E_s}}{\sigma}\Big) + \frac{1}{4} \cdot Q\Big(\frac{(1-h)\sqrt{E_s}}{\sigma}\Big) \\ &+ \frac{1}{4} \cdot Q\Big(\frac{(1-h)\sqrt{E_s}}{\sigma}\Big) + \frac{1}{4} \cdot Q\Big(\frac{(1+h)\sqrt{E_s}}{\sigma}\Big).\end{aligned} \tag{6.5}$$

With some mathematical manipulation, equation (6.5) becomes,

$$\mathbb{P}(A \neq \hat{A}) = \frac{1}{2} \sum_{k=0}^{1} Q\Big(\frac{\sqrt{E_s}[1 - (1-2k) \cdot h]}{\sigma}\Big). \tag{6.6}$$

Calculating the error probability of the symbol B is a little bit different. The general strategy of this calculation is similar with equation (6.3) and it is given as

$$\begin{aligned}\mathbb{P}(B \neq \hat{B}) &= E_{A,\hat{A},B}\big[Pr(error \mid A, \hat{A}, B)\big] \\ &= \sum_{a,\hat{a},b} Pr(A = a, \hat{A} = \hat{a}, B = b) \cdot Pr(B \neq \hat{B} \mid A = a, \hat{A} = \hat{a}, B = b).\end{aligned} \tag{6.7}$$

Notice that the error probability of symbol B is,

$$\begin{aligned}\mathbb{P}(B \neq \hat{B}) =& Pr(\hat{B} = -\sqrt{E_s} \mid B = \sqrt{E_s}) \cdot Pr(B = \sqrt{E_s}) \\ &+ Pr(\hat{B} = \sqrt{E_s} \mid B = -\sqrt{E_s}) \cdot Pr(B = -\sqrt{E_s}) \\ =& Pr(\hat{B} = -\sqrt{E_s} \mid B = \sqrt{E_s}).\end{aligned} \tag{6.8}$$

In order to reduce calculation cost, only $Pr(\hat{B} = -\sqrt{E_s} \mid B = \sqrt{E_s})$ is tried to find. If equation (6.7) and (6.8) are combined, we get

$$\begin{aligned}&\mathbb{P}(\hat{B} = -\sqrt{E_s} \mid B = \sqrt{E_s}) \\ &= E_{A,\hat{A}}\big[Pr(\hat{B} = -\sqrt{E_s} \mid A = a, \hat{A} = \hat{a}, B = \sqrt{E_s})\big] \\ &= \sum_{a,\hat{a}} Pr(A = a, \hat{A} = \hat{a} \mid B = \sqrt{E_s}) \\ &\cdot Pr(\hat{B} = -\sqrt{E_s} \mid A = a, \hat{A} = \hat{a}, B = \sqrt{E_s}) \\ &= \sum_{a,\hat{a}} Pr(A = a \mid B = \sqrt{E_s}) \cdot Pr(\hat{A} = \hat{a} \mid A = a, B = \sqrt{E_s}) \\ &\cdot Pr(\hat{B} = -\sqrt{E_s} \mid A = a, \hat{A} = \hat{a}, B = \sqrt{E_s}) \\ &\overset{(1)}{=} \sum_{a,\hat{a}} \frac{1}{2} \cdot Pr(\hat{A} = \hat{a} \mid A = a, B = \sqrt{E_s}) \cdot \\ &Pr(\hat{B} = -\sqrt{E_s} \mid A = a, \hat{A} = \hat{a}, B = \sqrt{E_s}) \\ &= \sum_{a,\hat{a}} \frac{1}{2} \cdot Pr(a + h \cdot \sqrt{E_s} + \eta \underset{\hat{a}=\sqrt{E_s}}{\overset{\hat{a}=-\sqrt{E_s}}{\lessgtr}} 0 \mid A = a, B = \sqrt{E_s}) \\ &\cdot Pr(a - \hat{a} + h\sqrt{E_s} + \eta < 0 \mid A = a, \hat{A} = \hat{a}, B = \sqrt{E_s}) \\ &= \sum_{a,\hat{a}} \frac{1}{2} \cdot Pr(\eta \underset{\hat{a}=\sqrt{E_s}}{\overset{\hat{a}=-\sqrt{E_s}}{\lessgtr}} -a - h \cdot \sqrt{E_s} \mid A = a, B = \sqrt{E_s}) \\ &\cdot Pr(\eta < -a + \hat{a} - h\sqrt{E_s} \mid A = a, \hat{A} = \hat{a}, B = \sqrt{E_s}) \\ &= \sum_{a,\hat{a}} \frac{1}{2} \cdot Q\Big(\frac{sgn[\hat{a}](-a - h\sqrt{E_s})}{\sigma}\Big) \\ &\cdot Pr(\eta < -a + \hat{a} - h\sqrt{E_s} \mid A = a, \hat{A} = \hat{a}, B = \sqrt{E_s}).\end{aligned} \tag{6.9}$$

where $sgn[.]$ is sign function. Step (1) comes from that since symbols A and B are independent, $Pr(A = a \mid B = \sqrt{E_s}) = Pr(A = a)$. Notice that in the last step

of the equation (6.9) for given A, $\hat{A}$ and B, corresponding η is not purely Gaussian distributed. For instance, if $A = \sqrt{E_s}$, $\hat{A} = -\sqrt{E_s}$ and $B = \sqrt{E_s}$, it means that $\sqrt{E_s} + h\sqrt{E_s} + \eta < 0$. Therefore the distribution of η for given A, $\hat{A}$ and B is truncated Gaussian.

Assume u is Gaussian distributed random variable with mean μ and variance σ^2. If u' is defined as

$$u' = \begin{cases} u & u \in [a,\ b] \\ 0 & o.w. \end{cases} \tag{6.10}$$

Probability density function (PDF) of u' in equation (6.10) is,

$$f(u') = \begin{cases} \frac{1}{\sigma\sqrt{2\pi}} \cdot e^{\frac{-(u'-\mu)^2}{2\sigma^2}} \cdot \frac{1}{Q\left(\frac{a-\mu}{\sigma}\right) - Q\left(\frac{b-\mu}{\sigma}\right)}, & u' \in [a,\ b] \\ 0, & o.w. \end{cases} \tag{6.11}$$

Notice that for given $A = a$ and $B = \sqrt{E_s}$ received signal is $a + h\sqrt{E_s} + \eta$. If $\hat{A}$ is also given as $\hat{a}$, η must satisfy following inequality,

$$\begin{aligned} a + h\sqrt{E_s} + \eta &\underset{\hat{a}=-\sqrt{E_s}}{\overset{\hat{a}=\sqrt{E_s}}{\gtrless}} 0, \\ \eta &\underset{\hat{a}=-\sqrt{E_s}}{\overset{\hat{a}=\sqrt{E_s}}{\gtrless}} -a - h\sqrt{E_s}. \end{aligned} \tag{6.12}$$

Then according to equation (6.11), PDF of η for given $A = a$, $\hat{A} = \hat{a}$ and $B = \sqrt{E_s}$ is

$$f(\eta \mid A = a,\ \hat{A} = \hat{a},\ B = \sqrt{E_s}) = \begin{cases} \frac{e^{\frac{-\eta^2}{2\sigma^2}}}{\sigma\sqrt{2\pi}} \cdot \frac{I_\eta[-a-h\sqrt{E_s},\ +\infty]}{Q\left(\frac{sgn[\hat{a}](-a-h\sqrt{E_s})}{\sigma}\right)}, & \text{if } \hat{a} = \sqrt{E_s} \\ \frac{e^{\frac{-\eta^2}{2\sigma^2}}}{\sigma\sqrt{2\pi}} \cdot \frac{I_\eta[-\infty,\ -a-h\sqrt{E_s}]}{Q\left(\frac{sgn[\hat{a}](-a-h\sqrt{E_s})}{\sigma}\right)}, & \text{if } \hat{a} = -\sqrt{E_s} \end{cases} \tag{6.13}$$

where $I_\eta[m,\ n]$ is 1 if $\eta \in [m,\ n]$ and 0 otherwise. If we proceed equation (6.9) with equation (6.13), the error probability of the symbol B becomes,

$$\begin{aligned}\mathbb{P}(\hat{B} \neq B) =& Pr(\hat{B} = -\sqrt{E_s} \mid B = \sqrt{E_s}) \\ =& \sum_{a,\hat{a}} \frac{1}{2} \cdot Q\Big(\frac{sgn[\hat{a}](-a - h\sqrt{E_s})}{\sigma}\Big) \\ & \cdot Pr(\eta < -a + \hat{a} - h\sqrt{E_s} \mid A = a, \hat{A} = \hat{a}, B = \sqrt{E_s}) \\ =& \frac{1}{2} \sum_{a} Q\Big(\frac{-a - h\sqrt{E_s}}{\sigma}\Big) - Q\Big(\frac{-a + \sqrt{E_s} - h\sqrt{E_s}}{\sigma}\Big) \\ & + Q\Big(\frac{a + \sqrt{E_s} + h\sqrt{E_s}}{\sigma}\Big).\end{aligned} \tag{6.14}$$

Equation (6.14) gives the exact error probability of the user B. Total error probability of the users is,

$$\begin{aligned}\mathbb{P}_{error} &= \mathbb{P}_{error}(A) + \mathbb{P}_{error}(B) \\ &= \frac{1}{2}\Big[Q\Big(\frac{-1-h}{\sigma/\sqrt{E_s}}\Big) - Q\Big(\frac{-h}{\sigma/\sqrt{E_s}}\Big) + Q\Big(\frac{2+h}{\sigma/\sqrt{E_s}}\Big) + Q\Big(\frac{1-h}{\sigma/\sqrt{E_s}}\Big) \\ &\quad - Q\Big(\frac{2-h}{\sigma/\sqrt{E_s}}\Big) + Q\Big(\frac{h}{\sigma/\sqrt{E_s}}\Big) + Q\Big(\frac{1+h}{\sigma/\sqrt{E_s}}\Big) + Q\Big(\frac{1-h}{\sigma/\sqrt{E_s}}\Big)\Big] \\ &= \frac{1}{2}\Big[1 + 2 \cdot Q\Big(\frac{h}{\sigma/\sqrt{E_s}}\Big) - 2 \cdot Q\Big(\frac{h-1}{\sigma/\sqrt{E_s}}\Big) + Q\Big(\frac{h-2}{\sigma/\sqrt{E_s}}\Big)\Big].\end{aligned} \tag{6.15}$$

Since the derivative of the Q-function is $Q'(\frac{x-\mu}{\sigma}) = -\frac{1}{\sigma\sqrt{2\pi}} e^{-\frac{(x-\mu)^2}{2\sigma^2}}$, according to [31], derivative of total error with respect to h is,

$$\begin{aligned}\frac{\partial \mathbb{P}_{error}(h)}{\partial h} =& \frac{-1}{2\sigma\sqrt{2\pi}}\Big[2 \cdot exp\big(\frac{-h^2}{2\sigma^2/E_s}\big) \\ & - 2 \cdot exp\big(\frac{-(h-1)^2}{2\sigma^2/E_s}\big) + exp\big(\frac{-(h-2)^2}{2\sigma^2/E_s}\big)\Big]\end{aligned} \tag{6.16}$$

where $exp(.)$ is exponential function. If $\frac{\partial \mathbb{P}_{error}(h)}{\partial h}$ is equaled to zero, then we get

$$\begin{aligned} 0 &= 2 \cdot e^{\frac{-h^2}{\gamma}} - 2 \cdot e^{\frac{-(h-1)^2}{\gamma}} + e^{\frac{-(h-2)^2}{\gamma}} \\ &= e^{\frac{-h^2}{\gamma}}[2 - 2 \cdot e^{\frac{2h-1}{\gamma}} + e^{\frac{4h-4}{\gamma}}] \\ &= 2 - 2 \cdot e^{\frac{-1}{\gamma}} \cdot e^{\frac{2h}{\gamma}} + e^{\frac{-4}{\gamma}} \cdot e^{\frac{4h}{\gamma}} \end{aligned} \tag{6.17}$$

where $\gamma = 2\sigma^2/E_s$. If $x = e^{\frac{2h}{\gamma}}$, equation (6.17) turns into,

$$e^{\frac{-4}{\gamma}} \cdot x^2 - 2 \cdot e^{\frac{-1}{\gamma}} \cdot x + 2 = 0. \tag{6.18}$$

According to the quadratic equation solution,

$$\begin{aligned} x &= e^{\frac{2h}{\gamma}} \\ &= \frac{2 \cdot e^{\frac{-1}{\gamma}} \pm \sqrt{4e^{\frac{-2}{\gamma}} - 4e^{\frac{-4}{\gamma}}2}}{2e^{\frac{-4}{\gamma}}} \\ &= e^{\frac{3}{\gamma}} \pm e^{\frac{4}{\gamma}} \sqrt{e^{\frac{-2}{\gamma}} - 2e^{\frac{-4}{\gamma}}} \\ &= e^{\frac{3}{\gamma}} \pm e^{\frac{2}{\gamma}} \sqrt{e^{\frac{2}{\gamma}} - 2}. \end{aligned} \tag{6.19}$$

In order to minimize total BER, h value should be,

$$\begin{aligned} h &= \frac{\gamma}{2} \cdot \ln\Big(e^{\frac{3}{\gamma}} \pm e^{\frac{2}{\gamma}} \sqrt{e^{\frac{2}{\gamma}} - 2}\Big) \\ &= \frac{\sigma^2}{E_s} \cdot \ln\Big(e^{\frac{3E_s}{2\sigma^2}} \pm e^{\frac{E_s}{\sigma^2}} \sqrt{e^{\frac{E_s}{\sigma^2}} - 2}\Big). \end{aligned} \tag{6.20}$$

The solution of the equation (6.20) is 0.54 for $E_s/\sigma^2 = 0$ dB and approximately 0.5 for $E_s/\sigma^2 = 3$ dB. When E_s/σ^2 increases, the solution almost remains same. As a result it can be said that, the optimum value of the h is 0.5 in order to minimize total error probability. Figure 6.1 illustrates total bit error rate for $E_s/\sigma^2 = 0$ dB. In addition to that, BER performances of the users A and B are given in figure 6.2 for $h = 0.5$. As it can be seen from these figures, analytical and simulation results are perfectly match.

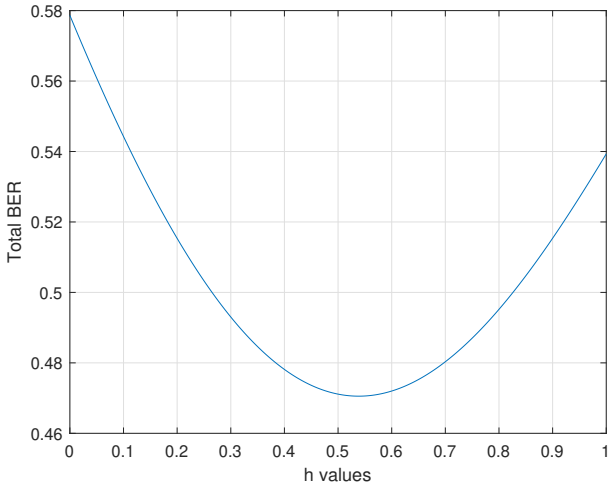

Figure 6.1. Total BER of the power domain NOMA for different h values. $E_s/\sigma^2 = 0$ dB

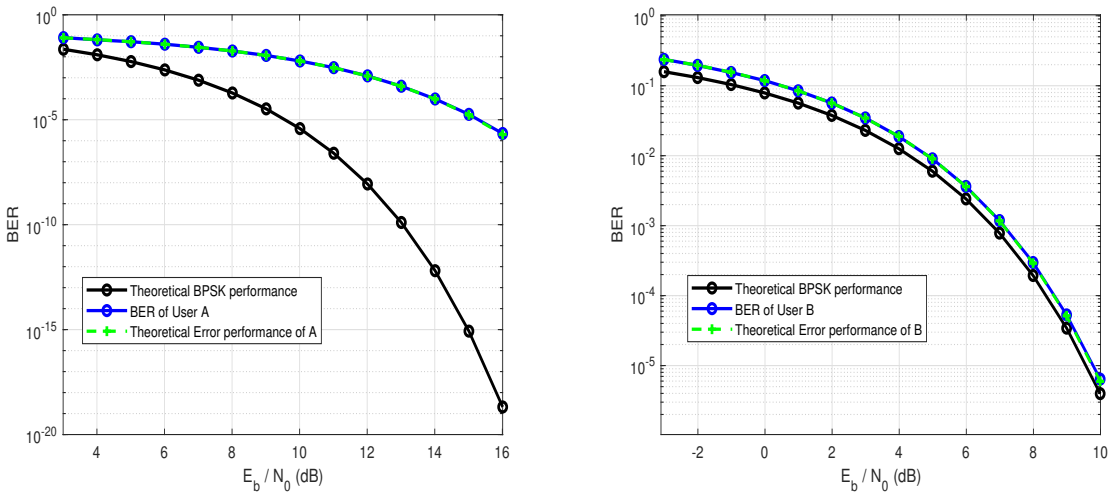

(a) BER of user A. (b) BER of user B.

Figure 6.2. Theoretical bit error rate of the power domain NOMA with $h = 1/2$. Symbols are BPSK modulated.

The relationship between symbol error rates of the BPSK and QPSK is given as in reference [32],

$$\mathbb{P}_{QPSK} = 1 - (1 - \mathbb{P}_{BPSK})^2. \tag{6.21}$$

When symbols A and B are QPSK modulated, equation (6.21) can be used to find corresponding error probabilities for power domain NOMA. Results are given in figure 6.3

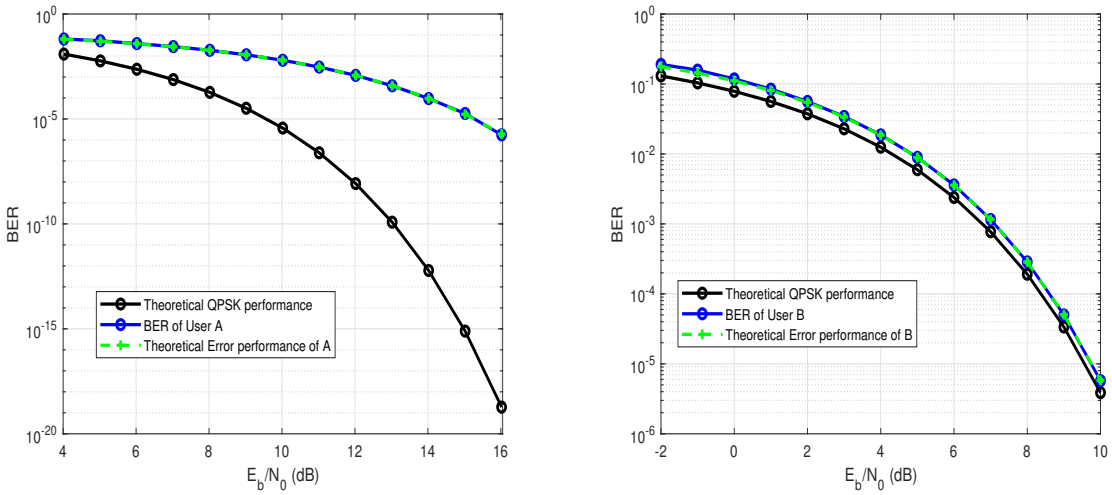

(a) BER of user A.

(b) BER of user B.

Figure 6.3. Theoretical bit error rate of the power domain NOMA with $h = 1/2$. Symbols are QPSK modulated.

6.2. Error Probability of the NOMA-2000

In this NOMA concept the error probability of N OFDMA with M MC-CDMA users scenario at the first iteration is investigated. At the receiver side, firstly OFDMA symbols are decoded with maximum likelihood detection. This process is shown in equation (6.22) for n^{th} sub-band.

$$\hat{a}_n = \underset{\hat{a}_n}{argmax}\ \mathbb{P}[x_n|\hat{a}_n] \tag{6.22}$$

where x_n is,

$$x_n = a_n + \frac{1}{\sqrt{N}} \sum_{m=1}^{M} w_{m,n} b_m + u_n. \tag{6.23}$$

Detected OFDMA symbols are subtracted from the received signal and the result is despreaded with Hadamard codes in order to insert MC-CDMA symbols. Assume that we would like to investigate i^{th} MC-CDMA symbol. The signal after despreading is z_k,

$$\begin{aligned} z_k &= \frac{1}{\sqrt{N}} \sum_{n=1}^{N} w_{k,n} \big(x_n - \hat{a}_n\big) \\ &= b_k + \frac{1}{\sqrt{N}} \sum_{n=1}^{N} w_{k,n} \big(a_n - \hat{a}_n + u_n\big). \end{aligned} \tag{6.24}$$

Detection method of k^{th} MC-CDMA symbol from z_k is maximum likelihood and it is given as,

$$\hat{b}_k = \underset{\hat{b}_k}{argmax}\ \mathbb{P}[z_k|\hat{b}_k]. \tag{6.25}$$

6.2.1. Exact Error Probability of the OFDMA Users

Assume that both OFDMA and MC-CDMA symbols are BPSK modulated for the sake of simplicity. The probability of the error is,

$$\begin{aligned}
\mathbb{P}_{OF}(error) &= \mathbb{P}[a_n \neq \hat{a}_n] \\
&= \mathbb{P}[a_n = 1]\mathbb{P}\big[x_n < 0 | a_n = 1\big] + \mathbb{P}[a_n = -1]\mathbb{P}\big[x_n > 0 | a_n = -1\big] \\
&= \frac{1}{2}\mathbb{P}\big[x_n < 0 | a_n = 1\big] + \frac{1}{2}\mathbb{P}\big[x_n > 0 | a_n = -1\big] \\
&= \mathbb{P}\big[x_n > 0 | a_n = -1\big] \\
&= \mathbb{P}\big[-1 + \frac{1}{\sqrt{N}} \sum_{m=1}^{M} w_{m,n} b_m + u_n > 0\big] \\
&= \mathbb{P}\big[u_n > +1 - \frac{1}{\sqrt{N}} \sum_{m=1}^{M} w_{m,n} b_m\big] \\
&= Q\Big(\frac{+1 - \frac{1}{\sqrt{N}} \sum_{m=1}^{M} w_{m,n} b_m}{\sigma}\Big).
\end{aligned} \tag{6.26}$$

With some mathematical manipulation equation (6.26) turns into,

$$\begin{aligned}
\mathbb{P}_{OF}(error) &= Q\Big(\frac{+1 - \frac{1}{\sqrt{N}} \sum_{m=1}^{M} w_{m,n} b_m}{\sigma}\Big) \\
&= \sum_{\vec{b}=[\mp 1,...,\mp 1]} P(\vec{b} = [\mp 1, ..., \mp 1]) \cdot Q\Big(\frac{+1 - \frac{1}{\sqrt{N}} \sum_{m=1}^{M} w_{m,n} b_m}{\sigma}\Big) \\
&= \sum_{\vec{b}=[\mp 1,...,\mp 1]} \frac{1}{2^M} \cdot Q\Big(\frac{+1 - \frac{1}{\sqrt{N}} \sum_{m=1}^{M} w_{m,n} b_m}{\sigma}\Big) \\
&= \sum_{m=0}^{M} \frac{\binom{M}{m}}{2^M} \cdot Q\Big(\frac{1 - (M - 2m)/\sqrt{N}}{\sigma}\Big).
\end{aligned} \tag{6.27}$$

Equation (6.27) gives the exact error probability of OFDMA at first iteration. By using equation (6.21) exact error probability can be found when both signal waveform is QPSK modulated.

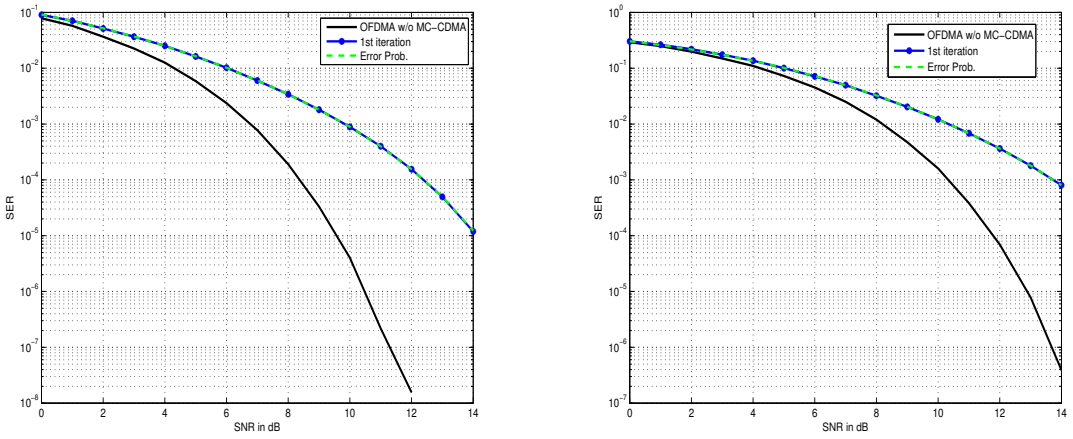

(a) BPSK modulated. (b) QPSK modulated.

Figure 6.4. Theoretical symbol error rate of the OFDMA at first iteration for NOMA-2000 in AWGN channel. There are 8 OFDMA and 2 MC-CDMA users.

6.2.2. Exact Error Probability of the MC-CDMA Users

Assume that OFDMA symbols are random variables and denoted as A_n. Their specific value is a_n. Both OFDMA and MC-CDMA symbols are BPSK modulated. In the same manner, MC-CDMA symbol is B_k (random variable). In order to find the probability of the error, general strategy is given in equation (6.28),

$$\begin{aligned}
\mathbb{P}_{CDMA}(error) &= P(B_1 = +1) \cdot P(\hat{B}_1 = -1 \mid B_1 = +1) \\
&\quad + P(B_1 = -1) \cdot P(\hat{B}_1 = +1 | B_1 = -1) \\
&= \frac{1}{2} \cdot P(\hat{B}_1 = -1 | B_1 = +1) + \frac{1}{2} \cdot P(\hat{B}_1 = +1 | B_1 = -1) \\
&= P(\hat{B}_1 = -1 | B_1 = +1) \\
&= E_{A_1, \hat{A}_1, .., A_N, \hat{A}_N, B_2, .., B_M} \big[P(\hat{B}_1 = -1 \\
&\quad \mid A_1, \hat{A}_1, ..., A_N, \hat{A}_N, B_1 = +1, B_2, .., B_M) \big] \\
&= \sum_{\vec{a}, \hat{\vec{a}}, b_2, .., b_M} P(A_1 = a_1, \hat{A}_1 = \hat{a}_1, .., \\
&\quad A_N = a_N, \hat{A}_N = \hat{a}_N, B_2 = b_2, .., B_M = b_M | B_1 = +1) \cdot \\
&\quad P\big(1 + \frac{1}{\sqrt{N}} \sum_{n=1}^{N} w_{1,n}(a_n - \hat{a}_n + u_n) < 0 | A_1 = a_1, ..., B_M = b_M\big).
\end{aligned} \tag{6.28}$$

Since all $w_{1,i}$ for $i = 1, .., N$ is 1, equation (6.28) becomes,

$$\begin{aligned}
\mathbb{P}_{CDMA}(error) = \sum_{\vec{a},\hat{\vec{a}},b_2,..,b_M} & P(A_1 = a_1, \hat{A}_1 = \hat{a}_1, .., A_N = a_N, \hat{A}_N = \hat{a}_N, \\
& B_2 = b_2, .., B_M = b_M | B_1 = +1) \cdot \\
& P\big(1 + \frac{1}{\sqrt{N}} \sum_{n=1}^{N} (a_n - \hat{a}_n + u_n) < 0 | A_1 = a_1, ..., B_M = b_M\big) \\
& = 2 \cdot \sum_{\vec{a},\hat{\vec{a}},b_2,..,b_M} P(\hat{A}_1 = \hat{a}_1, .., \hat{A}_N = \hat{a}_N \mid \\
& A_1 = a_1, .., A_N = a_N, B_1 = 1, B_2 = b_2, .., B_M = b_M) \cdot \\
& P(A_1 = a_1, .., A_N = a_N, B_1 = 1, B_2 = b_2, .., B_M = b_M) \cdot \\
& P(\sum_{n=1}^{N} u_n < -\sqrt{N} - \sum_{n=1}^{N} (a_n - \hat{a}_n) | A_1 = a_1, ..., B_M = b_M).
\end{aligned} \tag{6.29}$$

Because of all OFDMA and MC-CDMA symbols are independent, $P(A_1 = a_1, \cdots, A_N = a_N,\ B_1 = 1, B_2 = b_2, \cdots, B_M = b_M) = P(A_1 = a_1) \cdots P(A_N = a_N) P(B_1 = 1) \cdots P(B_M = b_M)$. Notice that, for example $\hat{A}_1$ is dependent on both all B's and A_1 however it is independent from $\hat{A}_j$ and A_j where $j \neq 1$. Therefore $P(\hat{A}_1 = \hat{a}_1, \cdots, \hat{A}_N = \hat{a}_N | A_1 = a_1, \cdots, A_N = a_N, B_1 = 1, B_2 = b_2, \cdots, B_M = b_M) = P(\hat{A}_1 =$

$\hat{a}_1|A_1 = a_1, \vec{B} = \vec{b}) \cdots P(\hat{A}_N = \hat{a}_N|A_N = a_N, \vec{B} = \vec{b})$. Then equation (6.29) is,

$$\begin{aligned}
\mathbb{P}_{CDMA}(error) = & \sum_{\vec{a},\hat{\vec{a}},b_2,..,b_M} \prod_{j=2}^{M} P(B_j = b_j) \\
& \cdot \prod_{i=1}^{N} P(\hat{A}_i = \hat{a}_i|A_i = a_i, B_1 = 1, B_2 = b_2, .., B_M = b_M) \\
& \cdot P(A_i = a_i) \cdot P\big(\sum_{n=1}^{N} u_n < -\sqrt{N} - \sum_{n=1}^{N}(a_n - \hat{a}_n\big) \\
& | \ \hat{\vec{A}} = \hat{\vec{a}}, \vec{A} = \vec{a}, B_1 = 1, B_2 = b_2, ..., B_M = b_M) \\
= & \frac{1}{2^{N+M-1}} \sum_{\vec{a},\hat{\vec{a}},b_2,..,b_M} \\
& \prod_{i=1}^{N} P(\hat{A}_i = \hat{a}_i|A_i = a_i, B_1 = 1, B_2 = b_2, .., B_M = b_M) \cdot \\
& P\big(\sum_{n=1}^{N} u_n < -\sqrt{N} - \sum_{n=1}^{N}(a_n - \hat{a}_n\big)|\hat{\vec{A}} = \hat{\vec{a}}, \vec{A} = \vec{a}, \vec{B} = \vec{b}).
\end{aligned} \tag{6.30}$$

The detail explanation of the expression $P(\hat{A}_i = \hat{a}_i|A_i = a_i, B_1 = 1, B_2 = b_2, .., B_M = b_M)$ is,

$$\begin{aligned}
P(\hat{A}_i = \hat{a}_i|A_i = a_i, \vec{B} = \vec{b}) &= P\big(a_i + \frac{1}{\sqrt{N}} \sum_{m=1}^{M} w_{m,i} b_m + u_i \underset{\hat{a}_i=-1}{\overset{\hat{a}_i=+1}{\gtrless}} 0\big) \\
&= P\big(u_i \underset{\hat{a}_i=-1}{\overset{\hat{a}_i=+1}{\gtrless}} -a_i - \frac{1}{\sqrt{N}} \sum_{m=1}^{M} w_{m,i} b_m\big) \\
&= Q\Big(\frac{\text{sgn}[\hat{a}_i](-a_i - \frac{1}{\sqrt{N}} \sum_{m=1}^{M} w_{m,i} b_m)}{\sigma}\Big) \\
&= Q\Big(\frac{\text{sgn}[\hat{a}_i](-a_i - \frac{1}{\sqrt{N}} W(i,:)\vec{b}}{\sigma}\Big).
\end{aligned} \tag{6.31}$$

where sgn[.] is sign function and $W(i,:)$ is i^{th} row of the Hadamard matrix W.

Notice that in equation (6.30), for given $\vec{A}$, $\hat{\vec{A}}$ and $\vec{B}$ corresponding u is not purely Gaussian. If $A_i = a_i$, $\hat{A}_i = \hat{a}_i$ and $\vec{B} = \vec{b}$, then interval for the u_i is $u_i \underset{\hat{a}_i=-1}{\overset{\hat{a}_i=+1}{\gtrless}} -a_i - \frac{1}{\sqrt{N}} W(i,:)\vec{b}$. It means that probability density function of the u_i for given A_i, $\hat{A}_i$

and $\vec{B}$ is truncated Gaussian. This distribution is given as,

$$\begin{aligned} & f(u_i|A_i = a_i, \hat{A}_i = \hat{a}_i, \vec{B} = \vec{b}) \\ & = \frac{\frac{1}{\sqrt{2\pi\sigma^2}} e^{-\frac{u_i^2}{2\sigma^2}}}{Q\big(\frac{\text{sgn}[\hat{a}_i](-a_i - (1/\sqrt{N})W(i,:)\vec{b})}{\sigma}\big)} \\ & \cdot I_{u_i}\big[\min(\infty\,\text{sgn}[\hat{a}_i], -a_i - \frac{1}{\sqrt{N}}W(i,:)\vec{b}), \max(\infty\,\text{sgn}[\hat{a}_i], -a_i - \frac{1}{\sqrt{N}}W(i,:)\vec{b})\big] \end{aligned} \tag{6.32}$$

where $I_z[x, y]$ is 1 if $x \leq z \leq y$, 0 otherwise. If equations (6.31) and (6.32) are inserted into equation (6.30), we get

$$\begin{aligned} \mathbb{P}_{CDMA}(error) =& \frac{1}{2^{N+M-1}} \cdot \sum_{\vec{a},\hat{\vec{a}},b_2,..,b_M} \cdot \prod_{i=1}^{N} Q\Big(\frac{\text{sgn}[\hat{a}_i](-a_i - (1/\sqrt{N})W(i,:)\vec{b})}{\sigma}\Big) \cdot \\ & P\big(\sum_{n=1}^{N} u_n < -\sqrt{N} - \sum_{n=1}^{N}(a_n - \hat{a}_n)|\hat{\vec{A}} = \hat{\vec{a}}, \vec{A} = \vec{a}, \vec{B} = \vec{b}\big) \\ =& \frac{1}{2^{N+M-1}} \cdot \sum_{\vec{a},\hat{\vec{a}},b_2,..,b_M} \cdot \prod_{i=1}^{N} Q\Big(\frac{\text{sgn}[\hat{a}_i](-a_i - (1/\sqrt{N})W(i,:)\vec{b})}{\sigma}\Big) \cdot \\ & \int_{-\infty}^{-\sqrt{N}-\sum_{n=1}^{N}(a_n-\hat{a}_n)} f_{u_1+\ldots+u_N}(u|\vec{A} = \vec{a}, \hat{\vec{A}} = \hat{\vec{a}}, \vec{B} = \vec{b})\,\mathrm{d}u. \end{aligned} \tag{6.33}$$

In order to calculate equation (6.33), probability density function of the summation of different truncated Gaussian noises has to be determined. Central limit theorem states that let say $X_1, X_2, \cdots, X_h$ are the sequence of the independent random variables with means $\mu_1, \mu_2, \cdots, \mu_h$ and variances $\sigma_1^2, \sigma_2^2, \cdots, \sigma_h^2$. Then pdf of $X_1 + X_2 + \cdots + X_h$ approaches normal distribution with mean $\mu_1 + \mu_2 + \cdots + \mu_h$ and variance $\sigma_1^2 + \sigma_2^2 + \cdots + \sigma_h^2$ when h goes to infinity. In this sense, equation (6.33) turns

into,

$$\begin{aligned}\mathbb{P}_{CDMA}(error) =&\frac{1}{2^{N+M-1}}\sum_{\vec{a},\hat{\vec{a}},b_2,..,b_M}\cdot\prod_{i=1}^{N}Q\Big(\frac{\text{sgn}[\hat{a}_i](-a_i-(1/\sqrt{N})W(i,:)\vec{b})}{\sigma}\Big)\cdot\\ &\int_{-\infty}^{-\sqrt{N}-\sum_{n=1}^{N}(a_n-\hat{a}_n)}\frac{1}{\sqrt{2\pi\overline{\sigma}^2}}e^{\frac{(u-\overline{\mu})^2}{2\overline{\sigma}^2}}\,\mathrm{d}u\\ =&\frac{1}{2^{N+M-1}}\sum_{\vec{a},\hat{\vec{a}},b_2,..,b_M}\cdot\prod_{i=1}^{N}Q\Big(\frac{\text{sgn}[\hat{a}_i](-a_i-(1/\sqrt{N})W(i,:)\vec{b})}{\sigma}\Big)\cdot\\ &Q\Big(\frac{\sqrt{N}+\sum_{n=1}^{N}(a_n-\hat{a}_n)+\overline{\mu}}{\overline{\sigma}}\Big)\end{aligned}\tag{6.34}$$

where $\overline{\mu}$ is expected value and $\overline{\sigma}^2$ variance of $f_{u_1+\ldots+u_N}(u|\vec{A}=\vec{a},\hat{\vec{A}}=\hat{\vec{a}},\vec{B}=\vec{b})$.

Assume that $f(.)$ is probability density function and $F(.)$ is cumulative distribution function. If y is normal distributed random variable with mean μ_y and variance σ_y^2 and it has only defined between $lB<y'<uB$. Then the expected value and the variance of y' are,

$$\begin{aligned}E[y'] =&\mu_y+\frac{f(\frac{lB-\mu_y}{\sigma_y})-f(\frac{uB-\mu_y}{\sigma_y})}{F(\frac{uB-\mu_y}{\sigma_y})-F(\frac{lB-\mu_y}{\sigma_y})},\\ Var(y') =&\sigma_y^2\Bigg[1+\frac{\frac{lB-\mu_y}{\sigma_y}f(\frac{lB-\mu_y}{\sigma_y})-\frac{uB-\mu_y}{\sigma_y}f(\frac{uB-\mu_y}{\sigma_y})}{F(\frac{uB-\mu_y}{\sigma_y})-F(\frac{lB-\mu_y}{\sigma_y})}\\ &-\left(\frac{f(\frac{lB-\mu_y}{\sigma_y})-f(\frac{uB-\mu_y}{\sigma_y})}{F(\frac{uB-\mu_y}{\sigma_y})-F(\frac{lB-\mu_y}{\sigma_y})}\right)^2\Bigg].\end{aligned}\tag{6.35}$$

By using equations (6.32) and (6.35) variance and expected value in equation (6.34) can be calculated. In addition to that, symbol error probability can be found if both signal group is QPSK modulated by using equation (6.21). Figure 6.5 demonstrates analytical and simulation results.

In this chapter the bit error analysis of the power domain NOMA and NOMA-2000 at the first iteration were given for AWGN channels. In addition to that optimum

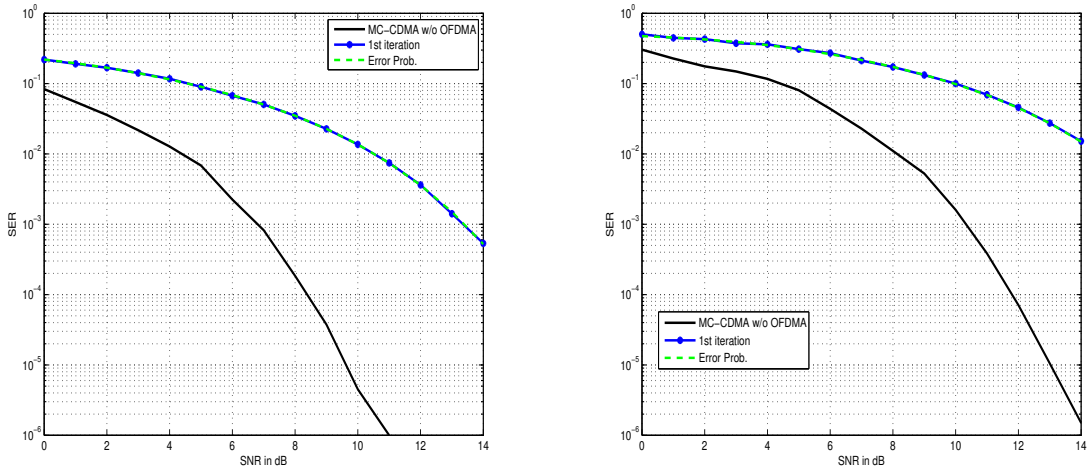

(a) BPSK modulated. (b) QPSK modulated.

Figure 6.5. Theoretical symbol error rate of the MC-CDMA at first iteration for NOMA-2000 in AWGN channel. There are 8 OFDMA and 2 MC-CDMA users.

power imbalance between users was shown for power domain NOMA in order to minimize total bit error rate. This imbalance is depend on channel SNR, however for practical applications, it can be taken as 4.

7. CONCLUSION

Non-orthogonal multiple access techniques are more bandwidth efficient then orthogonal multiple accesses for both uplink and downlink. Therefore it is the one of the promising technology to deal with bandwidth scarcity. However two main NOMA methods which are called as power and code domain NOMA have some disadvantages [2]. Power imbalance between non-orthogonal users is extremely critical for power domain NOMA. In addition, even if the number of the users is less then orthogonal resource blocks, non-orthogonality is unavoidable in code domain NOMA. This situation restrains the flexibility of the wireless communication system. However these problems are overcome by using two sets of orthogonal multiple access waveforms which are non-orthogonal to each others. These waveforms are chosen as MC-CDMA and OFDMA which are adaptable for today's technology.

Iterative successive interference cancellation method is proposed to separate waveforms. Moreover soft decision detection is used in order to increase performance. Its bit error rate performances are investigated for AWGN, frequency selective and non-frequency selective Rayleigh fading channels. Minimum mean square error equalizer is used as multi-user detection technique for fading channels. It is observed that power indifference between users is increased BER performance in Rayleigh flat fading channel. In this channel for uplink, 100% overload factor is achieved with zero SNR degradation thanks to dynamic user grouping method. MISO method is proposed for downlink Rayleigh flat fading and it also increases performances.

To avoid complexity of the iterative successive interference cancellation, channel overloading NOMA is proposed. It is basically combining 1 MC-CDMA user with N OFDMA users. Maximum likelihood detection is used at the receiver side. Its BER performances are also investigated for AWGN, flat and frequency selective Rayleigh fading channels.

Bit error probability of the power domain NOMA in AWGN channel is found. In order to minimize total BER, power ration between users is given. In addition exact error probability for proposed NOMA system is indicated at the first iterations.

REFERENCES

1. Osseiran, A., F. Boccardi, V. Braun, K. Kusume, P. Marsch, M. Maternia, O. Queseth, M. Schellmann, H. Schotten, H. Taoka, H. Tullberg, M. A. Uusitalo, B. Timus and M. Fallgren, "Scenarios for 5G Mobile and Wireless Communications: The Vision of the METIS Project", *IEEE Communications Magazine*, Vol. 52, No. 5, pp. 26–35, May 2014.

2. Dai, L., B. Wang, Z. Ding, Z. Wang, S. Chen and L. Hanzo, "A Survey of Non-Orthogonal Multiple Access for 5G", *IEEE Communications Surveys Tutorials*, pp. 1–1, 2018.

3. Sari, H., A. Maatouk, E. Caliskan, M. Assaad, M. Koca and G. Gui, "On the Foundation of NOMA and Its Application to 5G Cellular Networks", pp. 1–6, April 2018.

4. Goldsmith, A., *Wireless Communications*, Cambridge University Press, 2005.

5. Saito, Y., Y. Kishiyama, A. Benjebbour, T. Nakamura, A. Li and K. Higuchi, "Non-Orthogonal Multiple Access (NOMA) for Cellular Future Radio Access", *2013 IEEE 77th Vehicular Technology Conference (VTC Spring)*, pp. 1–5, June 2013.

6. Yang, S. C., *OFDMA System Analysis and Design*, Artech House, 2010.

7. Fazel, K. and S. Kaiser, *Multi-carrier and Spread Spectrum Systems: from OFDM and MC-CDMA to LTE and WiMAX*, John Wiley & Sons, 2008.

8. Cover, T. M. and J. A. Thomas, *Elements of Information Theory* 2^{nd} *Edition*, John Wiley & Sons.

9. Verdu, S., *Multiuser Detection*, Cambridge University Press, 1998.

10. Tse, D. and P. Viswanath, *Fundamentals of Wireless Communication*, Cambridge University Press, 2005.

11. Higuchi, K. and A. Benjebbour, "Non-Orthogonal Multiple Access (NOMA) with Successive Interference Cancellation for Future Radio Access", *IEICE Transactions on Communications*, Vol. 98, No. 3, pp. 403–414, 2015.

12. Saito, Y., A. Benjebbour, Y. Kishiyama and T. Nakamura, "System-Level Performance Evaluation of Downlink Non-Orthogonal Multiple Access (NOMA)", *2013 IEEE 24th Annual International Symposium on Personal, Indoor, and Mobile Radio Communications (PIMRC)*, pp. 611–615, September 2013.

13. Nikopour, H. and H. Baligh, "Sparse Code Multiple Access", *2013 IEEE 24th Annual International Symposium on Personal, Indoor, and Mobile Radio Communications (PIMRC)*, pp. 332–336, September 2013.

14. Chen, S., B. Ren, Q. Gao, S. Kang, S. Sun and K. Niu, "Pattern Division Multiple Access—A Novel Nonorthogonal Multiple Access for Fifth-Generation Radio Networks", *IEEE Transactions on Vehicular Technology*, Vol. 66, No. 4, pp. 3185–3196, April 2017.

15. Yuan, Z., G. Yu and W. Li, "Multi-User Shared Access for 5G", *Telecommun. Netw. Technol.*, Vol. 5, No. 5, pp. 28–30, May 2015.

16. Ding, Z., X. Lei, G. K. Karagiannidis, R. Schober, J. Yuan and V. K. Bhargava, "A Survey on Non-Orthogonal Multiple Access for 5G Networks: Research Challenges and Future Trends", *IEEE Journal on Selected Areas in Communications*, Vol. 35, No. 10, pp. 2181–2195, October 2017.

17. Guo, D. and C. Wang, "Multiuser Detection of Sparsely Spread CDMA", *IEEE Journal on Selected Areas in Communications*, Vol. 26, No. 3, pp. 421–431, April 2008.

18. Hoshyar, R., R. Razavi and M. Al-Imari, "LDS-OFDM an Efficient Multiple Access Technique", *2010 IEEE 71st Vehicular Technology Conference*, pp. 1–5, May 2010.

19. Zhang, S., X. Xu, L. Lu, Y. Wu, G. He and Y. Chen, "Sparse Code Multiple Access: An Energy Efficient Uplink Approach for 5G Wireless Systems", *2014 IEEE Global Communications Conference*, pp. 4782–4787, December 2014.

20. Nonaka, N., Y. Kishiyama and K. Higuchi, "Non-Orthogonal Multiple Access Using Intra-Beam Superposition Coding and SIC in Base Station Cooperative MIMO Cellular Downlink", *2014 IEEE 80th Vehicular Technology Conference (VTC2014-Fall)*, pp. 1–5, September 2014.

21. Kim, B., W. Chung, S. Lim, S. Suh, J. Kwun, S. Choi and D. Hong, "Uplink NOMA with Multi-Antenna", *2015 IEEE 81st Vehicular Technology Conference (VTC Spring)*, pp. 1–5, May 2015.

22. Ding, Z., M. Peng and H. V. Poor, "Cooperative Non-Orthogonal Multiple Access in 5G Systems", *IEEE Communications Letters*, Vol. 19, No. 8, pp. 1462–1465, August 2015.

23. Choi, J., "Non-Orthogonal Multiple Access in Downlink Coordinated Two-Point Systems", *IEEE Communications Letters*, Vol. 18, No. 2, pp. 313–316, February 2014.

24. Sari, H., F. Vanhaverbeke and M. Moeneclaey, "Multiple Access Using Two Sets of Orthogonal Signal Waveforms", *IEEE Communications Letters*, Vol. 4, No. 1, pp. 4–6, January 2000.

25. Cai, Y., Z. Qin, F. Cui, G. Y. Li and J. A. McCann, "Modulation and Multiple Access for 5G Networks", *IEEE Communications Surveys Tutorials*, Vol. 20, No. 1, pp. 629–646, Firstquarter 2018.

26. van de Beek, J. and B. M. Popovic, "Multiple Access with Low-Density Signa-

tures", *GLOBECOM 2009 - 2009 IEEE Global Telecommunications Conference*, pp. 1–6, November 2009.

27. Maatouk, A., E. Çalışkan, M. Koca, M. Assaad, G. Gui and H. Sari, "Frequency-Domain NOMA With Two Sets of Orthogonal Signal Waveforms", *IEEE Communications Letters*, Vol. 22, No. 5, pp. 906–909, May 2018.

28. Vanhaverbeke, F., M. Moeneclaey and H. Sari, "Turbo Multiple Access: Channel Overloading Using Two Sets of Orthogonal Signal Waveforms and Iterative Interference Cancellation.", *Proceedings 2nd International Symposium on Turbo Codes and Related Topics, Brest*, pp. 181–184, September 2000.

29. Caliskan, E., A. Maatouk, M. Koca, M. Assaad, G. Gui and H. Sari, "A Simple NOMA Scheme with Optimum Detection", *2018 IEEE Global Communications Conference (GLOBECOM)*, pp. 1–6, December 2018.

30. Caliskan, E., M. Koca, G. Gui and H. Sari, "Uplink Performance of NOMA-2000 with Dynamic User Grouping", *2019 IEEE 30th Annual International Symposium on Personal, Indoor and Mobile Radio Communications (PIMRC)*, to be published, 2019.

31. Severini, T. A., *Elements of Distribution Theory*, Vol. 17, Cambridge University Press, 2005.

32. Proakis, J. G., M. Salehi, N. Zhou and X. Li, *Communication Systems Engineering*, Vol. 2, Prentice Hall New Jersey, 1994.